Apoptosis Gene Expression Profiling in Lens Development

Thesis submitted to Cardiff University for the degree of Doctor of Philosophy

Jenny Geatrell

School of Optometry and Vision Sciences

Cardiff University

September 2007

ProQuest LLC
789 East Eisenhower Parkway
P.O. Box 1346
Ann Arbor, MI 48106-1346

Acknowledgements

This thesis is the result of a lot of hard work (and sleepless nights) and there have been many times since I embarked on this PhD that I thought this day would never come. There have been many highs and lows during this project and I would like to thank my two supervisors Dr. Mike Wride and Professor Mike Boulton for their support and guidance over the years, without them I would have lost all faith in my ability.

I would also like to thank my advisor Dr. Jon Erichsen. His support during the course of my PhD has been invaluable. My gratitude also goes to Dr. Fiona Mansergh for help in collecting the mouse tissue required for this project and for completing the submission of the raw array data to GEO. I would like to acknowledge Dr. Lesley Jones and Lyn Ellisten for the provision of the huntingtin knock-in mouse lenses. Many thanks go to Dr. Arwyn Jones in the Cardiff School of Pharmacy for allowing me to use the Typhoon Scanner to scan in my array results and Dr. Andrew Hollins for technical assistance with western blotting. I also need to acknowledge the help of the office staff who have always been very helpful, friendly and approachable during my time here.

Special thanks goes to my fellow postgrads, many of which I am glad to say have become good friends, especially Debbie, Tina, Linda, Llinos, Matt, Flick, Kat, Bablin, Charlotte and Yadan. They have been there during both the highs and lows of doing my PhD, providing me with cups of tea or something stronger when required.

I would also like to thank my parents for their constant support, both emotional and financial. You will never know how much that support meant to me, without it I would have given up a long time ago. Finally, I would like to thank Dave. He has been both a shoulder to cry on and someone to celebrate with. He has always believed in me. I hope I make you proud.

Jen

Abstract

During lens development, epithelial cells located at the equatorial region of the lens undergo terminal differentiation to form fibre cells; resulting in cell elongation and degradation of all intracellular organelles. Failure to complete this process successfully can result in cataract. This process is thought to be an attenuated form of classical apoptosis. This study was completed to give a comprehensive analysis of apoptosis genes in the developing mouse lens.

Macroarrays containing 243 immobilised cDNAs with a known role in apoptosis were utilised to examine the gene expression at different developmental stages. The stages examined were postnatal day 7 and postnatal day 14. Over 100 apoptosis genes were shown to be expressed above background with 20 genes demonstrating significantly differential expression (2-fold or greater change in expression, p-value < 0.05), with highest expression at P14. PCR confirmed expression of all the genes identified from the array results, and differential expression was confirmed for 52% of the genes. Protein expression of two selected genes, axl and mcl-1, was demonstrated using western blotting.

Lens morphology was examined in transgenic mice generated to contain an extended CAG repeat in the *huntingtin* gene (one of the genes identified from the arrays). Morphology was compared between homozygote, heterozygote and wild-type mice. The presence of the mutated gene did not affect denucleation during lens differentiation and no statistically significant difference was seen in the dimensions of the organelle free zone (OFZ) of the wild-type and homozygote mice.

A cross-species comparison was completed. Gene expression of the genes shown to be highly expressed and differentially expressed from the array results was examined in embryonic chick lenses. From the results of this part of the study expression was seen for 83% of genes. These results add to the argument that the process of differentiation is similar in both mouse and chick lenses.

Contents Page

List of Figures

List of Tables

Abbreviations

15-LOX	15 Lipoxygenase
4wk	4 weeks
AIF	Apoptosis Inducing Factor
APS	Ammonium Persulphate
BH	Bcl-2 homology
bp	Base pair
BMP	Bone Morphogenic Protein
BSA	Bovine Serum Albumin
Cdk4	Cyclin-Dependent Kinase 4
cDNA	Complimentary Deoxyribonucleic Acid
DAD-1	Defender Against Death 1
Dap1	Death associated protein 1
dATP	Deoxy Adenosine Triphosphate
Daxx	Death-domain-associated protein
dCTP	Deoxycytosine
DFF	DNA Fragmentation Factor
DLAD	DNase II-like acid DNase
DNA	Deoxyribonucleic acid
Dpc	Day Post Conception
ES	Embryonic Stem Cell
Ex	Embryonic day x
ECL	Enzyme Chemiluminescence
ECM	Extracellular Matrix
EQ	Equatorial Region
ER	Endoplasmic Reticulum
FGF	Fibroblast Growth Factor
Gal-3	Galectin-3
GPX	Glutathione Peroxidase
RT-PCR	Reverse Transcriptase Polymerase Chain Reaction
Hd	Huntingtin

IGF1	Insulin-like growth factor 1
IGF1r	Insulin-like growth factor 1 receptor
IOL	Intra Ocular Lens
IMS	Industrial Methylated Spirit
kDa	Kilo Daltons
LEC	Lens Epithelial Cell
LFC	Lens Fibre Cell
Mcl-1	Myeloid cell leukaemia-1
Mdm2	Mouse Double Minute Protein 2
Mfge8	Milk fat globule epidermal growth factor 8
MOPS	3-(N-morpholino) propanesulfonic acid.
NB	Newborn
OFZ	Organelle Free Zone
PARP	Poly ADP-Ribose Polymerase
P x	Postnatal day x
PBS	Phosphate Buffered Saline
PCO	Posterior Capsular Opacification
PCR	Polymerase Chain Reaction
RDZ	RNA Depleted Zone
RIPA	RadioImmunoPrecipitation Assay
RNA	Ribonucleic Acid
RT	Reverse Transcriptase
SD	Standard Deviation
SDS	Sodium Dodecyl Sulphate
SEM	Standard Error of the Mean
SREB	Super Conserved Receptor Expressed in Brain
TBS	Tris-buffered saline
TGFβ2	Transforming Growth factor beta 2
TNFα	Tumor Necrosis Factor α
TUNEL	Terminal Deoxynucleotidyl Transferase Mediated dUTP Nick End Labeling
UPP	Ubiquitin Proteasome Pathway
UV	Ultraviolet
WT	Wild-type

Chapter 1: Introduction

1.1. General Introduction

The lens is located in the eye between the iris and the vitreous body, where its function is to focus light onto the retina. The lens is made up of two different types of cells; a single layer of epithelial cells at the anterior and fibre cells which make up the remainder of the lens. The lens epithelial cells differentiate into fibre cells at the equatorial region of the lens. During this process, which has been likened to classical apoptosis (a type of programmed cell death), the intracellular organelles are degraded. This process of organelle degradation ensures that any potential light-scattering structures are removed from the visual axis.

Differentiation of lens epithelial cells into fibre cells continues throughout life, constantly covering underlying fibre cells with new ones. This leads to an increase in lens size throughout life. The cells contained within the lens persist throughout the lifetime of the organism and so protein turnover is limited to the outer epithelial cells. This means that the proteins of the lens have to be very stable to avoid denaturation. Any disruption to either the structure of the proteins within the lens, or the process of organelle removal during differentiation can result in cataract e.g. in Rubella syndrome (McAlister Gregg 2001).

The purpose of this introductory chapter is to give the reader background information about the lens including its development, differentiation and ageing. It will also provide details of the process of classical apoptosis to allow comparisons to be made between this process and that of organelle degradation in the lens.

1.2. Apoptosis

Apoptosis (programmed cell death) is essential in both development and tissue homeostasis, selectively deleting a cell. It is now known that apoptosis occurs at a low rate in most healthy mammalian tissues where it complements the role of mitosis, thus ensuring the maintenance of cell number. Apoptosis was first described in 1972 when a form of cell death that was morphologically distinct from necrotic death was observed (Kerr *et al.* 1972). It has since been shown that apoptosis pathways are evolutionarily conserved between species (Ameisen 2002).

Apoptosis is characterised by a series of distinct morphological changes. The cell and its nucleus are seen to shrink; chromatin condensation and marginalisation are seen to accompany this. Ultimately, the cell surface protuberances separate to produce membrane-enclosed apoptotic bodies in which the cytoplasmic organelles remain well preserved. The formation of these apoptotic bodies is completed in several minutes. They are then phagocytosed by macrophages or taken up by neighbouring cells and digested within lysosomes *in vivo*. The apoptotic bodies are recognised by the presence of phosphatidylserine on the outer surface which acts as a target signal for phagocytes (Kerr *et al.* 1972).

In 1980, it was shown that the morphological changes occurring during apoptosis are associated with a distinctive double-strand cleavage of nuclear DNA at the linker regions between nucleosomes (Wyllie *et al.* 1980). This results in multiples of 180-200 base pair oligonucleosomal fragments which when viewed on an agarose gel results in a distinctive DNA ladder. This DNA ladder is widely recognised as the major molecular criterion of apoptosis.

Three phases of apoptosis have been identified; firstly there is the initiation phase, followed by the effector phase and then finally the degradation phase (Kroemer *et al.* 1995). Apoptosis can be triggered by both extracellular signals, such as a withdrawal of growth factors or intracellular signals, such as DNA damage (Evan and Littlewood 1998; Green and Reed 1998; Nagata 1997).

The initiation phase is dependent on death-inducing primary stimuli, which are integrated by members of the Bcl-2 family of proteins. The signalling pathways generated during the initiation phase then converge on the mitochondria where they are amplified and then focused onto the caspase cascade. This then activates the degradation phase where mitochondrial proteins are released leading to the cleavage of key cellular proteins and DNA fragmentation.

1.2.1. Bcl-2 Family Members

Bcl-2 was the first mammalian regulator of apoptosis identified. Many more structurally similar proteins were recognised later, forming the Bcl-2 related family of proteins. There are at least 15 members of the Bcl-2 family found in mammalian cells (Adams and Cory 1998). The Bcl-2 family of proteins contains a number of apoptosis-regulatory proteins, which act upstream of the caspase cascade.

Bcl-2 family members can be organised into two groups, one group which inhibits apoptosis (e.g. Bcl-2, Bcl-X_L, Mcl-1_L) and one which promotes it (e.g. Bax, Bak, Bcl-X_S, and Mcl-1_S). The structures of these proteins vary with both their location and function. All family members have been shown to have at least one of four conserved Bcl-2 homology (BH) regions (Adams and Cory 1998). The proteins with the most structural similarity to Bcl-2 have been shown to inhibit apoptosis (as demonstrated in **Figure 1.1**); anti-apoptotic members of the Bcl-2 family typically contain all 4 BH domains, e.g. Bcl-X_L and Bcl-W (Antonsson 2001). In contrast, the pro-apoptotic proteins have few common domains with Bcl-2. This pro-apoptotic set of proteins can be further divided into two groups: the multidomain proteins including Bax and Bak, and the BH3 only proteins e.g. Bad and Bid (Burlacu 2003). One of the BH domains, the BH3 group, has been shown to be required for death-inducing activity (Chittenden *et al.* 1995; Hunter and Parslow 1996).

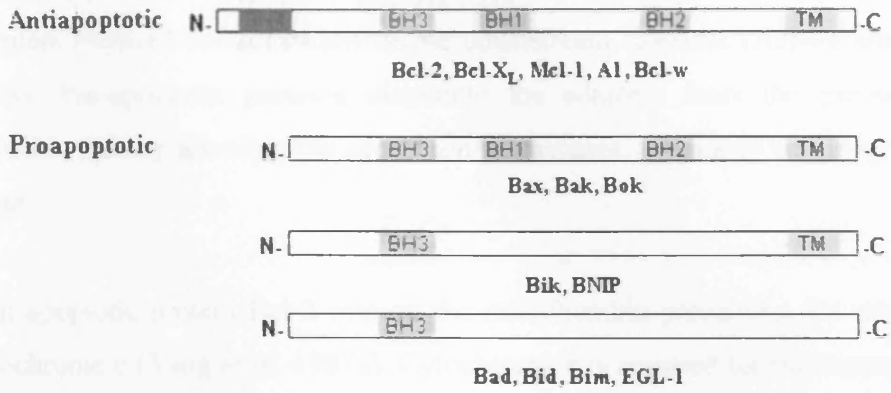

Figure 1.1: ***Diagram showing the structure of the different Bcl-2 family members.*** *BH1-4 represent the Bcl-2 homology domains; TM represents the transmembrane domain. Figure was adapted from Burlacu 2003*

Both pro- and anti-apoptotic members of this family have been shown to be localised to distinct compartments within the cell. Anti-apoptotic proteins, e.g. Bcl-2, are initially integral membrane proteins found in the mitochondria, endoplasmic reticulum and nuclear envelope (Akao *et al.* 1994). In contrast, the pro-apoptotic proteins, e.g. Bax, tend to be cytosolic proteins which, following the induction of apoptosis, undergo a conformational change following a death signal allowing them to integrate into the mitochondrial outer membrane (Wolter *et al.* 1997).

The fate of a cell (as to whether or not it will undergo apoptosis) is determined by posttranslational modifications (proteolysis and phosphorylation) to these proteins and the ratio of both pro- and anti-apoptotic proteins (Oltvai *et al.* 1993). The BH regions within the proteins affect their ability to interact with one another. Bcl-2 family members are capable of either hetero- or homodimerisation; by forming dimers, these proteins can seemingly control their function. It has been observed that Bcl-2 can form heterodimers with Bax suppressing its death-inducing activity (Oltvai *et al.* 1993). Bcl-2 has also been noted to form homodimers which have been shown to promote cell survival, whereas when Bax homodimerises it inserts into the mitochondrial membrane causing mitochondrial permeabilisation, leading to apoptosis.

Anti-apoptotic family members seem to promote cell survival by inhibiting adapters required for activation of the downstream caspases (Adams and Cory 1998). Pro-apoptotic proteins dismantle the adapters from the pro-survival proteins, thereby allowing the activation of caspases, ultimately resulting in cell death.

Anti-apoptotic protein Bcl-2 acts on the mitochondria preventing the release of cytochrome c (Yang *et al.* 1997a). Cytochrome c is required for the formation of the apoptosome, a protein complex composed of Apaf1, procaspase-9, dATP and cytochrome c (Li *et al.* 1997). This formation of the apoptosome leads to the activation of caspase-9 which subsequently cleaves and activates caspase-3. Following the activation of caspase-3, the recognised caspase substrates are cleaved and the morphological changes of apoptosis observed.

In contrast to the mechanism described above, Bax (a pro-apoptotic protein) has been suggested to cause cell death by damaging organelles, forming channels in the mitochondrial membrane (Antonsson *et al.* 1997). Even in the presence of caspase inhibitors, Bax and Bax-like proteins were shown to cause DNA condensation and membrane alterations, resulting in cell death (Gross *et al.* 1998).

1.2.2. The Role of Mitochondria in Apoptosis

The mitochondrial phase of apoptosis is characterised by an irreversible loss of mitochondrial membrane barrier function. The outer membrane becomes permeabilised leading to the release of intermembrane proteins into the cytosol. During the permeabilisation of the mitochondria membrane, the inner mitochondrial membrane potential ($\Delta\psi_m$) is lost (Newmeyer and Ferguson-Miller 2003).

Permeabilisation of the membrane leads to the release of intermembrane proteins including cytochrome c, apoptosis inducing factor (AIF), endonuclease G, and Smac/DIABLO (van Gurp *et al.* 2003). Cytochrome c forms the apoptosome, leading to the activation of caspase-9 as previously described above. AIF is usually localised in the mitochondria; although, following an apoptosis signal it

is translocated to the nucleus. Overexpression of AIF induces DNA fragmentation, chromatin condensation, exposure of phosphatidlyserine on the plasma membrane and dissipation of the mitochondrial potential (van Gurp *et al.* 2003). Endonuclease G is also translocated to the nucleus in the presence of an apoptotic signal, where it cleaves DNA independently of caspase activation (van Gurp *et al.* 2003). Smac/DIABLO has been shown to regulate apoptosis indirectly by interacting with inhibitors of apoptosis proteins (IAPs) (Verhagen *et al.* 2000). IAPs bind to activated caspases thereby inhibiting their enzymatic activity (Deveraux and Reed 1999). Smac/DIABLO dislodges caspases from IAPs upon reaching the cytosol, triggering caspase activity (Degli Esposti 2003).

1.2.3. The Caspase Family

Apoptotic cell death is accompanied by highly selective and specific proteolytic events. Members of the caspase (cysteine-containing aspartate-specific proteases) family play a significant role in this process by mediating the majority of proteolytic events. The caspases are involved in amplifying the initial death signal from initiator to effector caspases in a proteolytic cascade (Wilson 1999).

Caspases -8 and -9 are initiator caspases. Once activated, these initiator caspases trigger downstream effector caspases, such as caspases -3, -6 and -7. These downstream caspases can then in turn cleave key structural components such as DFF45, ICAD, poly (ADP-ribose) polymerase (PARP) and nuclear lamins (Vaux and Strasser 1996; Wilson 1999). Cleavage of these molecules results in the change in structural morphology characteristic of apoptosis.

DNA fragmentation factor (DFF) is a heterodimer made up of two subunits, DFF 40 (40kDa) and DFF 45 (45kDa). During apoptosis caspase-3 cleaves DFF 45 to release the active 40kDa subunit triggering DNA fragmentation and chromatin condensation (Liu *et al.* 1998; Liu *et al.* 1997). Following cleavage of DFF, caspase-3 plays no further role in DNA fragmentation although it still cleaves PARP and lamin B which may help the degradation of the nuclear envelope.

PARP is a nuclear enzyme which binds to DNA breaks. Following exposure to genotoxic agents PARP triggers the base excision repair pathway (Ding *et al.* 1992; Ding and Smulson 1994). Cleavage of PARP by caspase-3 during apoptosis incapacitates the DNA damage surveillance network, thereby preventing attempts at repairing the fragmented DNA. Cleavage of lamins, the major structural proteins of the nuclear envelope, has also been shown to accompany the apoptotic process (Lazebnik *et al.* 1995).

1.3. Vertebrate Eye Structure and Development

As a result of gastrulation, the embryo contains three germ layers; the ectoderm, the mesoderm and the endoderm. The ectoderm, the outer layer of cells, will give rise to the major parts of the eye (Gilbert 2003). The development of the lens begins once the optic vesicle and surface ectoderm are in close proximity. The opposing tissues thicken forming the lens placode. During this period of induction, the optic vesicle and the lens placode are held tightly together through a network of collagenous fibrils and cytoplasmic processes (Chow and Lang 2001).

Due to the close proximity of the lens ectoderm to the optic vesicle, it was believed that the optic vesicle was the lens inducer. Indeed, early experiments carried out by Spemann in 1901 seemed to show just that (Spemann 1901). The optic vesicle was removed from an amphibian, resulting in an absence of lens formation. Later experiments in other species showed contradictory results, suggesting that the optic vesicle was not the only tissue involved in lens induction.

This period of induction is the stage during development where the primitive lens structure first begins to appear. The primitive lens is composed of a spherical layer of epithelial cells surrounding a hollow interior (shown in **Figure 1.2.**). This cavity is filled by the elongation of epithelial cells located at the posterior of the lens vesicle. These cells are the primary fibre cells. The cells located at the anterior pole of the lens vesicle remain as epithelial cells, thus providing the lens with its characteristic polarity. Mitotically active cells are found around the

epithelial region just above the lens equator. These cells make up the germinative zone. Lens structure is shown in **Figure 1.3**.

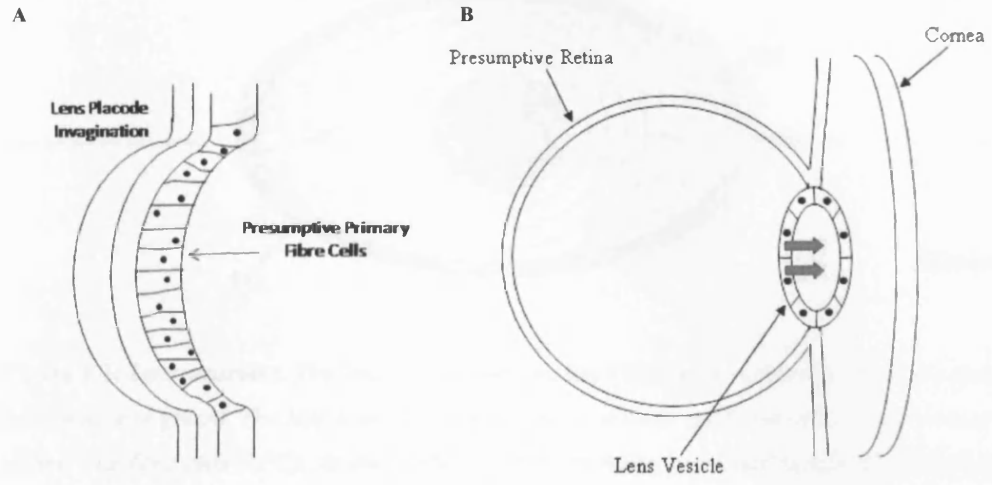

Figure 1.2: ***Overview of lens induction.*** *Induction of the lens is dependent on the close contact of the optic vesicle and surface ectoderm. The surface ectoderm thickens to form the lens placode which then invaginates forming the lens vesicle (**A**). This presumptive lens is composed of a spherical layer of cells surrounding a hollow lumen (**B**). Cells from the posterior of the lens vesicle elongate to fill the lumen forming the primary lens fibres (represented by the red arrows in the diagram). Figure adapted from Piatogorsky 1981.*

Daughter cells from this germinative zone migrate into the equatorial region of the lens where they elongate and differentiate into secondary lens fibres. New secondary lens fibres are continuously added to the fibre mass throughout life. Therefore, the lens continues to grow throughout the lifetime of the organism with new fibres successively added and retained for the entire life of the organism.

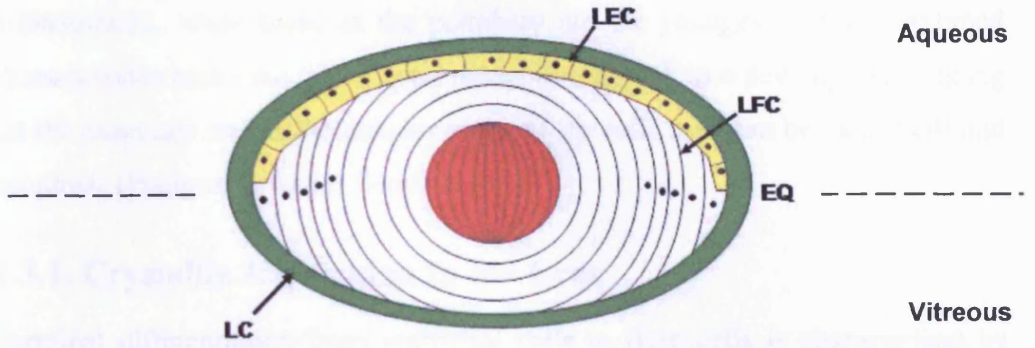

Figure 1.3: ***Lens structure.*** *The lens is contained within a basement membrane, the lens capsule (shown here in green). The lens is made up of two types of cells: epithelial cells (LEC) (shown in yellow) and fibre cells (LFC). As the epithelial cells reach the equatorial region (EQ) they begin to differentiate into secondary fibre cells. The primary fibre cells, formed during embryonic development, are shown here in red.*

Experiments carried out by Coulombre and Coulombre (1963) demonstrated that differentiation of lens epithelial cells is dependent on their location within the eye. They studied changes in the embryonic chicken lens after surgical reversal, so the lens epithelium faced the vitreous body. Just two days after the operation, all the epithelial cells were shown to be elongated. The fibres, which had differentiated previously were now located anteriorly and ceased to elongate as soon as the lens was reversed. A narrow ring of epithelium was left at the equator of the lens. The cells produced from this epithelial ring, which moved towards the neural retina, became fibre cells, whereas those that migrated towards the cornea became simple cuboidal epithelial cells. Eventually the lens reversed its organisation: producing new fibre cells posteriorly and rebuilding an epithelium anteriorly (Coulombre and Coulombre 1963). Later studies showed that the vitreous, but not the aqueous, induced the morphological changes characteristic of lens cell differentiation (Lovicu *et al.* 1995). Further details about the growth factors involved in lens differentiation are given in **Section 1.3.2**.

During differentiation, both primary and secondary fibre cells lose their nuclei and organelles. The way in which these cells differentiate leads to the formation of a concentric gradient of age and stage of differentiation. The cells at the

centremost region of the lens will be the oldest and the most highly differentiated, while those at the periphery are the youngest. These combined characteristics make the lens a good model for research into development, ageing (as the exact age and differentiation stage of the cells used can be identified) and apoptosis (Piatigorsky 1981; Wride 1996).

1.3.1. Crystallin Expression in the Lens

Terminal differentiation from epithelial cells to fibre cells is characterised by changes in protein expression. The level of crystallins is increased dramatically during this process, the synthesis of which is initiated by contact between the lens placode and the optic cup during induction. Crystallins are members of the small heat shock family of proteins and have been shown to be required for both generating and maintaining lens clarity (Harding 1991). Four distinct families of crystallins have been identified, α-, β-, γ- and δ-crystallin, (δ-crystallin is not found in mammalian lenses) which make up approximately 90% of the soluble proteins in the lens (Piatigorsky 1981).

The principle protein found in the lens is α-crystallin. Alpha-crystallin is a hetero-oligomeric complex composed of two different subunits αA- and αB-crystallin which has a known role as a molecular chaperone, preventing aggregation of proteins in the lens (Horwitz 1992). The expression of crystallins in the lens has been shown to alter during differentiation; firstly α-crystallin expression increases followed by observed increases in both β- and γ-crystallins (Peek *et al.* 1992).

Following the introduction of α-crystallins to bovine lens cultures the cells underwent morphological changes reminiscent of the changes observed during lens epithelial differentiation (Boyle and Takemoto 2000). Previously α-crystallin had been shown to bind to actin (Del Vecchio *et al.* 1984), type III intermediate filament proteins and the beaded filament proteins CP49 and CP115 (Carter *et al.* 1995). These findings along with the results of Boyle and Takemoto's study lead to the suggestion that the increase in expression of α-crystallin could play a role in the membrane cytoskeleton remodelling observed during lens epithelial cell differentiation.

A number of α-crystallin knockout mice have been generated to elucidate the physiological function of these proteins. The αA knockout mice presented with early-onset cataract (Brady *et al.* 1997) and increased cell death in lens epithelial cells (Xi *et al.* 2003). In contrast, the αB knockout lenses demonstrated hyperproliferation of the epithelial cells and an increase in genomic instability (Andley *et al.* 2001). In the lenses of the αA/αB double knockout mice lens fibre cells were observed to disintegrate following the degradation of all intracellular organelles. This disintegration of fibre cells was thought to be attributable to an increase in caspase activity; higher levels of both caspase-6 and caspase-3 were noted. An interaction between αA-crystallin and caspase-6 was observed leading to the suggestion that the α-crystallins could be suppressing caspase activity in the lens (Morozov and Wawrousek 2006). Members of the crystallin family of proteins have also been shown to interact with members of the Bcl-2 family of proteins, inhibiting their function (Mao *et al.* 2004). An anti-apoptotic role for the α-crystallins has previously been recognised; α-crystallins have been shown to protect cells from apoptosis induced by a variety of apoptotic agents (Andley *et al.* 1998; Andley *et al.* 2000).

1.3.2. Signals Involved in Lens Development

Contact between the optic vesicle and surface ectoderm is a critical period during eye development, during which inductive signals are exchanged between these two tissues. Many factors which influence lens development have now been identified (reviewed in Lang 1999). Proliferation has been shown to be restricted to the epithelial cells in the lens. However, there are areas of the epithelium in which the proliferative index varies. The epithelial cells with the highest level of proliferation are located near the ciliary body. The lowest level of proliferation is found in the centre of the epithelium (Zhou *et al.* 2006). This suggests that the factors regulating proliferation may be found in the ciliary body and the availability of these factors may be modulated by the surrounding tissues. This also suggests that regulation of these factors would be essential to maintain the rate and location of proliferation of these cells.

1.3.2.1. The Role of Pax6 in Lens Development

Pax6 is a transcription factor proven to be essential for lens formation (Grindley *et al.* 1995). It has been shown to be highly conserved across species suggesting its importance in this process (Graw 1996). Pax6 has been shown to be expressed in the lens during morphogenesis and is continually expressed in the lens epithelium. Pax6 expression was shown to be missing from lens fibre cells and overexpression of Pax6 in these cells was shown to inhibit fibre cell differentiation and maturation (Duncan *et al.* 2004). A number of other transcription factors have been observed in the lens during development, including Eya, Sox and Msx and it has been proposed that these transcription factors form a complex with Pax6, regulating eye development in both vertebrates and invertebrates (McAvoy *et al.* 1999).

1.3.2.2. FGFs in Lens Development

Fibroblast growth factors (FGFs) have been identified as potent inducers of fibre differentiation. Rat lens epithelial cells in explants containing FGF showed increased proliferation, cell migration and fibre differentiation. The inhibition of these processes by a bFGF antibody provides support for this molecule initiating all three processes (McAvoy and Chamberlain 1989). It has been observed that the response of epithelial cells to FGF is dependent on the concentration of the growth factor. As the concentration of FGF increases, the cells begin to proliferate. The concentration must then be increased further before they begin to migrate. Finally, fibre differentiation requires the highest concentration of FGF (McAvoy and Chamberlain 1989). This observation fits in with the spatial patterns of cellular behaviour observed in the lens. A concentration gradient of FGF is present in the eye; from negligible concentrations in the aqueous of the anterior chamber to concentrations in the vitreous high enough to induce fibre differentiation.

Epithelial cells in the central region of the epithelium do not undergo differentiation and are found to be non-proliferative. These cells are bathed by the aqueous. Epithelial cells at the equator and in the germinative zone still show no signs of differentiation, though they are highly proliferative. These cells are

exposed to the aqueous in the anterior chamber, so are still exposed to relatively low levels of FGF. Migration of the cells at the equator is achieved by exposure of the cells to a higher level of FGF as they are located at the junction between the aqueous and vitreous. Cells below the equator are bathed by the vitreous; therefore, they are exposed to a high enough concentration of FGF to allow them to differentiate, thereby becoming fibre cells. It has been suggested that the retina, due to its close proximity to the vitreous, may be the major source of FGF in the eye (McAvoy and Chamberlain 1989). However, the high inducing property of the vitreous may not only be due to the presence of FGF, other factors may also be present such as insulin-like growth factor (IGF-1) (Lang 1999). This observation of the vitreous inducing lens differentiation correlates with the findings from the Coulombres' experiment described previously (Coulombre and Coulombre 1963).

1.3.2.3. IGF

IGF was first implicated in lens differentiation when a factor in the chick vitreous was identified that could stimulate cell differentiation in culture (Beebe *et al.* 1980). Since then IGF-1 has been shown to have a potent differentiation effect on chick lens epithelial cells, but a minimal effect on proliferation (Hyatt and Beebe 1993). In contrast, explants of epithelial cells from the rat lens showed increased DNA synthesis but poor differentiation when exposed to IGF-1 alone (Liu *et al.* 1996). However, when the lens cells were exposed to IGF in addition to FGF, the differentiation effect of FGF was seen to be amplified (Liu *et al.* 1996) This has lead to the proposal that IGF-1 and FGF act together to regulate differentiation and proliferation in rodents, whereas IGF-1 alone stimulates cell division (Lang 1999).

1.3.2.4. BMP4

Bone morphogenetic protein 4 (BMP4) is another signalling molecule that has been implicated in embryonic tissue interactions (Trousse *et al.* 2001). It has been shown to be strongly expressed in the optic vesicle and weakly expressed in the surrounding mesenchymal tissue. It has been shown to have a crucial role in lens induction and in BMP4 homozygous null mice no lens induction occurs (Furuta and Hogan 1998). Another member of the BMP family, BMP7 has also

been shown to be essential for embryonic eye development (Furuta and Hogan 1998).

1.3.2.5. Other Factors Involved in Lens Differentiation

Other factors with a known role in lens development include members of the Wnt and TGFβ families. Several members of the Wnt family have been shown to be expressed in the lens epithelium of both rats and chicks, with expression extending into the germinative zone, their localisation suggests a role for this family in lens differentiation (Fokina and Frolova 2006; Stump *et al.* 2003).

When TGFβ receptor signalling was disrupted in lens fibre cells by the overexpression of a mutant truncated form impaired fibre maturation was observed, suggesting a role for this family in differentiation (de Iongh *et al.* 2001). However, despite the observations that these families have some influence over the differentiation of lens cells FGF still seems to be the main initiation factor of the differentiation process (Lovicu and McAvoy 2005).

1.3.3. Apoptosis in Lens Development

Mohamed and Amemiya (2003) investigated the development of the lens vesicle in rats. They suggested that the process of programmed cell death plays a fundamental role in the development of the lens vesicle. Results showed that by day 11 of gestation, apoptotic cells were present in the mesenchymal cells between the surface ectoderm and the optic vesicle, before the start of lens invagination, suggesting that these cells needed to be eliminated to provide space to enable contact between these two tissues. Apoptotic cells were also found at the junction of the surface ectoderm and lens placode as well as in the outer layer of the optic vesicle. These observations have shown that apoptosis plays a major role in lens vesicle development, from eliminating the cells between the surface ectoderm to aiding invagination of the lens and facilitating separation from the surface ectoderm (Mohamed and Amemiya 2003). In addition to these roles in development, an apoptosis-like process is thought to be responsible for the degradation of organelles in differentiating lens fibre cells.

1.4. Lens Organelle Degradation

During the terminal differentiation of lens epithelial cells to lens fibre cells a number of characteristic morphological changes are observed. The cell increases 50- to 100- times in length during differentiation. This elongation is accompanied by an increase in fibre-specific proteins including the intermediate filament proteins CP49 and CP95 (Ireland *et al.* 2000) and the crystallins (reviewed in Cvekl and Piatigorsky 1996). The process of terminal differentiation also results in the elimination of all the intracellular organelles. It has been suggested that the process of organelle elimination in lens fibre cells is analogous to programmed cell death (Bassnett 2002; Dahm 1999; Wride 2000). This process has been shown to have many similarities to apoptosis: known members of the apoptotic cascade have been shown to be active and all cytoplasmic organelles are removed as in apoptosis. However, unlike conventional apoptosis, the cells from which the organelles have been removed persist throughout life, rather than being destroyed. Other structural differences have also been observed. For example, the cytoskeleton persists in fibre cells that have completed organelle degradation whereas it is completely degraded during apoptosis (Bassnett and Beebe 1992; Dahm *et al.* 1998). Also, there is no flipping of phosphatidylserine to the outer membrane of the lens fibre cells as observed in apoptosis (Bassnett and Mataic 1997; Wride and Sanders 1998). This could suggest an underlying difference in these pathways or different regulation of the same pathway.

There are two types of lens fibre differentiation; primary and secondary. Primary fibre differentiation occurs early on during embryonic development when the cells at the posterior of the lens vesicle elongate to fill the vesicle. Secondary fibre differentiation occurs later when the epithelial cells at the lens equator differentiate and elongate. These two processes are thought to occur in different ways. In primary fibre differentiation condensation of the nucleoplasm and accumulation of dense bodies in the cytoplasm (most likely formed from chromatin) of the fibre cells has been observed (Vrensen *et al.* 1991). This is in contrast to the process of secondary fibre differentiation where the nucleoplasm is gradually degraded resulting in a density similar to that of the cytoplasm (Kuwabara and Imaizumi 1974).

Lens organelle degradation results in the formation of an organelle free zone (OFZ) in the centre of the lens. The OFZ begins to form between 17.5dpc and birth in mice (Kuwabara and Imaizumi 1974) and at around embryonic day 12 (E12) in chicks (Modak and Perdue 1970). In chick embryos, it has been observed that by E21 (hatching) the diameter of the OFZ is large enough to fill the pupil of the eye (Bassnett and Beebe 1992). This means that any existing organelles in the superficial cells are in the shadow of the iris and so are not disrupting the optical path. The degradation of cytoplasmic organelles in the lens eliminates potentially light scattering structures and is essential to the formation of an optically clear cytoplasm. Disturbances in this process have been shown to lead to congenital cataract, e.g. in Rubella syndrome (Gregg and Banatvala 2001) and disorganisation in the lens fibres (Bassnett and Mataic 1997).

Cells at the boundary of the OFZ have been studied extensively. It has been shown that, as in the case of apoptosis, mitochondrial permeability transition is an early event in lens organelle degradation. Mitochondria in cells bordering the OFZ suddenly fragment and lose their ability to retain rhodamine-123 (cationic $\Delta\psi_m$-sensitive dye) (Bassnett 1992; Bassnett and Beebe 1992). This indicates that the mitochondrial potential ($\Delta\psi_m$) is lost. There is no evidence to suggest whether the loss of mitochondrial potential occurs in all mitochondria throughout the lens or whether it occurs in a wave-like progression.

Previous studies using the chick lens have shown that the mitochondria and nucleus disappear coincidentally and abruptly (Bassnett and Beebe 1992). Experiments were also carried out to observe the fate of the Golgi apparatus and the endoplasmic reticulum. Towards the lens equator the Golgi apparatus was shown to fragment. The Golgi apparatus was only found in the superficial lens fibre cells. The endoplasmic reticulum was more abundant, extending to the edge of the OFZ where it was degraded along with the nucleus and mitochondria (Bassnett 1995). These observations suggest a wave of organelle degradation extending out from the centre of the lens. However, the actin cytoskeleton still remains after fibre cell differentiation, suggesting that this is a selective process rather than a global breakdown of the cell (Bassnett and Beebe 1992).

1.4.1. Denucleation of the Lens Fibre Cells

Lens denucleation occurs during the differentiation process of lens epithelial cells to fibre cells at the equatorial region of the lens. A similar situation has been observed in the terminal differentiation of both keratinocytes and erythrocytes (Lockshin and Zakeri 2004). Differentiation of epithelial cells to fibre cells includes a change in the morphology of the nucleus. The nuclear breakdown observed during this process has been noted to be morphologically similar to that seen in classical apoptosis (Dahm and Prescott 2002). Epithelial cells contain slightly round nuclei then, as they mature, they elongate and shrink to a more globular and highly condensed shape (Counis *et al.* 1998). A wave of nuclear degeneration spreads outwards from the centre of the lens, to the outermost fibres, which still contain intact nuclei (shown in **Figure 1.4**). This results in an increase in the size of the OFZ as development proceeds. Final DNA degradation and complete loss of the nuclei have been shown to be relatively late events in fibre cell differentiation occurring after the loss of the mitochondria, endoplasmic reticulum and the breakdown of the nuclear membrane (Bassnett and Mataic 1997). Morphological studies of lens fibre denucleation have documented the disintegration of the nuclear envelope into a chain of membrane vesicles with the nuclear contents eventually becoming indistinguishable from the cytoplasm (Kuwabara and Imaizumi 1974). Experiments have shown that DNA degradation is a gradual process with cells up to 100-200μm into the OFZ of an embryonic chick lens still containing collapsed nuclei. Small remnants of nuclear material have been observed in the centre of the chick lens (Bassnett and Mataic 1997) along with lamin B and histone proteins (Bassnett 1995).

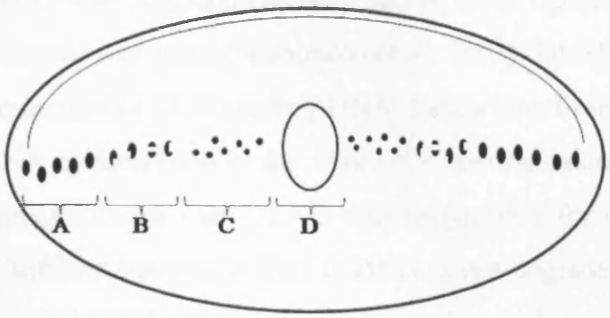

Figure 1.4: ***Nuclear degeneration of the lens.*** *A wave of denucleation in the lens is observed from the intact nuclei in the outermost fibre cells (A) to the OFZ in the centre of the lens (D).The intermediate stage of nuclear degeneration, pycknotic nuclei, are represented by B and C. Figure was adapted from the figure in Wride 2000.*

Non-random DNA degradation occurs during organelle degradation. The DNA degradation products resulting from lens fibre denucleation produce the same distinctive DNA ladder as apoptosis (Modak and Perdue 1970). It has been suggested that the cleavage of the DNA could be controlled by the protein environment. Counis et al (1998) proposed that the DNA is deprived of protective proteins during lens fibre differentiation, which would favour the action of endonucleases.

As described previously, DNA fragmentation factor (DFF) is a heterodimer made up of two subunits, DFF 40 (40kDa) and DFF 45 (45kDa). During apoptosis caspase-3 cleaves DFF 45 to release the active 40kDa subunit. In the chicken embryo lens, the active cleavage product of DFF45 is observed around E12 (Wride *et al.* 1999). This is also the stage at which organelle degradation is initiated (Modak and Perdue 1970). However, following the generation of a DFF knockout mouse with no reported ocular phenotype an absolute requirement for DFF in organelle degradation is unlikely (Zhang *et al.* 1998). Therefore, another endonuclease must be responsible for the degradation of the nucleus.

DNase II-like acid DNase (DLAD) has been shown to be uniquely expressed in the lens of both humans and mice (Nishimoto *et al.* 2003). DLAD deficient mice were shown to be incapable of degrading DNA during lens fibre differentiation; the undigested DNA accumulated in the fibre cells causing cataracts. The results from this experiment showed that DLAD was responsible for degrading DNA during lens fibre differentiation and that if DNA is not degraded then cataracts form (Nishimoto *et al.* 2003). A later study has shown that the expression of DLAD was confined to the lysosomes within the layer of cortical fibre cells immediately surrounding the OFZ; no expression was observed in the epithelial cells (Nakahara *et al.* 2007). In this study, DLAD was transiently activated during the later stages of organelle degradation with expression localised to the degenerating nuclei. The results from this study could suggest a role for DLAD and the lysosomes in this process of denucleation. To support this hypothesis microarray studies comparing gene expression of lens epithelial and fibre cells demonstrated increased expression of some lysosomal enzymes (cathepsins and lipases) in the fibre cells (Nakahara *et al.* 2007).

1.4.2. The Role of Apoptotic Proteins in the Lens

Despite the observations that complete apoptosis does not occur during terminal differentiation members of both the caspase family and the family of Bcl-2 related proteins have been shown to be present in lens fibre cells (Sanders and Parker 2002; Wride *et al.* 1999) and at least three classical caspase substrates have been shown to be cleaved at the border of the OFZ; poly (ADP-ribose) polymerase (PARP), lamin B and DFF (Bassnett and Mataic 1997; Ishizaki *et al.* 1998; Wride *et al.* 1999).

It has been noted that overexpression of Bcl-2 in both mouse and chick lenses resulted in abnormal lens fibre differentiation; the resulting lens fibre cells displaying incomplete elongation (Fromm and Overbeek 1997; Sanders and Parker 2003). Chick lenses overexpressing Bcl-2 were found to be morphologically different from the untreated controls (Sanders and Parker 2003). Fibre cells within the lenses appeared more disorganised and the lenses more spherical in shape when compared to controls. A greater number of nuclei was observed in the core region of the lenses overexpressing Bcl-2 in addition to a

reduction in the activation of caspase-9 and a failure of nuclear chromatin to condense within the lens core (Sanders and Parker 2003). Transgenic mice have also been generated which overexpress Bcl-2 in their lenses (Fromm and Overbeek 1997). In this study, the central lens fibres were shown to contain intact or fragmented nuclei. These results suggest that the overexpression of Bcl-2 interferes with the denucleation of secondary lens fibres.

The cleavage of the three known caspase substrates during lens fibre differentiation suggests a potential role for the caspases in this process. PARP, an 116kDa protein, is a known substrate for caspase-3 which, during apoptosis, cleaves PARP producing an 85kDa product (Lazebnik *et al.* 1994; Nicholson *et al.* 1995). During lens fibre differentiation, the PARP cleavage product was observed in outer lens fibre cells, but was not found in the anterior epithelium (Ishizaki *et al.* 1998). Following the addition of peptide caspase inhibitors to lens cell cultures PARP cleavage was prevented (Ishizaki *et al.* 1998; Wride *et al.* 1999). These results suggest a potential role for caspase-3, or a closely related protease, during lens fibre differentiation.

The nuclear lamina has been demonstrated to disintegrate during organelle elimination (Bassnett and Mataic 1997). Lamin B, a prominent component of the nuclear lamina, is ultimately degraded. During apoptosis, lamin B has been shown to be cleaved by caspase-3 (Slee *et al.* 2001). It has been suggested that this caspase is also active during organelle degradation causing the breakdown of lamin B. The presence of the cleavage product of DFF has also been noted during lens fibre differentiation. The role of DFF in apoptosis has been previously discussed in **Section 1.2.3**.

Further studies provided additional evidence that caspases are involved in this process. The general caspase inhibitor (Z-VAD-FMK) has been shown to abolish denucleation in rats (Ishizaki *et al.* 1998) and following the addition of peptide inhibitors of caspases-1, -2, -4, -6 and -9 to differentiating chick lens epithelial cells a 50-70% reduction in denucleation was observed (Wride *et al.* 1999). From the same study it was shown that inhibitors of caspases –3 and -8 did not have the same effect on denucleation.

However, recently the role of caspases in this process has come under scrutiny. The role of executioner caspases (caspase-3, -6 and -7) has been examined during lens differentiation (Zandy *et al.* 2005). In this study transcripts were identified for each of the executioner caspases in the fibre cells, although western blotting results detected no active forms of these caspases in the lens. Examination of lenses extracted from the mice deficient in each of the executioner caspases showed no significant difference in the size and shape of the OFZ between the knockout and the age-matched wild-type lenses, suggesting that the executioner caspases are not essential for lens organelle degradation.

TNFα has also been implicated in the process of denucleation (Wride and Sanders 1998). Wride and Sanders showed that the addition of TNFα to chick lens epithelial cell cultures increased the number of nuclei positively staining with TUNEL i.e. degenerating nuclei. TNFα was identified at embryonic day 8 (E8), the day at which nuclear degeneration in the embryonic chick lens begins (Modak and Perdue 1970), suggesting a role for this molecule in the denucleation process.

A recent study was completed to examine the role of the actin cytoskeleton in lens differentiation. The results of this study showed that the predominant actin filament structure of undifferentiated lens epithelial cells was stress fibres which, during differentiation, were disassembled and replaced with cortical filaments. Disassembly of actin stress fibres by cytochalasin D was shown to be sufficient to induce lens cell differentiation (Weber and Menko 2006). This disassembly of actin stress fibres was demonstrated to have an effect on members of the apoptotic pathway; disassembly of stress fibres was observed coincidently with the activation of caspase-3 and this depolymerisation of actin filaments was shown to inhibit Bcl-2 expression.

A suggested alternative to the classical apoptosis pathway in this terminal differentiation process is the ubiquitin/proteasome pathway (UPP). The UPP is used to selectively degrade proteins. It is a two-step process; the attachment of ubiquitin to the protein to signal degradation and the subsequent degradation of protein by the 26S proteasome (reviewed in Varshavsky 2005). Both lens

epithelial cells and fibre cells have been shown to contain a fully functioning ubiquitin pathway (Pereira *et al.* 2003; Shang *et al.* 1997) and components of the UPP have been shown to be upregulated during fibre differentiation (Shang *et al.* 1999; reviewed in Wride *et al.* 2006). Immunohistochemical studies examining the expression of UPP components in the lens demonstrated that the staining became progressively weaker moving towards the centre of the lens, where differentiation is already complete (Girao *et al.* 2005). The results of this study showed redistribution of UPP components during differentiation; demonstrated localisation of the UPP components in both the nuclei and cytoplasm in epithelial cells, whereas staining was only observed in the nuclei of fibre cells. This redistribution of the UPP proteins during lens differentiation supports the hypothesis that this pathway is involved in this process. Additional evidence that this pathway is involved in the process of lens differentiation comes from a later study which demonstrated that following the treatment of lens epithelial explants with a proteasome inhibitor FGF-induced proliferation and differentiation was delayed (Guo *et al.* 2006).

The onset of organelle degradation has been shown to correlate with a 6-fold increase in VEIDase activity (Foley *et al.* 2004). This increase in VEIDase activity is the only known proteolytic activity shown to increase with the onset of organelle degradation. VEID is an abbreviation for the amino acid sequence representing valine, glutamic acid, isoleucine and aspartic acid. The ability to cleave a VEID substrate is normally attributable to endogenous caspase-6 activity (Thornberry *et al.* 1997). However, following the results of the study completed by Zandy and Bassnett, the executioner caspases were shown not to be required for this process, with no observed morphological changes in the lenses of the knockout mice (Zandy *et al.* 2005). A later study was completed to identify the protease(s) responsible for this VEIDase activity. The resulting data showed that the VEIDase had a molecular weight of approximately 700kDa and following the addition of proteasome inhibition the degradation of succinate-ubiquione oxidoreductase (an integral mitochondrial membrane protein) was prevented. It was suggested, following these results, that the observed proteolytic activity was due to the proteasome (Zandy and Bassnett 2007).

Other alternatives to the apoptosis pathway in the process of organelle degradation include 15-lipoxygenase (15-LOX). This protein has previously been shown to be expressed in reticulocytes, a precursor of erythrocytes, with expression peaking immediately before organelle degradation. Lipoxygenase expression has been demonstrated in the lens and was shown to be limited to the area in which organelle degradation occurs (van Leyen *et al.* 1998). A decrease in endoplasmic reticulum staining was co-localised with an increase in lipoxygenase staining suggesting that 15-LOX initiates pore formation in organelle membranes allowing subsequent degradation by another pathway possibly the ubiquitin/proteasome pathway. A subsequent study showed that the inhibition of 15-LOX leads to the retardation of mitochondrial degradation during terminal differentiation of reticulocytes but does not prevent degradation entirely (Grullich *et al.* 2001).

1.4.3. Triggers of Organelle Degradation

In chicken embryos, the OFZ forms at around E12. At first, only the primary lens fibres are included within the OFZ, but it gradually increases in size such that it includes an increasing number of secondary fibre cells (reviewed in Bassnett 2002). Suggestions for triggers of organelle degradation include a drop in the cytoplasmic pH, a gradient of diffusion of a metabolic substance or an accumulation of waste products in the centre of the lens (Wride 2000). The concentration of oxygen has also been proposed as a trigger for this process (Bassnett and McNulty 2003). The oxygen concentration would be at the lowest level in the lens core. If the concentration in the lens core reaches a sufficiently low level, mitochondrial integrity would be compromised leading to the release of Ca^{+} which could result in the activation of an apoptotic cascade. Hypoxia is known to trigger apoptosis and it has been hypothesised that it could also trigger organelle degradation in the lens. It has been suggested that as fibre cells become buried by newer fibre cells they are subjected to increasing hypoxia. Recently, experiments have been carried out on chicken eggs under hyperoxic (50% O_2) and normoxic (21% O_2) conditions to test this hypothesis (Bassnett and McNulty 2003). The lens fibres in hyperoxic conditions should be exposed to higher oxygen concentrations and therefore organelle loss should be prevented to a degree. Results showed that in hyperoxic lenses, organelle loss was triggered at a

greater depth in the lens than in those lenses under normoxic conditions, (100μm deeper than normoxic lenses). This suggests that the critical level of oxygen concentration for organelle degradation is found deeper in hyperoxic lenses than in normoxic lenses (Bassnett and McNulty 2003).

1.4.4. RNA Stability in Differentiating Lens Fibre Cells

Transcription has been observed in fibre cells until the onset of nuclear condensation and their inclusion into the OFZ (Shestopalov and Bassnett 1999). However, in principle, translation could still occur in anucleated cells if the appropriate translational proteins and mRNA were present. Many studies have been carried out to try to identify when translation ceases.

1.4.4.1. Transcription in Anucleated Fibre Cells

Faulkner-Jones et al have identified a RNA-depleted zone (RDZ) in the lenses of chick embryos. Acridine orange was used to label the RNA. Intense fluorescence was observed in the lens epithelium and the outer fibres, but decreased towards the centre of the lens, an area the authors termed the RDZ. The RDZ was first visible at E13 and expanded in size after that time (Faulkner-Jones *et al.* 2003). By E19, central fibre cells were seen to lack nuclei and the RDZ was well defined. RNA concentration was seen to decrease sharply at the border of the RDZ suggesting the RNA is quickly degraded in this area of the lens.

1.4.4.2. Translation in Anucleated Fibre Cells

Experiments have been carried out to elucidate the ability of fibre cells to transcribe and translate microinjected templates (Shestopalov and Bassnett 1999). An absence of protein synthesis in the core of the lens was identified, suggesting that the cessation of translation also occurs at the time of organelle loss. This leads to the hypothesis that the protein contained within the centre of the lens had been present since foetal development (Ozaki *et al.* 1985; Shestopalov and Bassnett 1999). It is likely, therefore, that protein synthesis does not persist in the lens core for an extended period after denucleation and that the processes of both transcription and translation cease at the time of organelle degradation.

1.5. The Ageing Lens and Cataract

As described previously, the lens is constantly growing and changing shape due to the continuous addition of fibre cells, covering the underlying fibre cells. There is no protein turnover in the lens, leaving the lens susceptible to age-related changes. Cataract occurs when opacities form in the normally transparent lens. These opacities can be congenital or can form after exposure to toxic insults e.g. UV radiation. Cataract is a major ocular condition and is the commonest cause of blindness worldwide (Congdon 2001; Francis *et al.* 2000; Francis *et al.* 1999). There are a number of different types of cataract; nuclear, where the cataract forms in the lens nucleus, cortical where the cataract forms in the cortex of the lens and subcapsular where the opacities form under the lens capsule. Apart from opacification of the lens (cataract) other diseases of the lens are relatively uncommon (Graw 1999).

1.5.1. Congenital Cataracts

Congenital cataracts are rare in developed countries with an observed frequency of 30 cases among 100,000 births (Graw 2004). Many of the genetic causes of cataract are due to mutations affecting the structure and/or transparency of the lens. Mutations of genes required early in development can affect the formation of the lens vesicle. For example a mutation in the promoter for Pitx3, a transcription factor downstream of Pax6, leads to a decrease of Pitx3 expression resulting in the formation of small eyes which lack a lens (Semina *et al.* 2000). The role of Pax6 has already been described in **Section 1.3.2.1**, and mutations in this gene have been shown to lead to the lack of lens induction (Grindley *et al.* 1995). Mutations in the other transcription factors important for lens development, Maf, Sox, Fox and Eya, have also been shown to result in cataract (reviewed in Graw 2004).

Following the formation of the lens vesicle, cataracts can also be caused by mutations in proteins affecting the lens cell membranes; these include mutations in aquaporin0, important in forming the specialised junctions between fibre cells, and the connexins (reviewed in Graw and Loster 2003). The connexins are a well-characterised family of proteins shown to play a structural role in the lens as

functional building blocks of the gap junction channels. In the eye three connexins been shown to play major role in development Cx_{43}, Cx_{46} and Cx_{50} (Gong *et al.* 2007). Knockouts of both Cx_{46} and Cx_{50} have been shown to result in nuclear cataracts (Gong *et al.* 1997; White *et al.* 1998).

Observed mutations in the crystallin genes have been shown to result in the formation of cataracts. The αA-crystallin and αB-crystallin knockouts have already been described in **Section 1.3.1**. From the knockout mouse studies, it has been demonstrated that the knockout of αA-crystallin, and not that of αB-crystallin, resulted in the formation of cataract. However, point mutations in both the *Cryaa* and *Cryab* genes have been shown to cause dominant congenital cataract (reviewed in Graw and Loster 2003). Mutations in β- and γ-crystallin genes have also been shown to result in the formation of cataracts (Billingsley *et al.* 2006; Cohen *et al.* 2007; Pauli *et al.* 2007; Talla *et al.* 2006; Wang *et al.* 2007).

External factors can also lead to congenital cataract. Cases of maternal rubella have been shown to cause congential cataract. The cataract was normally present at birth, usually bilateral and was observed to fill the pupillary area (Gregg and Banatvala 2001). All of these data lead to the suggestion that dysregulation of any element essential for the maintenance of lens transparency could result in opacification.

1.5.2. Age-Related Cataract

The lens contains only a single epithelial layer on the anterior surface, which is essential for the maintenance of its metabolic homeostasis and transparency. The epithelial cells have a relatively long life span under normal conditions, although their viability is threatened when exposed to oxidative stress, UV radiation or other toxic agents (Robman and Taylor 2005).

Exposure to UV radiation has been shown to cause cataractogenesis. A study was completed by Li and Spector (1996) who tried to understand the progression of cataract after exposure to UVB radiation. Cultured rat lens epithelial cells were exposed to UVB radiation for 60 minutes and the extent of apoptosis was monitored by TUNEL labelling and DNA fragmentation assays. As shown in previous studies with hydrogen peroxide, (Li *et al.* 1995), opacification of the lens appeared to follow death of the epithelial cells suggesting that apoptotic death induced by UVB initiates cataract development (Li and Spector 1996).

A study by Pendergrass *et al.* showed that in cataractous old mouse lenses DNA and mitochondria were not degraded properly; fibre cells were noted to contain accumulations of DNA, nuclear fragments and aggregated mitochondria (Pendergrass *et al.* 2005). These inclusions were shown to colocalise with the subcapsular and cortical cataracts and resulted from the failure of the fibre cells in the bow region to undergo terminal differentiation.

1.5.3. Treatment for Cataract

Insights into the pathways that lead to the formation of cataract could lead to the development of novel treatments e.g. to delay the onset/ progression of cataract. At present the only available treatment for cataracts is surgery (Francis *et al.* 2000). During surgery, an opening is created in a portion of the anterior capsule, through which the cataractous lens is removed. An artificial intraocular lens (IOL) is then inserted into the remaining capsular bag.

1.5.4. Posterior Capsule Opacification

Although cataract surgery is usually very successful, a number of patients suffer from posterior capsule opacification (PCO). PCO is the commonest complication following cataract surgery and requires further treatment if it affects the visual axis (Marcantonio and Vrensen 1999; Spalton 1999). This condition is caused by the continued growth and differentiation of the residual LECs remaining in the capsular bag following surgery. These cells proliferate soon after surgery to form monolayers on the capsular surfaces. These monolayers can remain throughout life without any visual consequences. However, if the cells continue to differentiate, undertaking an epithelial-mesenchymal transition, larger structures

appear which are capable of scattering light, therefore reducing lens transparency (Marcantonio and Vrensen 1999). The epithelial-mesenchymal transition is driven by cytokines and leads to the expression of extracellular matrix proteins not normally found in the lens. PCO can be treated by Neodynium:Yttrium Aluminium Garnet (Nd:YAG) laser treatment.

Alternative treatments for PCO are being sought as treatment using the Nd:YAG laser is not completely risk free and a number of problems can result including retinal detachment and damage to the lens capsule (Pandey *et al.* 2004). Recently a study was completed using an adenovirus-mediated gene transfer to introduce the expression of proapoptotic molecules (P53, procaspase-3, Bax and TRAIL) into cultured lens cells in an attempt to induce programmed cell death. Injection of Bax or procaspase-3, but not P53 or TRAIL, into lens capsular bag following phacoemulisification prevented PCO in rabbits (Malecaze *et al.* 2005).

1.6. Aims of this Study

Although this process of organelle degradation may not be a direct form of conventional apoptosis, a number of apoptosis-related genes have been shown to be present in the lens (Wride *et al.* 2003; Wride *et al.* 1999) and further investigation is required to clarify the role of these apoptotic pathways in the process of denucleation and organelle degradation.

The studies described in this thesis have been designed to test the hypothesis that an apoptosis gene-specific macroarray is a useful tool for identifying apoptosis genes in the lens during development, therefore implicating them in the process of lens differentiation and identifying pathways of apoptosis gene expression involved in this process.

The aims of this study are:

- To examine the global apoptosis gene expression during mouse lens development using macroarrays. Once this has been completed the protein expression will be studied for selected proteins across the same developmental stages.
- To investigate the morphological changes of the lens in a transgenic mouse generated to contain a mutant copy of one of the genes identified from the array results.
- Finally, to complete a cross-species comparison identifying whether the genes identified in the mouse lens are also shown to be expressed in the embryonic chick lens.

Chapter 2: General Methods

2. Materials and Equipment

The composition of all chemicals and solutions prepared for this study is listed in **Appendix 1**. All other chemicals bought from the manufacturers are included in the text along with the supplier.

All protocols using RNA were carried out using RNase free filter tips and double autoclaved distilled water to prevent contamination of the samples. Solutions used for RNA work were made in autoclaved bottles and double autoclaved.

Due to the nature of the chemicals used, during the formaldehyde denaturing gels, the gels were set and run in the fume hood (Bigneat, Chemcap™ Laboratory Safety Cabinet).

The radioactive parts of these methods were carried out in a designated lab. Constant monitoring was carried out using a Geiger-Müller counter. Personal monitoring was also in place. Disposal of radioactive materials was carried out in accordance with the university guidelines.

2.1. Tissue Collection

2.1.1. Collection of Mouse Tissue

The mice used in this study were from the strain 129Sv/Ev. Lenses were extracted from mice at different stages of maturation. The stages used were new born (NB), postnatal day 7 (P7), postnatal day 14 (P14) and 4 weeks (4wk). The mice were sacrificed by a schedule 1 method (cervical dislocation) and enucleated. The lenses were then removed from a posterior incision in the eyeballs under a research stereo microscope (Nikon SMZ800) using No. 5 forceps (Sigma, UK).

Lenses were extracted from a litter of mice (average number = 7, range = 5-10) at each time point and then pooled to generate each sample of RNA. A different litter was used for each pooled lens RNA sample collected, this accounted for biological variation.

2.1.2. Collection of Chick Tissue

Lenses were also collected from White Leghorn chick embryos (Henry Stewart and Co, Lincolnshire, UK). Eggs were placed in an incubator at 37.5°C (40-50% humidity, turning every 45 minutes) until they reached the required time points (Brinsea Octagon 100, Jencons, UK). The embryos were placed in a fridge to cool down, then decapitated using a fresh scalpel blade before the lenses were removed using tungsten needles under a dissecting microscope (Nikon SMZ800). Lenses were collected from both eyes of embryos at embryonic days (E) 6, 8, 10, 12, 14 and 16. Lenses were pooled from a number of embryos to generate each RNA sample (ranging from 24 for an E6 sample to 16 for an E16 sample).

2.1.3. Obtaining RNA

Once collected, the lenses were immediately homogenised in TRIzol® reagent (Invitrogen, UK) using a tissue grinder (Wheaton). RNA was then isolated from these lenses using the protocol provided by Invitrogen, briefly described here. Chloroform (0.2ml per 1ml of TRIzol® originally used) was added to the sample before centrifugation (12,000 x g for 15 minutes at 4°C) in an eppendorf bench-

top centrifuge (Sorvall® fresco). After centrifugation, the mixture was separated into three phases; a lower pink phenol-chloroform phase, an interphase, and a colourless upper aqueous phase. RNA from the sample remained in the colourless aqueous phase. The aqueous phase was removed and placed in a new eppendorf tube before isopropyl alcohol (0.5ml per 1ml of TRIzol® originally used) was added. The samples were placed into isopropyl alcohol in the freezer at -20°C overnight to precipitate the RNA from the sample collected. The sample was then removed from the freezer and centrifuged again (12,000 x g for 10 minutes at 4°C). The RNA precipitate formed a white pellet on the bottom of the tube. This pellet was then washed by the addition of 75% RNase free ethanol (1ml per 1ml of TRIzol® originally used). After addition of ethanol, the sample was then mixed and centrifuged, (7,500 x g for 5 minutes at 4°C). The pellet that formed on the bottom of the tube was then allowed to air dry for 5-10 minutes. Finally, the pellet was resuspended in RNase free water (Sigma, UK) (10-60µl) by pipetting it up and down before being incubated at 60°C for 10 minutes.

2.1.4. Quantification of RNA Samples

The RNA samples collected were quantified using a spectrophotometer (GeneQuant II, Pharmacia Biotech). Nuclease-free water (Sigma, UK) was used as a reference sample. RNA (2µl) was added to water (98µl) before the absorbance was read at 260nm. An absorbance value was also taken at 280nm and a ratio calculated. The RNA concentration was then calculated by multiplying the absorbance at 260nm by the dilution factor and then by 40 (the RNA constant).

2.1.5. Checking Integrity of RNA

Following isolation from the lenses, the RNA was run out on a formaldehyde denaturing gel to check its integrity. Intact RNA should show two distinct bands corresponding to the 28S and 18S ribosomal species. If there was any smearing on the gel, it would suggest that the RNA had been degraded.

One hundred millilitres of gel solution was made (composition of the gel is given in **Appendix 1**), poured into the gel mould and left to set for 1-2 hours in the fume cupboard. The denaturation reaction for each sample of RNA was then set

up in an eppendorf tube (components for one reaction are given overleaf in **Table 2.1**).

Component	Volume
RNA	4.0µl
10x MOPS electrophoresis buffer	2.0µl
Formaldehyde	3.5µl
Formamide	10.0µl
Ethidium bromide	0.5µl

Table 2.1: ***Components of RNA denaturation reaction***

Once all the components of the denaturation reaction had been added, the eppendorf tubes were incubated for 15 minutes at 55°C in a water bath (Grant, JB Series). The samples were then chilled on ice for a minute. Sufficient running buffer (composition given in **Appendix 1**) was then added to the gel dock tray to cover the gel to a depth of approximately 1mm. Loading buffer (composition given in **Appendix 1**) was then added (5µl) to each sample prior to loading onto the gel. To begin with, the gel was run at 40V (Consort E122 Power Pack). This was increased to 80V when the samples or loading dye could be visualised on the gel.

The RNA bands were visualised by placing the gel on a UV transilluminator and photographed under UV illumination using a Gel Doc system and digital camera (UVP BioDoc-It™ System).

2.2. Apoptosis Arrays

2.2.1. Generating Labelled cDNA

After the integrity of the RNA had been confirmed, the RNA could then be used to generate radiolabelled cDNA, incorporating ^{33}P-dCTP (Amersham Biosciences, UK). The labelling reactions are performed in two steps. The first step, the annealing reaction, shown in **Table 2.2**, involves the annealing of mouse apoptosis cDNA primers (Sigma-Genosys, UK) to the RNA template. The mouse apoptosis primers used contained 250 apoptosis-gene-specific primers optimised for generating cDNA from total RNA extracted from mice. During the second step, radiolabelled nucleotides and reverse transcriptase (Sigma-Genosys, UK) were added to initiate the cDNA synthesis reaction.

Final Concentration	Volume for One Reaction
2µg total RNA	2-11µl
Mouse Apoptosis cDNA Labelling Primers	4µl
Sterile distilled water to	15µl

Table 2.2: ***Composition of the Annealing Reaction.*** *Table taken from Panorama™ Mouse Apoptosis Gene Arrays Protocol provided by Sigma-Genosys.*

For the annealing step, the components from the table above were added to an eppendorf tube. The primers were annealed to the RNA template by heating at 90°C for 2 minutes and then transferring to a heating block set at 42°C for 20 minutes.

The components of the annealing reaction were added to the components of the reverse transcriptase reaction, (shown in **Table 2.3**), mixed and then incubated at 42°C for 2-3 hours on a heating block (Grant, QBT2).

Final Concentration	Stock Reagent	Volume for One Reaction
Components from table 2.1		15 µl
1x Reverse Transcriptase Buffer	5x	6 µl
333µM dATP	10 mM	1 µl
333µM dGTP	10 mM	1 µl
333µM dTTP	10 mM	1 µl
1.67µM dCTP	100 µM	0.5 µl
20µCi [α-^{33}P] dCTP	10 µCi/µl	3 µl
20 U Ribonuclease Inhibitor	40 U/µl	0.5 µl
50 U AMV Reverse Transcriptase	25 u/µl	2 µl
Sterile distilled water to a final volume of		30 µl

Table 2.3: ***Composition of the Reverse Transcriptase Reaction.*** *Table adapted from Panorama™ Mouse Apoptosis Gene Arrays Protocol provided by Sigma-Genosys.*

2.2.2. Pre-Hybridisation of the Arrays

Panorama™ mouse apoptosis arrays (Sigma-Genosys, UK) were used for this set of experiments. These arrays are nylon membranes containing 243 known apoptosis related genes. The complete list of genes present on the array is given in **Appendix 2**. Before the arrays were hybridised with the radiolabelled cDNA they were first pre-hybridised to prevent non-specific binding of DNA to the arrays. The arrays were washed in 50ml 2x SSPE (containing NaCl and EDTA, pH 7.4, Sigma, UK) at room temperature for 5 minutes. The arrays were then pre-hybridised in hybridisation solution (Sigma, UK) containing salmon testes DNA (100µl Salmon testes DNA in 10ml hybridisation solution) at 65°C for at least an hour before the addition of the radiolabelled cDNA.

2.2.3. Removal of Unincorporated Radiolabelled Nucleotides

The unincorporated radiolabelled nucleotides had to be removed from the reaction mix before it was added to the arrays. This should result in a reduction in the background signal during the hybridisation reaction. To remove the unincorporated radiolabelled nucleotides a spin column containing sephadex beads (Sigma-Genosys, UK) was used. The spin column was centrifuged to remove any excess buffer before the sample was added. Once the sample had been added to the centre of the spin column, the column was centrifuged at 1100

x g for 4 minutes. The eluate from the column contained the purified cDNA sample; this sample could then be added to the arrays.

2.2.4. Hybridisation of the Arrays

The purified labelled cDNA was then added to 2-3mls hybridisation solution (containing 100µl salmon testes DNA per 10ml hybridisation solution). The DNA was then denatured by heating at 95°C for 10 minutes. The hybridisation solution containing the labelled cDNA was then added to the arrays, which were hybridised overnight for 18 hours in the hybridisation oven at 65°C (UVP, HC-3000 Hybricycler).

2.2.5. Washing the Arrays

After the hybridisation reaction was complete, the arrays were then washed to remove any unbound DNA with increasing concentrations of salt solution. The hybridisation solution was decanted and discarded and 40-50ml of wash solution I (composition in **Appendix 1**) was added to the roller bottles. The arrays were washed by gently inverting the bottles by hand at room temperature for 2-3 minutes. This process was repeated twice more, with a new aliquot of wash solution I each time. 80-100ml of wash solution I (pre-warmed to 65°C) was then added to the roller bottles and the arrays were washed in the hybridisation oven at 65°C for 20 minutes, before the wash solution was discarded. This process was repeated once more. Wash solution II (pre-warmed to 65°C: composition given in **Appendix 1**) was then added to the roller bottles (80-100ml) and washed for a further 20 minutes in the hybridisation oven. The wash solution was then discarded and the arrays were wrapped in clingfilm before placing them into a storage phosphor screen (Amersham Biosciences, UK). The arrays were exposed to the phosphor screen for 5-7days.

2.2.6. Scanning the Arrays

The phosphor screen was then scanned using the Typhoon scanner (Amersham Biosciences, Typhoon 9410 Variable Mode Imager) which extracted the energy from the screen and converted it into a computer image which could later be analysed by use of image analysis software.

2.2.7. Stripping the Arrays

Once the phosphor screen had been scanned, the arrays were stripped removing any residual bound DNA. This ensured that each array could be reused. The arrays were added to 200ml of stripping solution (composition given in **Appendix 1**), which had been brought to the boil. The arrays were then added to the stripping solution, which was then allowed to cool. The arrays were then removed from the solution, the excess drained and the arrays wrapped in clingfilm. Once stripped, the arrays were stored at -20°C. Some stripped arrays were exposed to the phosphor screen to check that the residual radiolabelled cDNA had been removed.

2.2.8. Analysing the Results

The results were analysed using an image analysis program, ImaGene 5 (Biodiscovery). Using ImaGene, a virtual grid was placed over the image of the arrays assigning each spot a know grid reference; this allowed for the intensity of each spot to be calculated and also allowed the correct gene ID to be allocated to each spot (see **Figure 3.2.**). Once ImaGene had calculated the spot intensities, the data were then exported to Microsoft® Excel for further analysis. The data obtained from ImaGene produces a spot intensity and a background signal value for each individual spot. The background value for each spot was calculated as a mean of the intensity of a set number of pixels surrounding the spot (as shown in **Figure 2.1.**).

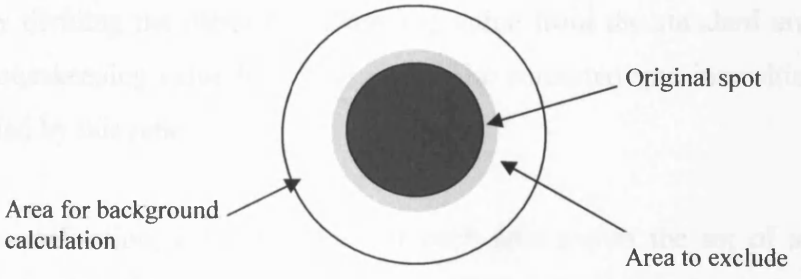

Figure 2.1: ***Diagram demonstrating how spot intensity was measured.*** *Diagram shows the area used to measure the spot intensity. An excluded area was included around the original spot to prevent false background values due to contamination from the original spot (approximately 10 pixels wide).*

The data produced were normalised using the mean expression of the housekeeping genes from the arrays; housekeeping genes are genes continuously expressed throughout development. The normalisation process allowed comparisons of gene expression to be made between the completed arrays; accounting for variations of the signal between arrays.

2.2.8.1. Normalisation with Housekeeping Genes

The mean and standard deviation were calculated using the individual background values for each spot; these values were subsequently used to filter the data later on in the analysis process. The spots whose original signal (signal value generated from the analysis completed using ImaGene) was lower than the mean plus two standard deviations of the background values were removed from the rest of the results following normalisation.

The individual background values were then subtracted from the corresponding spot intensity, to give a corrected intensity. Each corrected spot value was normalised before being filtered. The spots were normalised using the housekeeping genes printed on the apoptosis arrays. A mean value was calculated from the corrected spot intensities from each of these housekeeping genes as well as GAPDH (a standard housekeeping gene), which was also printed on the array. The array data were then normalised using the ratios of these mean values.

One of the arrays was designated as standard. A ratio was calculated for each array by dividing the mean housekeeping value from the standard array by the mean housekeeping value from that array. The corrected spot intensities were all multiplied by this ratio.

After normalisation, a mean value for each spot across the set of arrays was calculated using the corrected intensities. The mean values for each spot were then compared for P7 and P14 using an unpaired t-test. Spots with a 2-fold difference between these two time points and a p-value <0.05 were considered to have a significant change in gene expression.

2.2.8.2. Global Normalisation

The mean corrected gene intensity (corrected intensity = original spot intensity minus background value) was calculated for each spot on each array; housekeeping genes, negative controls and positive controls were excluded from the data set. One of the arrays was designated as the standard. For the other arrays a normalisation ratio was calculated by dividing the mean spot intensity for the standard array by the mean intensity calculated for each array. All the corrected spot intensities were then multiplied by the ratio for each array. This allowed the spot intensities to be compared across arrays.

Following normalisation, a mean value was calculated for each gene across the arrays at each time point. The mean values were compared between P7 and P14 using an unpaired t-test. Genes were considered to be significantly differentially regulated if they showed a 2-fold or greater difference between values and a *p*-value of less than 0.05.

2.3. PCR Confirmations

2.3.1. DNase Digestions

Before cDNA synthesis, the RNA samples were first treated with the addition of a DNase to remove any contaminating genomic DNA. DNase digestion was completed using Ambion's TURBO DNase protocol, briefly described here. 10 x DNase I buffer ($^1/_{10}$ of the volume of the original sample) and 1µl of DNase I (Ambion, UK) was added to each RNA sample. This mixture was then gently mixed and incubated at 37°C for 30 minutes. DNase inactivating reagent (typically 2µl or $^1/_{10}$ volume of the sample, whichever was greatest) was then added to the samples and the samples left at room temperature for 2 minutes, mixing occasionally. The samples were then centrifuged at 10,000 x g for 1 minute. The supernatant (containing the DNase digested RNA sample) was then removed from the pellet of the DNase inactivation reagent and transferred to a new eppendorf tube. Samples with a concentration of 200µg/ml or above had to be diluted (to approximately 10µg/50µl) before addition of the DNase.

2.3.2. Reverse Transcriptase Reaction

This DNase digested RNA was then used to generate cDNA. Synthesis of cDNA was completed in accordance with the protocol provided by Invitrogen in the Superscript™ First-Strand Synthesis System for RT-PCR kit. The sample (5µl) was added to 1µl of oligo(dt) primers (Invitrogen, UK) and 1µl of 10mM dNTP mix (Invitrogen, UK). Double autoclaved water was then added to bring the volume of the sample up to 12µl. These reactions were set up in duplicate; one was used to synthesise the cDNA, the other was used as a control to which no reverse transcriptase would be added. The mixtures were then heated to 65°C for 5 minutes before being chilled on ice. The tubes containing these mixtures were then briefly centrifuged before 2µl of 10 x RT buffer, 4µl of 25mM $MgCl_2$, 2µl of 0.1M DTT and 1µl of RNaseOUT™ were added, before incubation at 42°C for 2 minutes. Following this incubation, 1µl Superscript™ II RT (Invitrogen, UK) was added (except to the no RT controls). The tubes were then incubated for 50 minutes at 42°C. The reaction was inactivated by heating the tubes at 70°C for 15 minutes. RNase H (1µl) was added to each tube and the samples were

incubated at 37°C for 20 minutes. Finally, samples were diluted by the addition of 30µl nuclease free water.

2.3.3. Primer Design

Mouse primers were designed for the genes shown to be differentially expressed from the array results using the primer design programme Primer3 (http://frodo.wi.mit.edu/cgi-bin/primer3/primer3_www.cgi) using the FASTA sequence of the gene. The sequence for the gene in question was looked up on Gene (provided by NCBI). The first primer pair suggested by Primer3 was used. Primers for the housekeeping genes were taken from published work; mouse housekeeping gene (GAPDH) used for the PCR confirmations was taken from Mansergh *et al.* (2004). Primers were ordered from Operon and were resuspended in nuclease free water (Sigma, UK) in the amounts specified.

Chick primers were designed for the genes shown to be highly expressed and differentially expressed. The sequence for most of the genes was available on Gene; the FASTA sequence was used to design primers using Primer3 (as described above). However, some of the sequences were not available on Gene and so BLAST searches had to be completed to try to identify the chick homologue of the gene. The accession number for the mouse sequence was compared to the chick genome. Sequences with an identity of 70% or greater were used to design primers. The primer sequences for the housekeeping gene used, GAPDH, was taken from Faulkner-Jones *et al. 2003*. Both the mouse and chick primer sequences used are shown in **Appendix 4.**

2.3.4. PCR Reactions

Primers were run out on a gel prior to the PCR reactions to ensure that they were all at similar concentrations. Promega's GoTaq® protocol was used to complete the PCR reactions. The components of the PCR reaction (shown in **Table 2.4**) were added to a sterile microcentrifuge tube on ice. The PCR reaction mix was overlaid by 50µl mineral oil (Sigma, UK) to prevent evaporation before the microcentrifuge tubes were placed into the PCR machine (Techne Flexigene). PCR was completed using the parameters shown in **Table 2.5**. Equal loading of cDNA was monitored using the products of the GAPDH PCR reaction and

subsequent image analysis. Adjustments were made to the amount of cDNA used in the PCR reactions until the resulting bands from the GAPDH PCR reaction were shown to be the same intensity.

Component	Final Volume	Final Concentration
5x Green GoTaq Flexi Buffer	10µl	1x
$MgCl_2$ Solution, 25mM	3µl	1.5mM
PCR Nucleotide Mix, 10mM	1µl	0.2mM each dNTP
Forward Primer	Xµl	0.1-1.0µM
Reverse Primer	Yµl	0.1-1.0µM
GoTaq DNA polymerase (5u/µl)	0.25µl	1.25u
Template DNA	Zµl	<0.5µg/50µl
Nuclease-Free water to	50µl	-

Table 2.4: ***Components of PCR Reaction***

The PCR products were then loaded onto a 2% agarose gel alongside a 1Kb DNA ladder (Invitrogen, UK). The products were visualised due to the addition of ethidium bromide (Sigma, UK) to the agarose gel. The resulting gels were visualised by placing the gel on a UV transilluminator and photographed under UV illumination using a Gel Doc system and digital camera (UVP BioDoc-It™ System). Three PCR reactions for each gene were completed; using a different pooled RNA sample for each repetition.

Step	Temperature	Time	Number of Cycles
Initial Denaturation	95°C	2 minutes	1
Denaturation	95°C	1 minute	25-35
Annealing	42-65°C	1 minute	
Extension	72°C	1 minute 20 seconds	
Final Extension	72°C	5 minutes	1
Soak	4°C	Indefinate	1

Table 2.5: ***PCR Parameters***

2.3.5. PCR Image Analysis

The images of the gels were imported into Scion Image for analysis. This programme allowed for the band intensities to be calculated (measured as mean pixel intensity). A background reading was measured, which was later subtracted from the band intensities measured for the bands of the gel. These measurements from Scion Image were then imported into Microsoft® Excel. Data were collected from all the repetitions of PCR reactions in Excel and normalised using the band intensities from the GAPDH bands from the first set of reactions. A mean normalised value of band intensity along with the standard error of the mean (SEM) was calculated for each gene at each time point.

The mean normalised band intensity value was compared across the time points to identify any statistically significant changes in expression using a one-way ANOVA with Tukey's post-hoc test. Statistical significance was only observed if the resulting p-value was less than 0.05.

2.4. Western Blotting

2.4.1. Isolation of Protein

Protein was isolated from postnatal mouse lenses using RadioImmunoPrecipitation Assay (RIPA) buffer (0.5M Tris-HCl pH 7.4, 1.5M NaCl, 2.5% deoxycholic acid, 10% NP-40, 10mM EDTA, Upstate, USA). Lenses were collected from a litter of mice at each of the time points to generate each protein sample. Prior to the addition of RIPA buffer to the lenses, the buffer first had to be diluted 10-fold. Immediately before the addition of RIPA buffer to the lenses, protease inhibitor cocktail (Sigma, UK) was added to the buffer (100µl of protease inhibitor cocktail per 10ml diluted RIPA buffer). RIPA buffer (500µl) was added to the lenses before homogenisation. The sample was then transferred to an eppendorf tube before incubation at 4°C on a rotator for 30 minutes. The sample was then centrifuged at 13,000 x g for 30 minutes at 4°C. The supernatant was removed and aliquoted into new eppendorf tubes before storage at -20°C.

2.4.2. Quantification of Protein

The protein samples collected were quantified using a BCA assay (Pierce, UK). The assay was completed using the protocol provided by the manufacturer; briefly described here. A number of bovine serum albumin (BSA) standards of varying concentrations (2,000µg/ml-0µg/ml) were made by diluting the BSA stock solution provided. Enough working solution (50 parts of reagent A: 1 part reagent B) was prepared to run each unknown sample (plus BSA standards) in duplicate. Each sample and standard (25µl) was added to a microplate, 200µl of working reagent was added to each sample/standard. The microplate was then covered in foil and incubated at 37°C for 30 minutes. The absorbance of each of the samples were then measured at 570nm using a plate reader (Multiskan Ascent, Labsystems). The absorbance readings for the standards were used to produce a standard curve allowing for the concentrations of the unknown samples to be calculated.

2.4.3. SDS-PAGE

The Bio-Rad Mini-Protean® 3 cell system was used to run the SDS-PAGE. Glass plates were cleaned with ethanol before using. A short plate was placed on top of a tall plate before placing into the casting frame, where it was locked into position. Distilled water was used to check for leaks from the apparatus. The resolving and stacking gels were made up as described in **Tables 2.6** and **2.7**. The percentage of the resolving gel used was altered depending on the molecular weight of protein; for mcl-1 and axl a 10% resolving gel was used. The resolving gel was allowed to set for 20 minutes before the stacking gel mixture was layered on top of the resolving gel. A comb was then inserted into the glass spacers. The gel was then allowed to set for an hour, damp tissue was placed over the casting frame to prevent the gel from drying out. After an hour, the glass plates, with the gel inside, were removed from the casting frame and placed into the electrode assembly (short plate facing inwards, creating the inner buffer chamber). The electrode assembly was then locked into the clamping frame which in turn was placed into the mini tank. Approximately 125ml running buffer (100ml 10x Tris/glycine/SDS buffer, Bio-Rad, and 900ml distilled water) was added to the inner buffer chamber. 200ml was added to the outer buffer chamber.

Resolving gel to a final volume of 10ml			
Final %age Gel	10%	12%	15%
Range (MW)	20-100	10-70	8-50
Acrylamide (30%)	3.3ml	4ml	5ml
Water	4ml	3.3ml	2.3ml
1.5M Tris pH 8.8	2.5ml	2.5ml	2.5ml
10% SDS	100µl	100µl	100µl
10% APS	100µl	100µl	100µl
TEMED	20µl	20µl	20µl

Table 2.6: ***Components of the resolving gel for SDS-PAGE***

Stacking gel to a final volume of 10ml	
Acrylamide (30%)	1.67ml
Water	5.83ml
1.5M Tris pH 8.8	2.5ml
10% SDS	100µl
10% APS	50µl
TEMED	10µl

Table 2.7: ***Components of the stacking gel for SDS-PAGE***

2.4.4. Preparation of Protein Samples

The protein samples were diluted to the same concentration (~2.5µg/µl) by addition of the lysis buffer (RIPA buffer, Upstate). Equal amounts of the diluted protein sample and sample loading buffer (Bio-Rad, UK) were added to an eppendorf. These samples were then boiled at 100°C for 5 minutes on a heating block (Grant QBT2) to denature the proteins. Following boiling, the protein samples were added to the gel using the lane guide provided by Bio-Rad. 8µl of protein/loading buffer mix was added to each well (~10µg protein). 8µl of molecular weight marker (Bio-Rad Precision Plus Molecular weight marker) was added to the outermost lanes. The lid was the placed on the mini tank and the gel run for 30 minutes at 200 volts, 300mA.

2.4.5. Transfer of Proteins onto the Nitrocellulose Membrane

Transfer buffer was made up (200ml methanol, 100ml Tris/glycine buffer and 700ml distilled water). The nitrocellulose membrane (Hybond™-ECL™, Amersham Biosciences, UK) was cut to size using a short glass plate as a template. After completion of electrophoresis, the inner chamber assembly was removed from the mini tank. The gel was removed from the glass plates by gently separating the plates. The stacking gel was discarded, whilst the resolving gel was placed into transfer buffer. Following the completion of the SDS-PAGE the nitrocellulose membranes, filter paper, fibre pads and the gels were soaked in transfer buffer on the rocker for 15 minutes

A gel sandwich was then made up in a gel holder cassette composed of two fibre pads, two pieces of filter paper, the gel and the nitrocellulose membrane. This sandwich was then placed into the mini tank, which had been filled with transfer buffer (~600ml), alongside a frozen cooling unit. A magnetic stirrer was placed into the mini tank to keep the buffer circulating during the transfer process in order to prevent overheating of the system. Transfer conditions used were 100V, 350mA for 45 minutes. Following completion of the transfer, the gel sandwich was unpacked in the same order as it was packed. The membrane was placed in 1 x TBS/Tween where it was stored in the fridge for up to a week. Proteins were visualised on the membrane using Ponceau S (Sigma, UK), this allowed the success of the transfer to be visualised. Following staining with Ponceau S the membranes were photographed under white light (UVP BioDoc-It™ System). Membranes were then washed with 1 x TBS/Tween to remove the Ponceau S before the blocking step in the protocol.

2.4.6. Blocking the Membrane

5% milk was used to block the membrane in order to prevent non-specific binding. Approximately 20ml of blocking solution was added to each membrane. The membranes were then left on the rocker for 1 hour at room temperature. After an hour the blocking solution was removed from the membranes and the membranes were washed 6 times with 1 x TBS/Tween for 5 minutes each time.

2.4.7. Incubation with the Primary Antibody

Antibody dilutions were made up in 1% milk. A range of dilutions were used to try to optimise the conditions used. 20ml of antibody solution was added to the membrane. The membranes were then left on the rocker for an hour at room temperature. Following incubation with the primary antibody the membranes were washed in 1x TBS/Tween for 30 minutes (6 x 5 minute washes).

2.4.8. Incubation with the Secondary Antibody

20ml of secondary antibody solution (1% milk and antibody) was added to the membrane. Incubation with the secondary antibody was also an hour at room temperature, with the membrane on the rocker. Following incubation, the

membrane was washed for 30 minutes with 1x TBS/Tween (6 x 5 minute washes).

2.4.9. Exposing the Membrane to Film

The membranes were then placed inside a plastic wallet in the developing cassette (Hypercassette™, Amersham Biosciences). The cassette was then taken into the dark room. The ECL reagents were mixed (50 parts of reagent A: 1 part reagent B) (ECL Plus Western Blotting Detection Reagents, Amersham Biosciences, UK). Approximately 1ml of the mixed solution was added to each membrane. It was allowed to incubate for 5 minutes at room temperature before the membranes were exposed to the first film. The plastic wallet was closed and a film (Hyperfilm™, Amersham Biosciences, UK) was placed on top of the plastic wallet. The developing cassette was then closed and the exposure time measured. A number of different exposure times were used in an attempt to obtain the best picture, ranging from 1 to 10 minutes. Following exposure the film was then placed in developer solution (Photosol Limited, UK) for 3 minutes, then fixer solution (Photosol Limited, UK) for 3 minutes, before being rinsed in water. The film was then dried.

2.4.10. Stripping the Membranes

Following membrane exposure to the film, the membrane was stripped to remove the bound antibody. This allowed for the expression of a secondary protein to be examined; in this case, actin expression was used as a loading control. Stripping buffer (~20ml) was added to each membrane (composition given in **Appendix 1**). The membranes were washed twice with stripping buffer at room temperature for 10 minutes each time. Following the removal of the stripping buffer the membranes were washed with 1x PBS twice for 10 minutes each time. The membranes were then placed into 1x TBS/Tween for 5 minutes before they were ready for the blocking stage. Blocking and incubating with antibodies were completed as described previously (**Sections 2.4.6.-2.4.8.**) before the membrane was again exposed to film.

2.4.11. Analysis of the Western Blotting Results

The films produced from the western blotting experiments were scanned (Epson Expression 1680 Pro). The resulting images were imported into the Labworks™ software (Media Cybernetics, UK) to enable the completion of densitometry analysis. The optical denisity was recorded for each of the bands observed and these results were imported into Microsoft® Excel. Data were collected from all the sets of experiments and normalised to the actin results. This was completed to ensure that any differences observed would be true differences in expression rather than due to varying quantities of protein at each time point. Mean normalised band intensity along with the standard error of the mean was calculated for each protein at each time point. Statistical analysis was completed to identify any significant changes in expression (one-way ANOVA with Tukey's post-hoc test, statistical significance is only observed if the resulting *p*-value is less than 0.05).

2.5. Histology Examination of Lens Morphology

2.5.1. Tissue Collection

Eyeballs were collected from mice at postnatal day 2 (P2) and fixed in 4% paraformaldehyde (PFA). At the same time tail-tips from each of the pups were collected; DNA extracted from these tail-tips allowed the genotype of each pup to be established. The eyeballs were left in the fixative for 24 hours. The fixative was then removed and the eyeballs were washed in 1x PBS three times for 30 minutes each time. The tissues were then left in PBS overnight. The following morning the eyes were soaked in increasing concentrations of ethanol (50% for 30 minutes, 70% for 1 hour, 90% for 5 hours then 100% for 3 hours). The tissue was then submerged in 50:50 ethanol:xylene for 15 minutes. The 50:50 ethanol:xylene solution was then replaced and the tissue was left overnight in this solution.

The tissue was then moved to xylene, in which it was washed twice, for 1 hour each time. The eyeballs were then placed in hot wax and allowed to soak in the oven for 2 hours. The wax was then replaced and the tissues left in wax for another 2 hours (65°C). Following this incubation in wax the eyeballs were removed from the molten wax and placed onto a pre-cooled base of wax in a mould tray. Molten wax was then added so that it covered the tissue and then left to cool. Once cooled the mould trays were then transferred to the fridge for storage overnight. The blocks were left for 24 hours at room temperature before being sectioned.

2.5.2. Sectioning of Tissue

Once the wax blocks had set, they could then be sectioned. The wax blocks were secured to the microtome (HM 325, Microm), trimmed around the tissue and sections were cut at 7μm intervals. Sections were floated on water to ensure they were flat before placing them onto slides.

2.5.3. Haematoxylin and Eosin Staining

Haematoxylin and eosin were used to stain the sections obtained in order to examine lens morphology. The slides of sections were placed in xylene twice for 5 minutes each time. The slides were then placed in decreasing concentrations of IMS: 100% IMS twice for 5 minutes each time, then 90%, 70% and 50% with 2 minutes in each concentration. Slides were then placed in haematoxylin for 2 minutes before being washed under running water for 10 minutes. Following washing, the slides were placed in eosin for 2.5 minutes, before being washed for the last time in running water for 10 minutes.

Finally, following staining with haematoxylin and eosin, the slides were placed into a slide holder and dehydrated: slides were placed in 50% IMS through increasing concentrations of IMS, before being placed into xylene. Two drops of mounting medium (DPX, Raymond Lamb Laboratories, UK) was added to each slide. A coverslip was gently lowered onto the slide to avoid the introduction of air bubbles. The slides were left in the mounting hood overnight to dry, before being examined under a microscope (Leica DMRA2). Photographs were taken of the slides which were later analysed using Image-Pro Plus (MediaCybernetics), which allowed the dimensions of the lens to be measured.

As the samples for one of the genotypes (heterozygotes) were not of sufficient quality, results were only examined from two genotypes. Prior to the use of statistical analysis to compare the data collected an F-test was first completed to check for equal variation across the data sets. If the result from the F-test produced a value greater than 0.05 the result is not deemed significant and equal variation can be assumed. Following this an unpaired t-test was used. Statistical significance is only observed if the resulting p-value is less than or equal to 0.05.

Chapter 3: Examination of Apoptosis Gene Expression in the Postnatal Mouse Lens

3.1. Introduction

The removal of potential light-scattering organelles during differentiation of lens epithelial cells into fibre cells is thought to involve apoptosis signalling (Bassnett 2002; Dahm 1999; Wride 2000) . This process has been shown to have similarities to apoptosis and a number of apoptosis-related genes have been shown to be present in the lens (Wride *et al.* 1999) (described in more detail in the introduction). However, this process does not result in the plasma membrane changes characteristic of apoptosis, suggesting the presence of different control systems.

Previously, microarrays have enabled the global gene expression of the lens to be identified in both development and disease. A study by Wride *et al.* (2003) used microarrays to gain insight into the gene expression of the lens. Gene expression of the lens tissue was compared to non-lens tissue in order to identify genes preferentially expressed in the lens. Lenses of different ages were also compared to investigate the changes in gene expression during maturation. 1,668 genes were expressed in one or more of the time points examined at levels significantly above background. A number of the genes identified were previously unknown to be expressed in the lens. A selection of apoptosis-related genes and various isoforms of haemoglobin were also shown to be present (Wride *et al.* 2003).

In addition to looking at genes specifically expressed in the lens, this technique has also been used to examine the gene expression between different cell types in the lens. Ivanov *et al.* demonstrated that there was differential gene expression between young elongating fibre cells and the mature non-elongating fibre cells in the lens (Ivanov *et al.* 2005). From this study 65 genes were demonstrated to have differential expression; 25% were shown to be activated in maturing fibre cells, 75% were downregulated. Included in the number of genes shown to be downregulated were 7 genes encoding metabolic enzymes. This result was expected as metabolic activity decreases in the centre of the lens as cells become separated from the nutritious ocular humors. From this study several classes of apoptosis-related genes were also shown to be activated during differentiation. For example, DNase II-like acid DNase (DLAD) demonstrated elevated

expression during differentiation. This enzyme has been shown to be the DNase responsible for nuclear degradation during lens cell differentiation (Nishimoto *et al.* 2003). Data from this study confirms the expression of both pro- and anti-apoptotic genes during fibre maturation suggesting a potential role for the apoptotic pathway in this process.

Recently a study has been completed examining the gene expression in embryonic mouse lenses. Microarrays were utilised to compare the expression in lenses at embryonic days 10 and 12 (Xiao *et al.* 2006). From this study 1573 genes were confirmed as having differential expression; 965 were downregulated at E12, 617 shown increased expression. Genes that promote the cell cycle were seen to be downregulated at E12 as the progenitor cells from the lens pit exit the cell cycle and begin to differentiate into primary fibre cells. Members of both the IGF and Wnt families were shown to be differentially regulated between these two time points. Between E10 and E12 positive regulators of Wnt signalling were seen to be downregulated whilst negative regulators were upregulated. This seems to suggest that modulation of the Wnt family is necessary for normal lens differentiation. Expression of crystallins, markers of fibre cell differentiation, was also seen to increase.

Microarrays have given researchers the ability to study the underlying global gene expression changes of diseases, allowing the classification of diseases and possibly leading to the identification of potential targets for treatments. Recently, studies have been carried out to elucidate the genetic causes of a number of ocular diseases, including cataract (Wilson *et al.* 2002). Mansergh *et al.* (2004) looked at the changes in gene expression in the progression of cataract in the SPARC knockout mouse; a mouse model known to develop age-related cataract. Using microarrays, 54 genes were shown to be differentially expressed after the formation of cataract, these included 5 of the mouse globin genes (Mansergh *et al.* 2004). The identification of the differentially expressed genes from this study allowed for the generation of hypothesises about the role these genes play in the pathogenesis of cataract. The presence of globins in the lens has lead to suggestions that these proteins could play a role in lens ion transport and/or metabolism, oxygen transport or could potentially act to promote apoptosis.

Microarray studies have also been completed to identify the gene expression changes between human cataractous and normal age-matched lenses (Hawse *et al.* 2003; Hawse *et al.* 2004; Ruotolo *et al.* 2003; Segev *et al.* 2004). These studies demonstrated differential expression between cataractous lenses and age-matched controls. A number of structural proteins were included in the list of genes shown to be down-regulated in cataract, suggesting that the structural changes associated with age-related cataract could be due to the decreased expression of structural components.

This study aims to identify which apoptosis genes are present in the mouse lens during postnatal maturation through the use of a macroarray containing 243 genes with known roles in apoptosis. The presence of these genes in the lens could suggest a potential role in the processes of lens differentiation and organelle degradation. Incomplete organelle degradation has been shown to result in the formation of cataract. Prevention of DNA degradation in a mouse model, due to DLAD deficiency, was shown to lead to DNA accumulation in the lens causing cataract (Nishimoto *et al.* 2003). A study by Pendergrass *et al.* demonstrated the accumulation of nuclear and mitochondrial fragments in cortical cataract as a result of incomplete differentiation of fibre cells at the equatorial region (Pendergrass *et al.* 2005).

3.2. Experimental Design

The arrays used during this study are nylon macroarrays (Panorama™ Mouse Apoptosis Arrays) on which 243 apoptosis-related cDNAs are immobilised. The genes on the array included both pro- and anti-apoptotic factors including members of the caspase family, cell cycle regulators and signalling molecules amongst others. The housekeeping genes, where present, were used to normalise the array data so that comparisons could be made across the repetitions in each time point. Genes shown to be differentially expressed between the time points examined or shown to have high expression levels were identified from the arrays to try to elucidate the role of apoptosis signalling pathways in lens organelle degradation.

The macroarrays used in this study were hybridised with cDNA synthesised from RNA collected from whole lenses of newborn, postnatal day 7 and 14 mice (array methods given in **Section 2.2**). Following hybridisation and exposure to the phosphor imaging screen the arrays were stripped to remove any residual radiolabelled cDNA (see **Section 2.2.7** for more details).

These postnatal stages were used as they avoided the ethical considerations connected with collecting tissue from embryonic time points. The three time points examined using the arrays are prior to eye-opening, seen to occur at P14 (Kuwabara and Imaizumi 1974). By eye-opening the OFZ fills the pupillary area, therefore, a large amount of organelle degradation will have occurred before this time and the genes involved in this process could potentially be identified.

Semi-quantitative PCR was used to confirm array results (see **Section 2.3** for methods) as well as to examine the expression of selected genes at other postnatal time points. RNA was isolated from whole lenses of newborn and 4 week old mice in addition to that collected from lenses of mice at postnatal days 7 and 14. This RNA was used to synthesise cDNA, which was later used in PCR reactions.

Primers were designed for genes shown to be differentially expressed from the array results (sequences shown in **Appendix 4**). PCR reactions using each set of primers were completed three times; each time with a different cDNA sample. Each cDNA sample was synthesised from a litter of pooled lenses. The resulting gels were photographed and the band intensities quantified using Scion Image (see **Section 2.3.5.** for details).

GAPDH was used as a loading control, ensuring that the same amount of cDNA was used for each time point. This meant that any expression differences observed should be representative of the true differences of gene expression rather than discrepancies in the quantity of cDNA used for the reactions. The PCR reactions for each set of cDNAs were first normalised to GAPDH before being used to examine the expression of other genes identified from the arrays. Normalisation to GAPDH was completed by taking densitometry readings of the bands produced on the gel from the GAPDH products; as a result the amounts of cDNA were altered in the PCR reactions until the densitometry values were the same across all time points.

Following the completion of the three sets of PCR results for the genes shown to have differential expression, an average band intensity value was calculated to show the change in expression between the time points examined. Standard error of the mean was calculated for each time point/gene to give an idea of the variation observed from the three sets of results.

Subsequently protein expression of selected genes was examined using western blotting. Protein was extracted from lenses of postnatal mouse lenses at birth, postnatal days 7 and 14 and 4 weeks old, and quantified using a BCA assay (Pierce). Western blotting was used to examine the presence of mcl-1 and axl. A 10% resolving gel was used to separate the proteins. Primary antibodies used were raised in rabbit: mcl-1 (Santa Cruz, sc-819), axl (Santa Cruz, sc-20741). The secondary antibody used was goat anti-rabbit IgG (Santa Cruz, sc-2004). Both the mcl-1 and axl antibodies were used at a dilution of 1:2000. The secondary antibody was used at a dilution of 1:5000. The films were exposed for

three different periods of time for each of the antibodies used (1, 5 and 10 minutes) before developing and fixing.

Following film exposure the membranes were stripped (see **Chapter 2** for methods) and reprobed using a goat polyclonal actin antibody (Santa Cruz, sc-1616). The secondary antibody used was donkey-anti goat IgG (Santa Cruz, sc-2020). Reprobing the membranes with the actin antibody allowed for confirmation of equal loading. The resulting films were scanned (Epson Expression E1680 Pro). Three sets of protein were used to complete the western blots for each of the antibodies.

3.3. Results

3.3.1. Checking the Integrity of RNA Samples

Following isolation, RNA integrity was confirmed using a denaturing gel (an example of which is shown in **Figure 3.1**). Intact RNA should produce two distinct bands on a denaturing gel corresponding to the 28S and 18S ribosomal bands. These bands should be in a ratio of 2:1, with the 28S band twice as intense as the 18S band. If the RNA has degraded a smear would be observed on the gel.

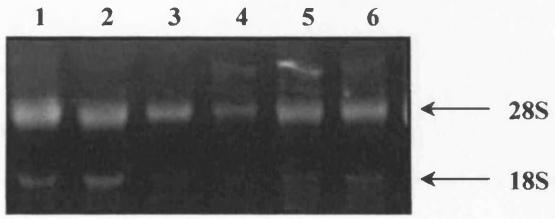

Figure 3.1: ***An example of an RNA denaturing gel.*** *Samples run on the gel were isolated from whole mouse lenses using TRIzol®. Lane contents as follows; lane 1: P7 RNA, lanes 2 and 3: P14 RNA, lanes 4-6: 4 week RNA.*

3.3.2. Array Results

The arrays were completed as described previously (see **Section 2.2**). Results from the arrays hybridised with the RNA collected from newborn mice were not of sufficient quality for further analysis. Consequently data were only collected from the arrays hybridised with P7 and P14 RNA. Four arrays were hybridised with the P7 RNA and 3 were hybridised with P14 RNA. The first two arrays from each time point were completed on fresh arrays i.e. they had never been used. The remainder, however, were carried out on arrays which had been previously stripped to remove the bound cDNA. An example of the array results obtained is shown in **Figure 3.2**.

To confirm the effectiveness of the stripping protocol the stripped arrays were exposed to the phosphor screen for 5-7 days before scanning. Any residual cDNA bound to the arrays would show up during scanning as small spots on the array. After the arrays were scanned, no spots were observed (data not shown); demonstrating that the stripping protocol was effective.

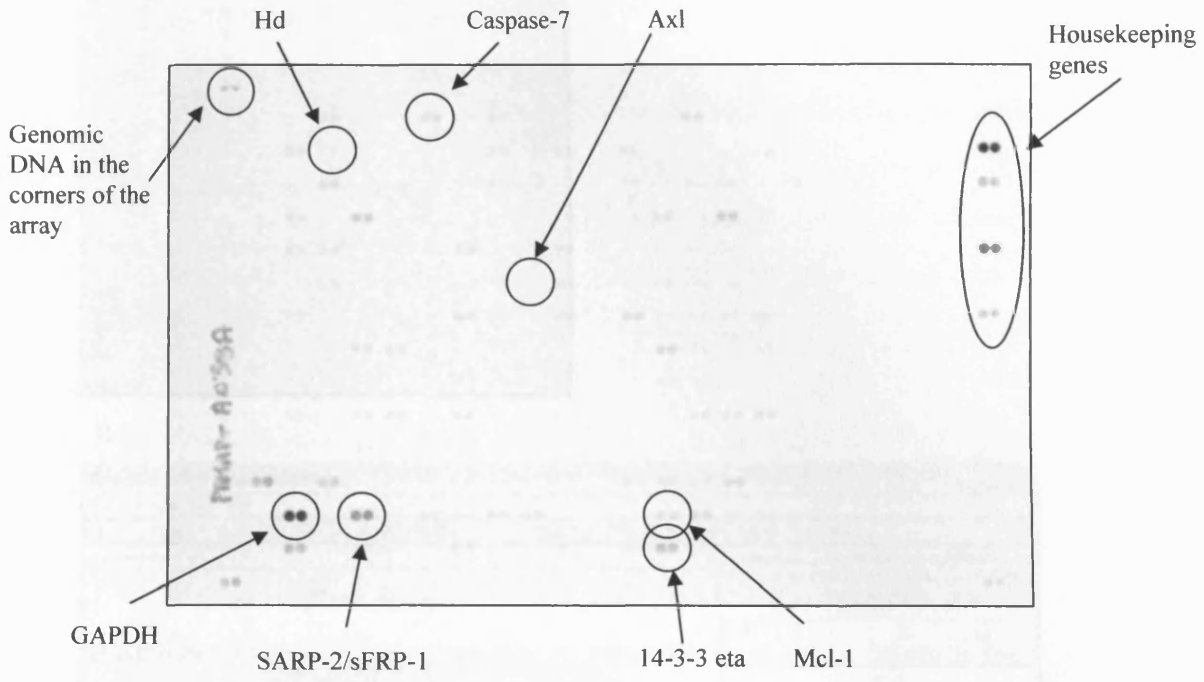

Figure 3.2: ***An example of array results obtained****. Phosphoimage of an array hybridised with P7 RNA. The arrays used were fresh; i.e. they had not been previously stripped. Genes identified on the array include the genomic DNA used to align the arrays, the housekeeping genes, the intensity of which was used for analysis. A few of the highly expressed genes, 14-3-3 eta, caspase-7 and SARP-2/sFRP-1 are also identified. The position of the genes of interest used for further studies is also indicated. The spots for two of these genes (axl and hd) are hard to visualise, but these genes were shown to have a higher expression at P14 and so would not show up intensly on this array.*

3.3.2.1. Analysis of Array Data

The computer image generated by the typhoon scanner was imported into ImaGene (Biodiscovery, USA). A virtual grid was placed over the image using the genomic DNA in the corners of the array as orientation points. A screenshot from ImaGene demonstrating the analysis process is shown in **Figure 3.3**. The results were then analysed in Microsoft® Excel as described in the methods section (**Section 2.2.8**). The raw array data have been submitted to GEO, an online database of results generated from array experiments (http://www.ncbi.nlm.nih.gov, GEO accession: GSE8731).

A

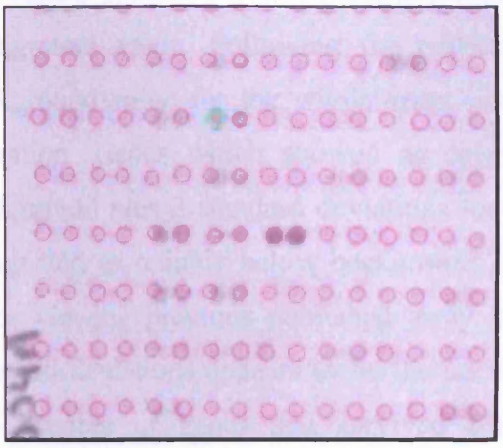

B

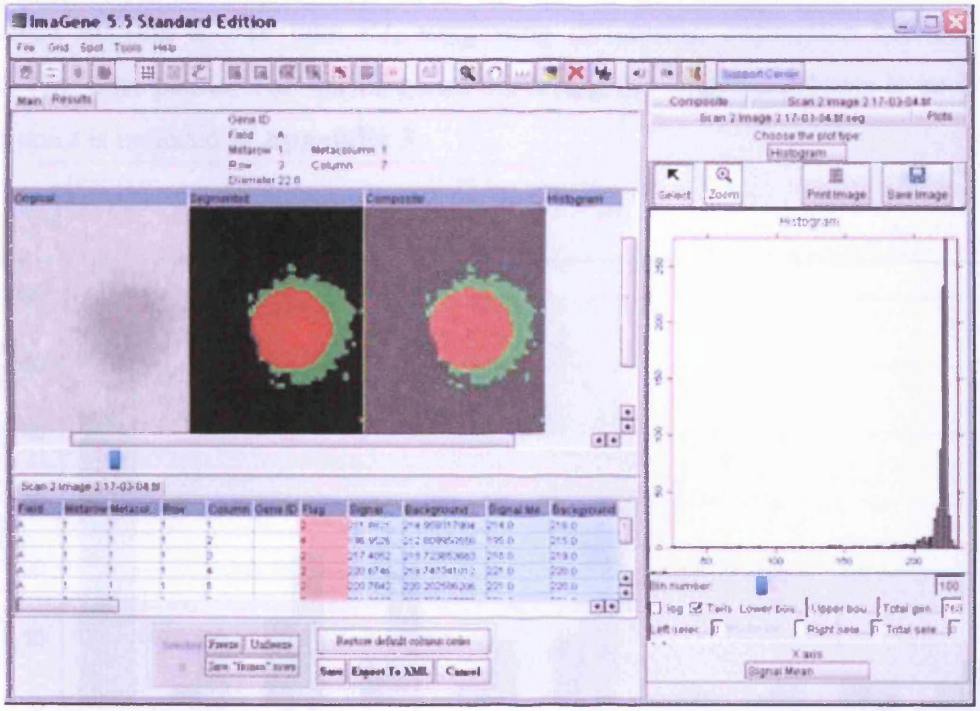

Figure 3.3: ***Screenshots taken from ImaGene.*** *Figure 3.3A shows the spot alignment process. A virtual grid is aligned over the spots to allow assignment of grid references to each spot. Grid spots could be moved manually to allow correct alignment. Figure 3.3B shows the analysis screen generated for each array by ImaGene. In the top left corner is a representation of the spot being analysed. Next to the original spot is a diagram showing the areas used to calculate both the mean signal intensity and the mean background value. The pixels coloured in red are used to calculate the mean signal intensity, those in green are used to calculate the background value. The area immediately around the spot was ignored for the background value; this prevents the generation of an artificially high background value (see* ***Figure 2.1****). Underneath the spots is an example of the data produced for each spot on the array, including the mean signal and mean background values used to analyse the results. On the right of the picture is a histogram which represents the mean signal intensities for all the spots on the array.*

The results produced from ImaGene included a mean spot intensity and a mean background value. Following the collection of the array results, the mean background value for the whole array was calculated along with the standard deviation. Genes which showed an original spot intensity below the mean background plus 2 standard deviations for at least half of their data spots were designated as reliably below background and were filtered out of the data set. After viewing previous published array articles the mean background plus 2 standard deviations appears to be the standard value used to filter the data set. The number of genes that survived filtering from each gene family was calculated and plotted on a graph (**Figure 3.4**). A greater number of genes survived filtering at P14 than P7, suggesting differential expression between these two time points. The list of genes surviving the filtering process at each time point is included in **Appendix 3**.

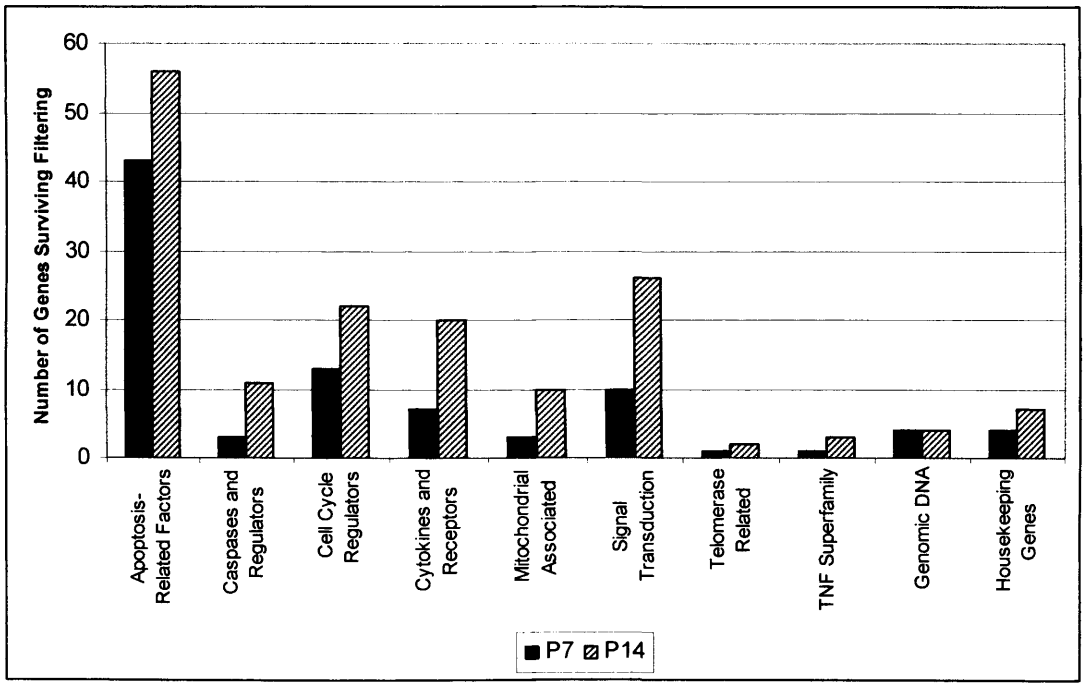

Figure 3.4: ***Graph showing the number of genes surviving the filtering process at the two time points examined.*** *The average background intensity was measured along with the standard deviation. The mean background value was calculated along with the standard deviation. Spots were considered to be below background if their original intensity was lower than the mean background intensity plus 2 standard deviations. Genes have been grouped into the gene families assigned by Sigma.*

Following filtering, the ten genes, which were not housekeeping genes, with the highest expression at each time point were identified. These are shown in **Table 3.1**.

Highly Expressed Transcripts

Gene Name	Accession Number	Normalised Band Intensity P7	Normalised Band Intensity P14	Gene Family
Clusterin	NM_013492	75.36	63.25	Apoptosis-Related Factors
Gpx1	NM_008160	55.09	48.46	Apoptosis-Related Factors
Pin	NM_019682	50.64	42.09	Apoptosis-Related Factors
14-3-3 eta	NM_011738	47.45	28.95	Signal Transduction
SARP-2/sfrp-1	NM_013834	39.34	56.28	Apoptosis-Related Factors
Dad-1	NM_010015	32.63	27.49	Apoptosis-Related Factors
Cyclin G1	NM_009831	28.61	51.28	Cell Cycle Regulators
Myd118	NM_008655	28.61	20.37	Signal Transduction
Mts-1	NM_011311	23.74	28.27	Apoptosis-Related Factors
Caspase-7	NM_007611	18.92	18.79	Caspases and Regulators

Table 3.1: ***Highly expressed genes.*** *This table lists the ten genes shown to have the highest expression at both P7 and P14.*

Two normalisation methods were used to analyse the array data; normalisation with housekeeping genes and global normalisation (see **Section 2.2.8** for more details). Genes that demonstrated a 2-fold or greater change in expression and a *p*-value of less than 0.05 (i.e. statistically significant difference in gene expression) after each normalisation method were identified and are shown in **Tables 3.2** and **3.3**.

The array results were first normalised using a mean housekeeping gene value; this was Sigma's recommended method of analysis for the arrays. This method of analysis showed 20 genes to be significantly differentially expressed between the two time points. An alternative method of normalisation was utilised as three of the housekeeping genes were not shown to be expressed on the arrays, possibly affecting the normalisation process. Global normalisation was the second method of analysis to be used. This method involved calculating a mean spot intensity and using that to normalise the values across the arrays (more detail given in **Section 2.2.8.2**). From this method of analysis 60 genes were shown to have differential expression; included in the 60 genes identified were the 20 previously identified by the housekeeping method of analysis. Following this analysis, it was decided to continue using the housekeeping method of normalisation as it appears to be a more stringent method. The 20 genes identified by this method were also identified by the global normalisation, suggesting that these genes were worthy of further investigation.

Differentially Expressed Transcripts Identified by Normalisation with Housekeeping Genes

Gene Name	Accession Number	Mean Normalised Expression P7	Mean Normalised Expression P14	Fold Difference	*p*-value
P2rx1	NM_008771	2.05	18.05	8.81	1.6E-05
Hd	NM_010414	2.97	21.96	7.34	4.5E-06
Icad/Dffa	NM_010044	3.91	15.03	3.84	0.0002
Mdm2	NM_010786	4.78	16.8	3.51	4.6E-07
Mfge8	NM_008594	2.52	7.89	3.13	0.0004
IGF1r	NM_010513	2.33	6.84	2.93	0.0001
Axl	NM_009465	2.85	8.27	2.9	0.0017
Galectin-3	NM_010705	2.49	6.67	2.68	0.0002
A1	NM_009742	2.46	6.53	2.66	0.0014
Cdk4	NM_009870	2.79	7.2	2.58	0.0005
Srebf2	XM_127995	4.62	11.86	2.57	0.0062
Tgfβ2	NM_009367	3.83	9.32	2.43	2.5E-06
Integrin-αV	NM_008402	6.56	14.61	2.23	0.0002
Dap1	NM_146057	7.56	16.85	2.23	0.0013
Trp53/p53	NM_011640	3.17	7.01	2.21	0.0101
Srebf1	NM_011480	2.49	5.43	2.18	0.007
IGF-1	NM_010512	3.52	7.65	2.17	0.035
Mcl-1	NM_008562	3.79	8.04	2.12	5.9E-06
Thrombospondin	NM_0011580	2.99	6.04	2.02	0.003
Daxx	NM_007829	2.14	4.32	2.01	0.024

Table 3.2: ***Significant genes identified using normalisation with housekeeping genes.*** *This table lists the genes shown to have a 2-fold or greater difference in expression between P7 and P14 and a p-value less than 0.05.*

Differentially Expressed Transcripts Identified by Global Normalisation

Gene Name	Accession Number	Mean Expression P7	Mean Expression P14	Fold Difference	*p*-value
*P2rx1**	NM_008771	1.78	22.23	12.50	4.36E-06
*Hd**	NM_010414	2.62	27.08	10.33	9.28E-07
*Icad/Dffa**	NM_010044	3.50	18.38	5.25	6.18E-06
*Axl**	NM_009465	2.44	10.16	4.16	1.85E-05
*Mdm2**	NM_010786	5.05	20.62	4.08	3.55E-08
*Mfge8**	NM_008594	2.52	9.64	3.83	1.62E-05
Ar	NM_013476	1.13	4.16	3.69	0.0044
*IGF R**	NM_010513	2.28	8.38	3.67	2.52E-06
*A1**	NM_009742	2.21	8.08	3.66	1.34E-05
*Galectin-3**	NM_010705	2.40	8.20	3.41	2.54E-06
*Cdk4**	NM_009870	2.76	8.84	3.21	8.01E-06
*Srebf2**	XM_127995	4.55	14.52	3.19	0.0012
TR/TeRc	U33831	2.31	7.04	3.05	0.0012
*TRP53/p53**	NM_011640	2.84	8.62	3.04	0.0001
*IGF-I**	NM_010512	3.12	9.38	3.00	0.0025
Bak	NM_007523	2.21	6.43	2.91	0.0014
*Tgf-β2**	NM_009367	3.98	11.45	2.88	9.99E-10
*Daxx**	NM_007829	1.89	5.33	2.87	0.0003
*Srebf1**	NM_011480	2.38	6.62	2.78	0.0002
Caspase-3	NM_009810	2.18	5.99	2.75	8.58E-05
Calcyclin	NM_011313	2.99	8.05	2.69	0.0004
RARβ2	S56660	2.20	5.74	2.61	0.0012
CRADD	NM_009950	1.53	3.96	2.59	0.0062
*Thrombospondin**	NM_0011580	2.90	7.42	2.56	2.54E-05
Cyclin D1	M64403	2.72	6.95	2.56	0.0004
FLIPL/Cash	NM_009805	1.56	3.99	2.56	0.0117
DNAse1	NM_010061	2.03	5.12	2.53	0.0019
TRAF2	NM_009421	1.67	4.20	2.52	0.0055
DEDD	NM_011615	3.55	8.77	2.47	0.0006
*Integrin-αV**	NM_008402	7.28	17.97	2.47	0.0002
Bcl-10	NM_009740	2.04	5.01	2.45	0.0027
TGF-β3	NM_009368	2.44	5.97	2.45	0.0012
TFAR15	AF159368	2.01	4.90	2.43	0.0040
*Mcl-1**	NM_008562	4.13	9.88	2.39	1.41E-06
TDAG8	NM_008152	2.62	6.19	2.36	0.002
Sp1	NM_013678	2.18	5.09	2.34	0.006
TRAF6	NM_009424	3.53	8.17	2.32	5.16E-06
IFN-γ R1	NM_010511	1.85	4.26	2.31	0.0107
RP105/Ly78	NM_008533	1.56	3.54	2.28	0.0206
CDC2	NM_007659	2.04	4.63	2.27	0.0053
CAS/CSE1	AI549625	2.01	4.57	2.27	0.0166
*Dap1**	NM_146057	9.11	20.69	2.27	0.0029
TWEAK/TNFSF12	AF030100	1.77	3.97	2.24	0.0215
PDCD2	NM_008799	2.10	4.68	2.23	0.0124
NF-κBp65	NM_009045	3.71	8.25	2.23	2.38E-05
E2F1	NM_007891	4.12	8.93	2.17	2.62E-05
PARP-2	NM_009632	2.08	4.49	2.16	0.0058
Cytochrome p450 oxidoreductase	NM_008898	2.62	5.64	2.15	0.0177

Table 3.3. continued overleaf

Gene Name	Accession Number	Mean Expression P7	Mean Expression P14	Fold Difference	p-value
TRANK	NM_016764	2.62	5.58	2.13	0.0018
IL-2	NM_008366	1.98	4.19	2.12	0.016
TRAF3/CRAF1	NM_011632	2.34	4.94	2.11	0.0059
CD47	NM_010581	2.08	4.37	2.10	0.0102
Cox-1/Ptgs1	NM_008969	1.76	3.64	2.06	0.0453
Cyclin G1	NM_009831	30.89	63.73	2.06	0.0010
IFN-γ R2	NM_008338	2.37	4.89	2.06	0.0030
PDCD1	NM_008798	1.39	2.85	2.05	0.0377
53BP2	U58881	1.74	3.56	2.04	0.0330
CLDN3	NM_009902	1.72	3.48	2.02	0.0034
CDK5	NM_007668	2.83	5.72	2.02	0.0001
Bim	NM_009754	2.04	4.10	2.01	0.015
erbB2	U71126	2.04	4.10	2.01	0.0265

Table 3.3: ***Significant genes identified using global normalisation.*** *This table lists the genes shown to have a 2-fold or greater difference in expression between P7 and P14 and a p-value less than 0.05. Gene names marked with an asterisk were also identified through normalisation with the housekeeping genes.*

3.3.2.2. Reproducibility of Array Data

To examine the reproducibility of array results obtained, normalised signal intensities were compared. Results observed from arrays hybridised with P7 cDNA were compared by plotting them on an X-Y scatter plot (**Figure 3.5A-C**). Two of the arrays hybridised with P7 cDNA were fresh, i.e. they had never been used before. The remainder had previously been stripped (methods described in **Section 2.2.7.**). If the data are reproducible, a straight line should be generated at a 45° angle dissecting equal values on both the X and Y axes. When the results from the fresh arrays were compared (**Figure 3.5A**) the resulting graph demonstrated a general trend towards the expected 45° line (R^2-value: 0.95). When the results from the two stripped arrays were compared (**Figure 3.5B**) again this trend towards the expected 45° line was observed (R^2-value: 0.88). However, when the results were compared from arrays hybridised under different conditions (fresh versus stripped, **Figure 3.5C**) the trendline generated did not dissect equal values on both the X and Y axes, but instead demonstrated a bias towards the results generated from the fresh array (R^2-value: 0.41). This was not unexpected, as the stripping process may have removed some of the original bound cDNA on the arrays, which could lead to a reduction in the resulting signal. To counteract this potential problem, all of the array results were normalised with respect to the mean housekeeping gene expression so the weaker signals observed from the stripped arrays should not affect the overall results.

Three arrays were completed using P14 cDNA. The results from the arrays hybridised with P14 cDNA are shown in **Figure 3.5D-E**. Again, when the results were compared from the arrays treated identically there was a general trend towards the expected 45° line (R^2-value: 0.94).

Scatter Plots Demonstrating Reproducibility of the Array Results

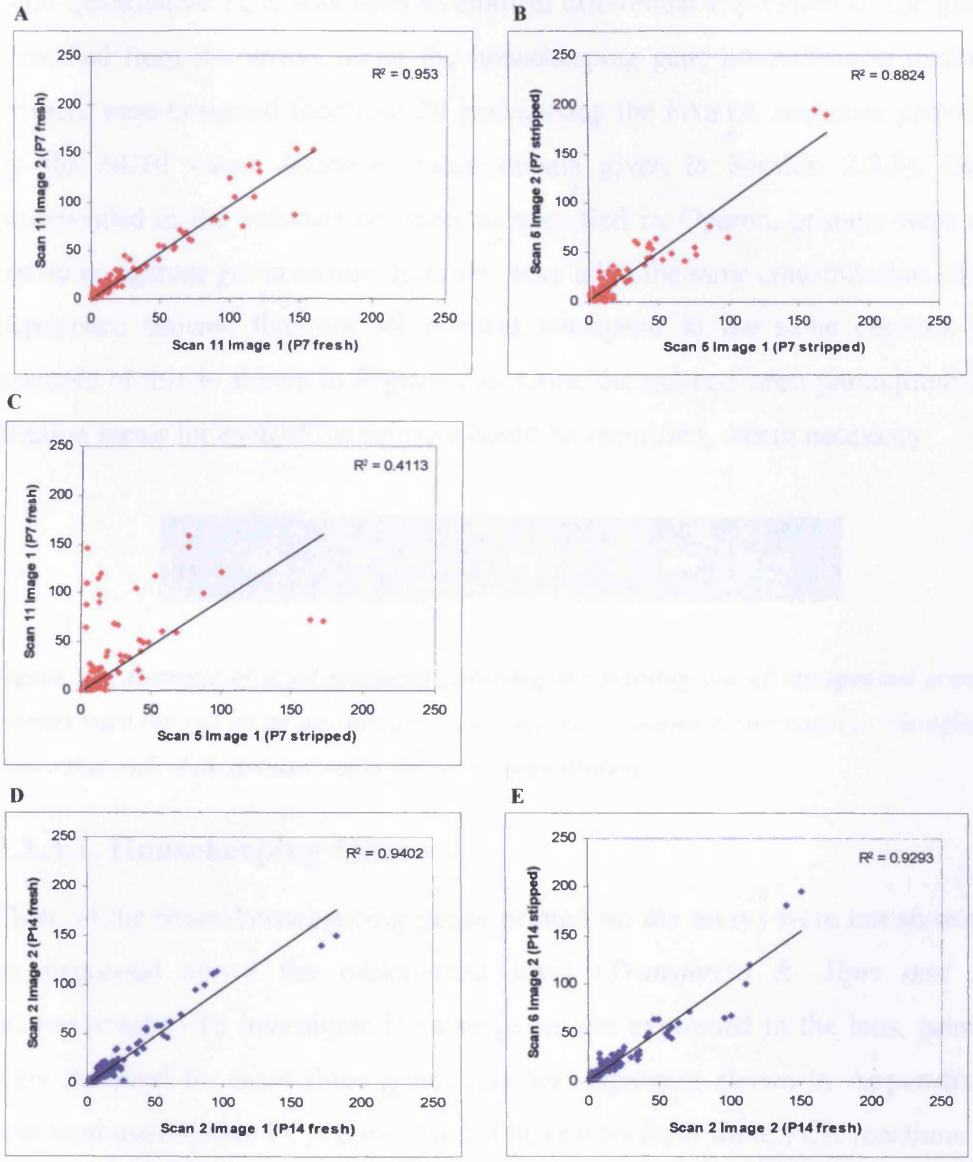

Figure 3.5: ***Reproducibility of array results.*** *These graphs were produced by plotting the normalised signal intensities from one array against another. Array results were compared between arrays which had been treated identically (i.e. fresh array compared with a fresh array, or a stripped array compared with a stripped array) or that had been treated differently (fresh versus stripped). Results from the arrays hybridised with P7 cDNA (A-C) or P14 cDNA (D-E) show that when arrays are compared with others that have been treated identically they have a high level of reproducibility. However, when the results were compared from two different conditions the trendline did not dissect equal values on both the X and Y axes (C). The R^2-value is shown on each graph. The closer this value is to 1, the greater the correlation between the two sets of data.*

3.3.3. PCR Confirmations

Semi-quantitative PCR was used to confirm differential expression of the genes identified from the arrays using the housekeeping gene normalisation method. Primers were designed for these 20 genes using the FASTA sequence provided by the NCBI Gene database (more details given in **Section 2.3.3**). Once resuspended in the volumes of water as specified by Operon, primers were run out on an agarose gel to ensure that they were all at the same concentration (since experience showed that not all primers resuspend to the same degree). An example of this is shown in **Figure 3.6**. Once the gel had been photographed a dilution factor for each of the primers could be identified, where necessary.

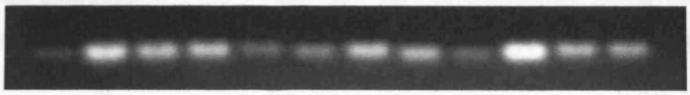

Figure 3.6: ***Example of a gel produced following the running out of resuspended primers.*** *Primers were run out on an agarose gel; following this a dilution factor could be identified to ensure that each of the primers was at the same concentration.*

3.3.3.1. Housekeeping Genes

Three of the seven housekeeping genes printed on the arrays were not shown to be expressed above the background level (*Transferrin R, Hprt and β2-microglobulin*). To investigate if these genes are expressed in the lens, primers were designed for these three genes (primer sequences shown in **Appendix 4**) and semi-quantitative PCR completed. The results from these PCR reactions are shown in **Figure 3.7**.

As shown in **Figure 3.7.**, all three of the housekeeping genes were found to be expressed in the lens at both P7 and P14. This result suggests that there could have been a problem with the spotting of these genes on the original arrays.

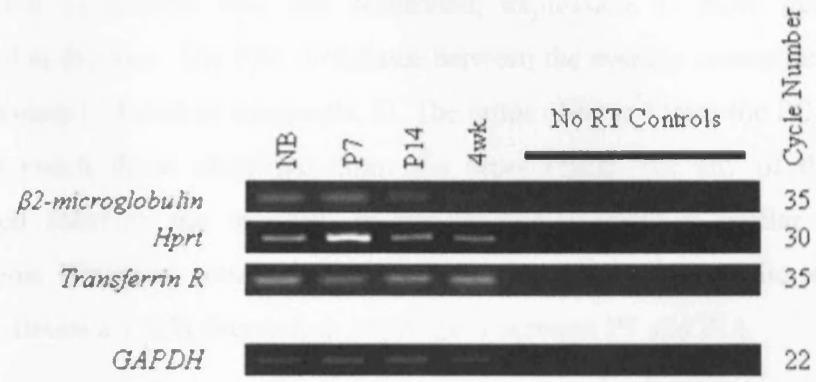

Figure 3.7: ***Semi-quantitative PCR results for the housekeeping genes not shown to be expressed using the arrays.*** *Three housekeeping genes were not shown to be expressed above background from the array results. Semi-quantitative PCR was used to examine the expression of these genes. PCR results demonstrated expression of all three of these genes at the stages examined. Gels presented are representative of the three sets of results produced.*

3.3.3.2. Differentially Expressed Genes

A number of different cycle numbers and annealing temperatures were tried in order to obtain the optimum results for each PCR reaction. DNA gels representative of the PCR results for the differentially expressed genes are shown in **Figure 3.8**. The gels produced from the PCR reactions were analysed using Scion Image (USA), producing average pixel intensities for each band. The band intensities were then normalised with respect to GAPDH, before being compared to the other repetitions. The average band intensity was calculated along with the standard error of the mean, this is shown graphically in **Figure 3.9**. The original band intensities are included in **Appendix 5**.

From the PCR results differential expression between P7 and P14 was confirmed for 10 of the 19 genes tested (52%). For the remaining 9 genes, although differential expression was not confirmed, expression of these genes was observed in the lens. The fold difference between the average normalised values was calculated (shown in **Appendix 5**). The ratios observed from the PCR results did not match those identified from the array results for any of the genes examined although the majority of results demonstrated a similar trend in expression. However, some of the results demonstrated the opposite, e.g. *igf-1* showed almost a 7 fold decrease in expression between P7 and P14.

Statistical analysis of the PCR results was completed using a one-way ANOVA with Tukey's post-hoc test. This analysis would demonstrate whether there were any significant changes in expression of the genes between the time points examined. Following the completion of this analysis, 2 genes were shown to have significant differences in expression; *thrombospondin* and *igf-1*. *Thrombospondin* demonstrated a statistically significant change in expression between the newborn and 4 week stages, and P7 and 4 weeks. A significant change in expression of *igf-1* was noted between P7 and P14, and P7 and 4 weeks. Results from the statistical analysis are shown in **Appendix 6**.

Results for the *P2rx1* PCR were not obtained, despite altering both the cycle number and annealing temperature. PCR reactions were also completed using two different sets of primers for this gene, but to no avail.

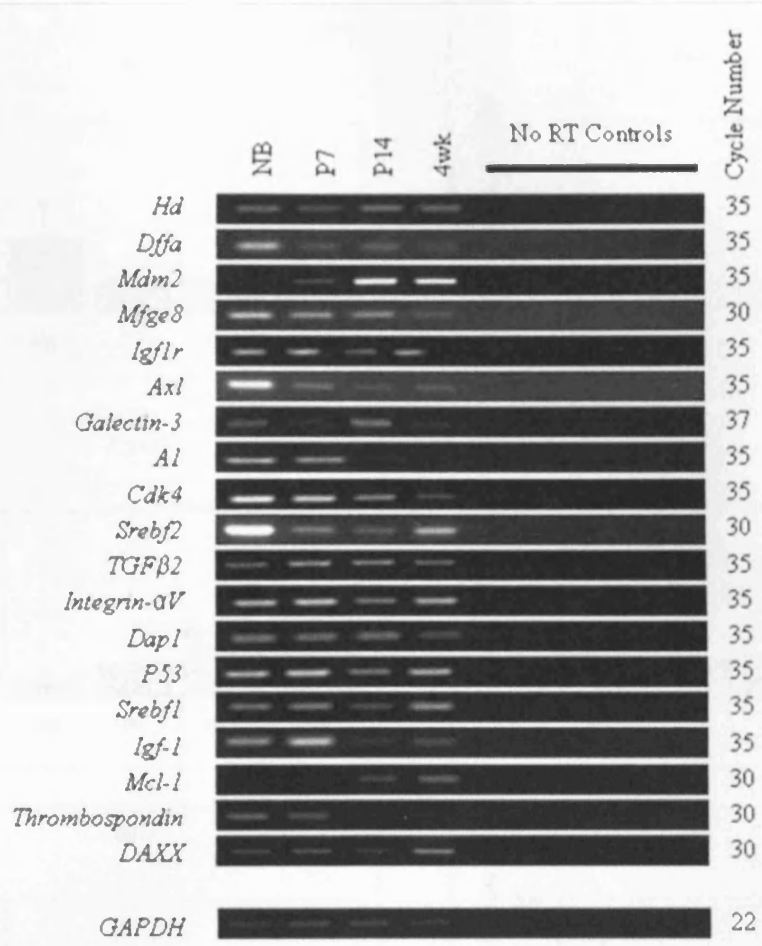

Figure 3.8: ***Semi-quantitative PCR results for differentially expressed genes.*** *Gels presented are representative of the three sets of results produced. Results are arranged in order of the fold difference observed from the array results.*

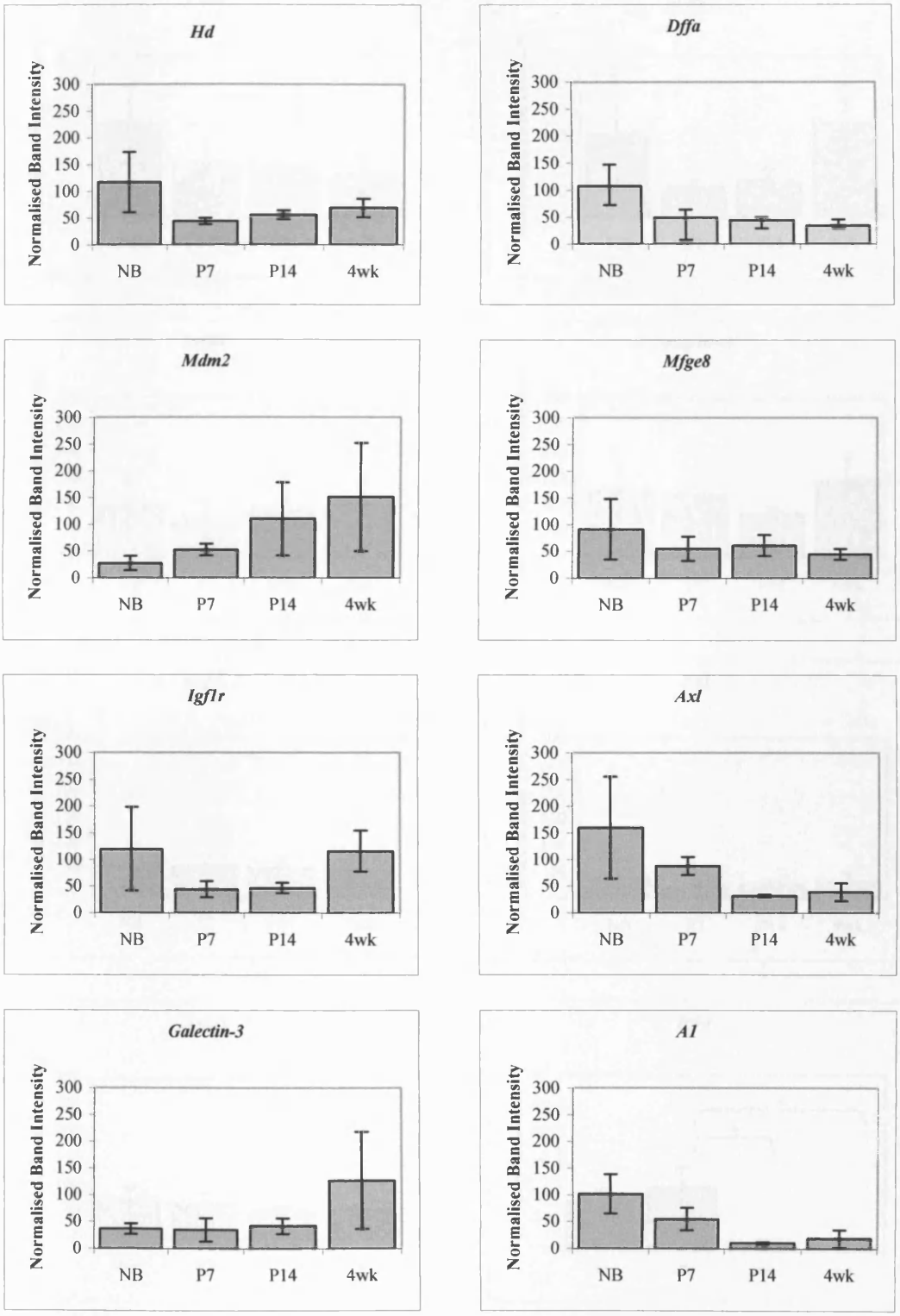

Figure 3.9 continued overleaf

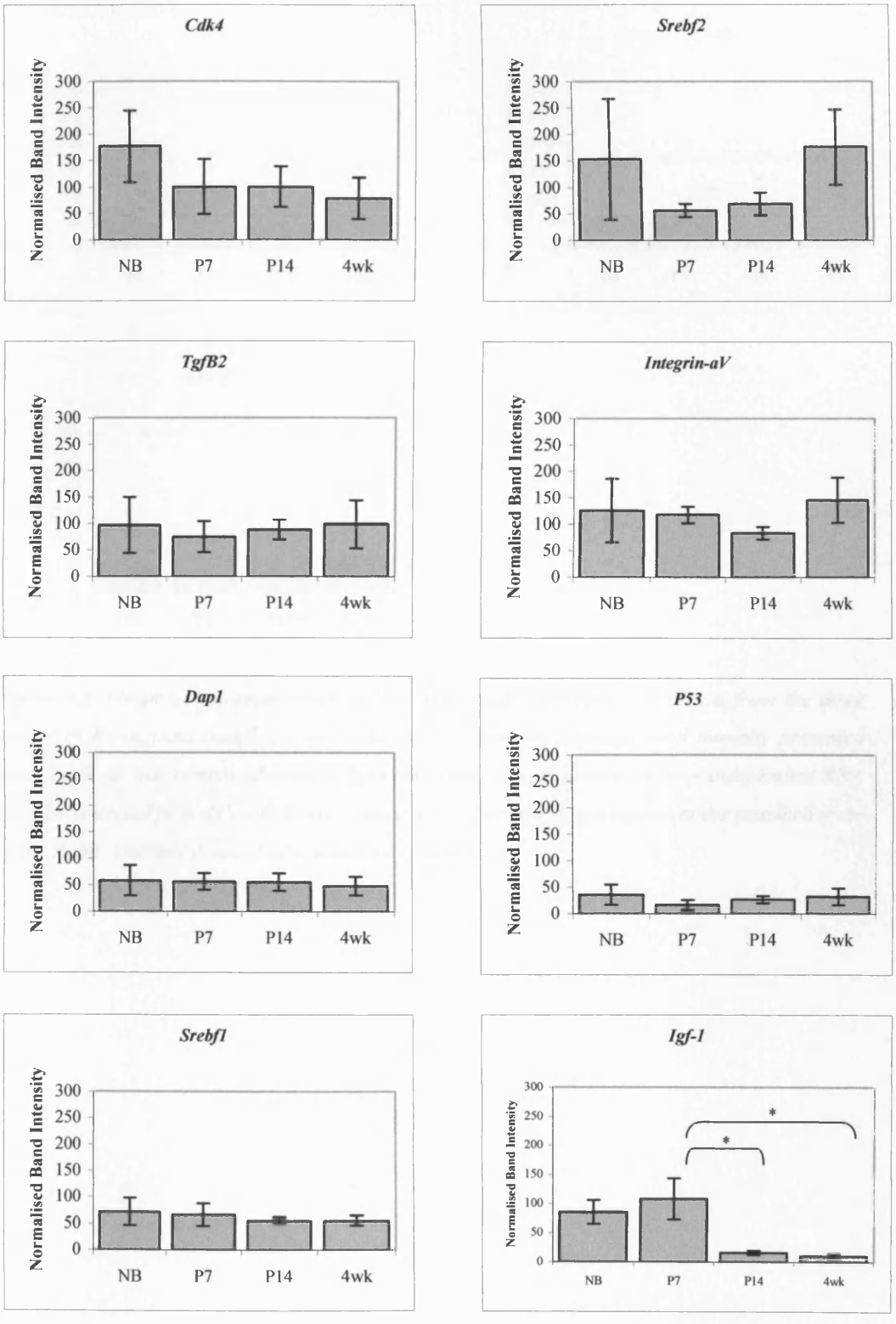

Figure 3.9 continued overleaf

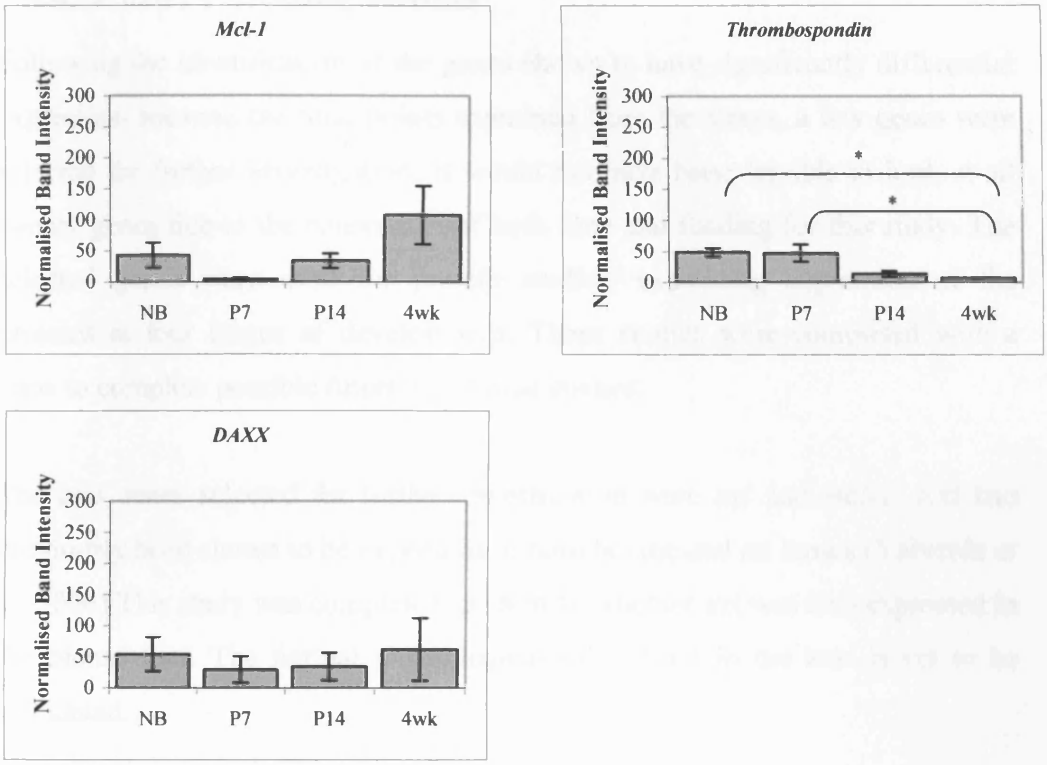

Figure 3.9: Graphical representation of the PCR results obtained. *The results from the three sets of PCR reactions completed were combined to give the average band intensity presented here. Each set was completed using a different cDNA sample generated from independent RNA samples collected from different litters of mice. Error bars displayed represent the standard error of the mean. Asterisks demonstrate statistical significance.*

3.3.4. Western Blotting Results

Following the identification of the genes shown to have significantly differential expression between the time points examined from the arrays, a few genes were selected for further investigation. It would not have been feasible to look at all twenty genes due to the constraints of both time and funding for this study. The selected genes were used for protein studies; examining expression of the proteins at four stages of development. These studies were completed with a view to complete possible future functional studies.

The two genes selected for further investigation were *axl* and *mcl-1*. Axl had previously been shown to be expressed in both bovine and rat lenses (Valverde *et al.* 2004) This study was completed to identify whether axl was also expressed in the mouse lens. The normal physiological role of axl in the lens is yet to be elucidated.

Mcl-1 demonstrated differential expression from both the PCR and array results. It is a member of the Bcl-2 family, members of which have been shown to be present in the lens previously. Overexpression of Bcl-2 has been shown to result in abnormal differentiation of fibre cells (Fromm and Overbeek 1997; Sanders and Parker 2003). There are two known isoforms of mcl-1, a short pro-apoptotic form and a longer anti-apoptotic form (Bae *et al.* 2000). The shorter isoform is formed as a result of alternative splicing of the mcl-1 gene. The presence of these two isoforms was examined to see if there was any change in expression of these two isoforms over the developmental stages examined.

Western blotting was completed to examine the expression of these two proteins in the lens during maturation. Four developmental stages were used: NB, P7, P14 and 4 weeks. Results are shown in **Figure 3.10**. Both axl and mcl-1 protein expression was confirmed in the mouse lens. Densitometry analysis was completed to identify differences in expression between the time points; results are shown in **Figure 3.11**. Statistical analysis of the western blotting results is given in **Appendix 7**. The only comparison that showed a statistically significant difference was between new born and P7 for the long isoform of Mcl-1.

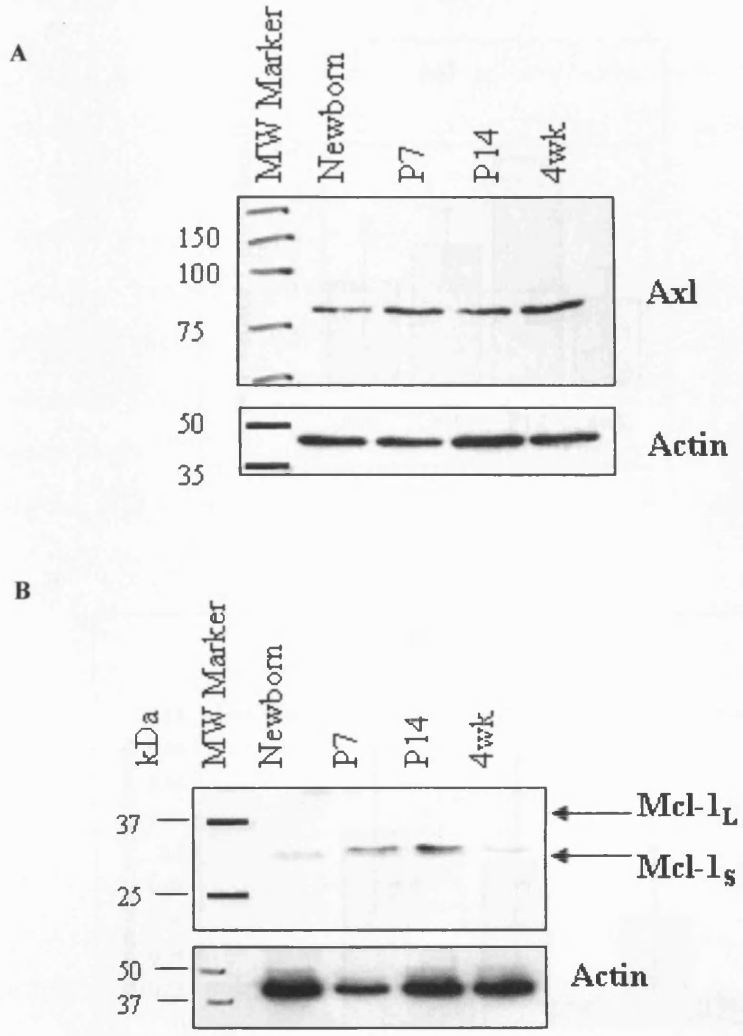

Figure 3.10: ***Western blotting results.*** *10μg of each protein sample was loaded onto the gel. Following the addition of ECL reagents to the membrane, the membranes were exposed to the film for 10 minutes (actin exposure was 1 minute). The membranes were stripped and reprobed with an actin antibody to confirm equal loading of protein in each well. Results presented demonstrate protein expression for both axl (A) and mcl-1 (B). Figures are representative of the three sets of results produced. Each western blot was completed using an individual protein sample for each of the time points extracted from the lenses of a litter of pups (between 5 and 8 pups).*

A

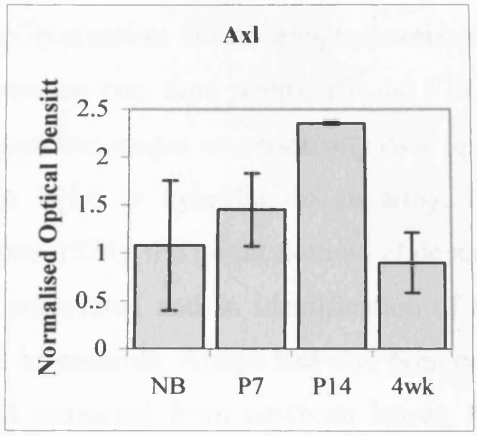

B

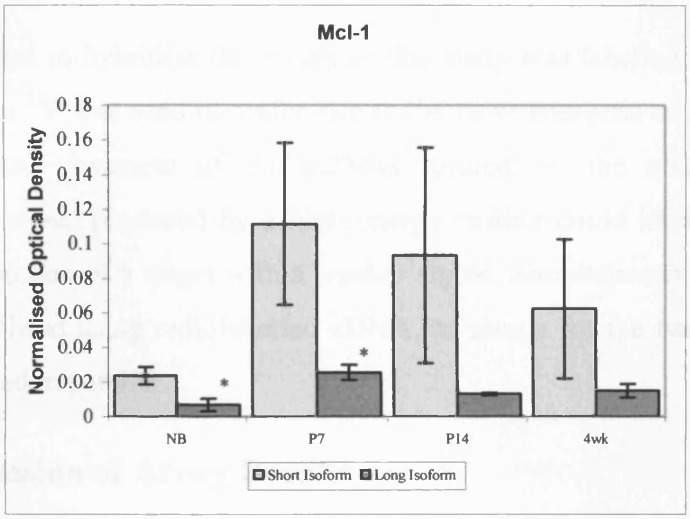

Figure 3.11: Graphical representation of the western blotting results obtained. *Results presented demonstrate the densitometry results obtained for the bands produced from the western blotting films. Protein expression for both axl (A) and mcl-1 (B) was observed. The results from the three sets of western blotting experiments completed were combined to give the average optical density presented here. The results obtained from the blots of the protein of interest were normalised to the intensity measured for the actin loading control for each time point. Error bars represent the standard error of the mean. A statistically significant difference was observed in expression for mcl-1_L between NB and P7; statistical significance is demonstrated by the presence of the asterisk.*

3.4. Discussion

In this study, the gene expression of 243 apoptosis-related genes in the mouse lens was compared between two time points, P7 and P14, using a macroarray. Tissue at these developmental stages was relatively easy to obtain and an average litter provided enough RNA to hybridise to an array. By P14, eye opening (Kuwabara and Imaizumi 1974), the initial flourish of denucleation and organelle degradation has been completed and so identification of the genes involved in these processes should be possible. Arrays had also been completed using cDNA synthesised from RNA extracted from newborn lenses, but these arrays were unsuccessful. This result was probably due to limited quantities of RNA extracted from the newborn lenses.

The cDNA used to hybridise the arrays in this study was labelled with ^{33}P. For array detection ^{33}P was used in preference to the more energetic emitter ^{32}P. Due to the physical closeness of the cDNAs located on the arrays a strong hybridisation signal produced by a high energy emitter could interfere with, or mask, the detection of a target with a weaker signal. Simultaneous hybridisation can not be utilised using radiolabelled cDNA, so arrays for the two time points were completed in parallel.

3.4.1. Discussion of Array Results

The onset of organelle degradation precedes the postnatal stages examined in this study; secondary fibre cell denucleation begins at E17.5, with the maturation of the lens complete by P14 (Kuwabara and Imaizumi 1974). However, as organelle degradation continues throughout life, some cells from the whole lens would be going through this process at each of the stages examined and so identification of the genes identified in these processes should be possible when compared to an earlier stage such as P7.

As discussed previously in **Section 1.3.3**, lens fibre cells have been shown to cease both transcription and translation at the time of organelle degradation (Faulkner-Jones *et al.* 2003; Ozaki *et al.* 1985; Shestopalov and Bassnett 1999). From the research discussed in **Section 1.3.3**, large quantities of RNA would not

be expected to be extracted at the later stages due to its degradation in lens fibre cells. To overcome this potential problem, whole lenses were used to collect the samples in this study; as the lens continues to grow throughout the lifetime of the organism the epithelial cells will be constantly differentiating into fibre cells. During differentiation, the genes involved in the process of organelle degradation should still be expressed in the cells in the equatorial region and the outermost fibre cells of postnatal mouse lenses.

Over 100 (86 at P7 and 161 at P14) of the genes immobilised on the array were shown to be expressed above background levels + 2SDs of background in at least one of the time points examined. Twenty genes showed significant differential expression, with higher expression at P14. From the array results a larger number of genes were shown to be expressed above background at P14 when compared to P7. This was an unexpected result; by P14 the majority of lens maturation is complete. The only cells undergoing differentiation at this time point are those located at the equatorial region. Cells located in the epithelium near the ciliary body will still be proliferating and it is these cells along with those in the equatorial region that will still be actively transcribing RNA. The difference in gene expression observed could potentially be explained by the increase in size of the lens between P7 and P14. Previous studies have observed that the OFZ increases in size by approximately 80μm/day encompassing more of the secondary fibre cells (Bassnett and Beebe 1992). The increase in size of the lens between these two time points would suggest an increase in proliferating epithelial cells and differentiating fibre cells; this could be a possible reason for the increase in number of genes expressed between these developmental stages.

In support of the suggestion that the apoptosis pathway has a role in lens differentiation, over one hundred apoptosis-related genes were shown to be present in the lens in this study. It is likely that even though these genes were identified at stages after the initial formation of the OFZ they could still be involved in its formation. However, the identification of these genes from the array results does not indicate where they are expressed (i.e. in which sub-compartment in the lens). These genes may be expressed in the equatorial region where differentiation is beginning, or they could be located in the lens epithelium

where they could be involved in epithelial remodelling or in the outer cortical lens fibre cells, which have yet to lose their nucleus.

Following the completion of the array results, 3 housekeeping genes were shown not to be expressed above background. Subsequently PCR reactions were completed which demonstrated expression of these genes in the lens, results of which demonstrate varying expression across the developmental time points. Normalisation of the array results was completed using the results obtained for the remaining housekeeping genes as standards. The variability of results for the three housekeeping genes tested by PCR could suggest that the expression of the remaining housekeeping genes used for the normalisation process could also vary during development. This correlates with the observation that the number of housekeeping genes surviving filtering differs between the two time points. This could then affect the normalisation process. However the 20 genes identified from normalisation with the housekeeping genes were also identified by global normalisation, adding weight to the suggestion that they are significantly differentially expressed.

3.4.2. Functions of the Genes Identified by the Arrays

Twenty genes were shown to have a significant change in gene expression between the two time points examined (shown in **Table 3.1.**); all with highest expression at P14. A brief description of function of these genes is included here.

P53 is a well-characterised tumour-suppressor gene which has been shown to play a role in a number of cellular processes including responding to DNA damage (Kastan *et al.* 1991), apoptosis (Shaw *et al.* 1992) and cell cycle progression (Kuerbitz *et al.* 1992). Recently, p53 has been shown to be expressed in the lens epithelial cells of central and pre-germinative zones and in the lens fibre bow in the lens of adult mice (Pokroy *et al.* 2002). The role of p53 in lens cells has been examined through the use of transgenic mice generated to express wild-type human p53. These mice developed microphthalmia as a result of apoptosis induction in differentiating lens fibre cells (Nakamura *et al.* 1995). P53 has also been observed to play a role in the differentiation of normoblasts; the advanced stage of erythropoiesis (Peller *et al.* 2003).

Mouse double minute protein 2 (**Mdm2**) has been shown to have affects on the cell cycle, apoptosis and tumourogenesis through its interactions with other proteins including p53 and retinoblastoma 1 (reviewed in Momand *et al.* 2000). Mdm2, which has been shown to have intrinsic E3 ligase activity, is the main inhibitor of p53 maintaining low levels of p53 expression in non-stressed cells by increasing the degradation of p53 by the 26S proteasome (reviewed in Michael and Oren 2003).

Death-domain-associated protein (**Daxx**) was originally identified as a protein demonstrating specific binding to the death domain of the transmembrane death receptor FAS and was thought to be involved in the promotion of Fas-induced apoptosis (Yang *et al.* 1997b). However, homozygous deletion of Daxx was seen to results in embryonic lethality, with widespread apoptosis observed in Daxx-deficient embryos (Michaelson *et al.* 1999). This suggests that Daxx plays an important role in embryonic development. This protein has also been shown to play a role in regulating transcription. RNAi was used to prevent the expression of Daxx; cells showed increased apoptosis, suggesting an anti-apoptotic role for Daxx. Transcriptional activity was also observed to decrease (Michaelson and Leder 2003). Daxx is also known to be involved in the p53/mdm2 pathway. Downregulation of Daxx was seen to decrease mdm2 expression levels and it was noted that Daxx enhances the E3 activity of mdm2 towards p53 (Tang *et al.* 2006).

The exact physiological function of the normal Huntingtin (**hd**) protein has yet to be elucidated. The mutant form of protein, containing a CAG expansion region in the first exon, has been shown to result in a progressive neurodegenerative disorder (reviewed in Reddy *et al.* 1999). Huntingtin has been shown to interact with a wide range of proteins, including caspase-3, and has been proposed to play a role in both membrane trafficking and apoptosis (Harjes and Wanker 2003).

Transforming growth factor β2 (**tgfβ2**) has been shown to induce an epithelial-mesenchymal transition, characteristic of the changes observed in PCO (Wormstone *et al.* 2002). A role for this family in lens differentiation has also been suggested with a previous study demonstrating that disruption of TGFβ receptor signalling in lens fibre cells impaired fibre maturation (de Iongh *et al.* 2001).

Insulin-like growth factor 1 (**IGF1**) and insulin-like growth factor 1 receptor (**IGF1r**) have previously both been shown to be expressed in the lens. IGF-1 was shown to be expressed exclusively in the epithelial cells within the lens of chick embryos (Caldes *et al.* 1991). The highest expression of IGF-1r was observed in the mouse lens at the lens periphery where the germinative and transitional zones are located (Xie *et al.* 2007). IGF-1 has been shown to be a potent differentiation factor in embryonic chick lenses inducing epithelial-fibre cell differentiation (Beebe *et al.* 1987). In comparison, in rodent lenses IGF-1 was not shown to have the same effect on the cells, although it was shown to be capable of enhancing or maintaining the differentiation induced by FGF (Richardson *et al.* 1993). Overexpression of IGF-1 in the mouse lens resulted in an observed change in the morphology of the lens; a posterior expansion of the transitional zone. This suggests that IGF-1 may provide a spatial cue for this region of the lens (Shirke *et al.* 2001).

DNA fragmentation factor (**DFF**) is a heterodimer composed of 40kDa and 45kDa subunits (Liu *et al.* 1997). It was demonstrated that caspase-3 cleaves 45kDa subunit (**DFFA**) at two sites to generate an active factor, resulting in DNA fragmentation without any further requirement for caspase-3 or other cytosolic proteases. DFFA has been shown to be cleaved in the chick lens during organelle degradation (Wride *et al.* 1999), although this could be a caspase-independent process as cleavage still occurred in the presence of general caspase inhibitor Boc-D-FMK.

Galectin-3 (gal-3) has been localised to the plasma membrane of ovine lens fibre cells where an interaction with MP20, an intrinsic membrane protein, was observed (Gonen *et al.* 2000). Expression patterns of gal-3 in the human, mouse

and rat lenses have since been identified (Dahm *et al.* 2003). In human lenses, highest expression was observed during embryonic stages of development, although it continued to be expressed in adult lenses in both epithelial cells and early differentiating fibre cells (Dahm *et al.* 2003). Its expression was seen to decrease with maturation of the lens fibre cells; with no expression detected in mature lens fibres. The observations of the spatio-temporal expression of gal-3 lead to the suggestion that this molecule could play a role in cell-cell interactions and the differentiation of fibre cells. Gal-3 is also thought to play an anti-apoptotic role; a high level of both functional and structural similarity between gal-3 and Bcl-2 has been observed and gal-3 has been shown to prevent apoptosis induced by staurosporine in a human cell line (Yang *et al.* 1996).

Axl, a receptor tyrosine kinase, has previously been shown to be expressed in both bovine and rat lens epithelium (Valverde *et al.* 2004). The presence of its ligand, Gas6, was observed in the aqueous humor. Experiments completed in this study demonstrated both mitogenic and anti-apoptotic roles of Gas6. It was proposed from this finding that the Gas6/Axl interaction could play a role in regulating the normal growth of lens epithelial cells.

Myeloid cell leukaemia-1 (**Mcl-1**) is a member of the Bcl-2 family of proteins predominantly localised in the mitochondrial membrane (Yang *et al.* 1995). Two isoforms of Mcl-1 have been identified; a short isoform, containing only a BH3 domain, which is pro-apoptotic (Bae *et al.* 2000) and the originally identified long form, containing Bcl-2 homology domains 1, 2 and 3, shown to be anti-apoptotic (Kozopas *et al.* 1993). The long and short isoforms are capable of forming heterodimers and the balance between the two isoforms could determine the fate of the cells expressing both proteins. The long isoform was also shown to be capable of interacting with other proapoptotic Bcl-2 family members but not with anti-apoptotic members (Bae *et al.* 2000).

Milk fat globule epidermal growth factor 8 (**Mfge8**) was first identified in the membrane of milk fat globules (Stubbs *et al.* 1990). It has since been shown to be secreted by activated macrophages recognising apoptotic cells by binding to aminophospholipids such as phosphatidylserine (Hanayama *et al.* 2002).

Macrophages have been shown to be present during mammalian lens development. Immunohistochemical studies have shown the presence of macrophages in the ectoderm, lens vesicle, lens cavity and surrounding mesoderm where they were observed to remove degenerating epithelial cells. Macrophage localisation was shown to correlate with areas of cell death (Nishutani and Sasaki 2006). However, during the process of lens cell differentiation flipping of phosphatidylserine from the inner to the outer leaflet of the membrane is not observed, so the presence of this gene in the lens may not have been predicted.

The family of integrins are heterodimeric membrane receptors which act as signalling molecules between the cytoplasm and the cell membrane (Wederall and De Longh 2006). The integrin family have previously been shown to have a role in organisation of the cytoskeleton and have demonstrated ability to generate intracellular signals inducing proliferation (Giancotti 1997). Western blotting was used to examine the expression of intergrins in the embryonic chick lens (Menko and Philip 1995). The results of this study did not show **Integrin-αV** expression.

Cyclin-dependent kinase 4 (**cdk4**) belongs to a family of serine/threonine protein kinases which are essential for the progression of the cell cycle (Sherr 1993). The kinase activity of this protein is regulated by a member of the cyclin family (cyclin D). Cdk4 has been shown to have role in the regulation of the G1/S transition (G1 is the first gap phase, S is the DNA synthesis phase) (Sherr 1993). Both the mRNA and protein for cdk4 have previously been identified in both the epithelial and fibre cells of the rat lens during early development, E16 to P8, alongside other members of the same family (Gao *et al.* 1999). Other members of the cyclin-dependent kinase family have been shown to be involved in the process of primary fibre cell denucleation in the embryonic chick lens (He *et al.* 1998) so the presence of cdk4 in the rat lens during the stages of development described by Gao *et al.* could suggest a role for cdk4 in this process as well.

Death associated protein 1 (**Dapl**) is a small proline rich protein shown to be located in the cytoplasm. Dapl belongs to a family of 5 novel genes, shown to mediate cell death induced by interferon-γ (Levy-Strumpf and Kimchi 1998). Dapl is known to interact with the cytoplasmic death domain of TNF-R1 and overexpression of this protein has been shown to induce apoptosis (Liou and Liou 1999).

Five other genes were shown to be differentially expressed: **P2rx1** belongs to the family of P2x class of cell surface receptors. It functions as a ligand-gated ion channel activated by the binding of ATP. P2x family members have been noted to play a role in cellular signalling (Khakh and North 2006). Bcl-2 family member Bcl2a1a (**A1**) is an anti-apoptotic protein shown to bind to bid and prevent apoptosis caused by cytochrome c release induced by TRAIL and CD95 (Werner *et al.* 2002). Two members of the sterol regulatory binding family, ***srebf1*** and ***srebf2***, were also shown to be differentially regulated. These genes are transcription factors with a role in lipid biosynthesis (reviewed in Shimano 2001). The last of the genes shown to be differentially expressed was ***thrombospondin.*** Thrombospondin has previously been shown to be expressed in the eye where it was shown to have a role in modulating interactions between cells and the cellular environment (Hiscott *et al.* 2006). It is also known to play a role in the inflammatory response and angiogenesis (Adams and Lawler 2004).

3.4.3. Discussion of PCR confirmations

Semi-quantitative PCR results confirmed expression in the mouse lens of all differentially expressed genes identified from the arrays. The expression levels of the genes of interest at both P7 and P14 demonstrated by the PCR results were compared to that obtained from the arrays. 52% of the genes tested (10/19) confirmed the differential expression observed from the array results; with higher expression at P14 observed. Gene expression for all genes was also observed in newborn and 4 week old lenses.

The gene expression differences seen from the arrays were not observed from the PCR results, although a similar trend in expression was observed for the majority of the genes examined. Some genes e.g. *IGF-1* and *A1* showed the opposite expression from the PCR results, demonstrating increased expression at P7.

The level of gene expression observed from the array results was seen to have no bearing on whether the expression would be confirmed by PCR (see **Table 3.4**). For example, from the array results *integrin-αV* was shown to have a 2.2 fold change in expression with original intensities of 6.5 at P7 and 14.6 at P14 but the PCR results for the gene demonstrated higher expression at P7.

Gene Name	Ratio Observed from Array Results	Ratio Observed from PCR Results
P2rx1	8.81	Unsuccessful
Hd	7.34	1.27
Dffa	3.84	0.91
Mdm2	3.51	2.08
Mfge8	3.13	1.11
Igf1r	2.93	1.06
Axl	2.9	0.36
Galectin-3	2.68	1.21
A1	2.66	0.19
Cdk4	2.58	1.00
Srebf2	2.57	1.22
TGFβ2	2.43	1.18
Dap1	2.23	0.99
Integrin-αV	2.23	0.71
P53	2.21	1.59
DAXX	2.18	1.17
Thrombospondin	2.17	0.30
IGF-1	2.12	0.15
Srebf1	2.02	0.84
Mcl-1	2.01	7.07

Table 3.5: ***Ratio of gene expression observed from the array and PCR results.*** *The average expression was compared between P7 and P14 for each of the techniques and a ratio (P14/P7) was calculated. The ratios of expression observed from the array results were not corroborated by the subsequent PCR reactions.*

Previously published lens microarray papers (Hawse *et al.* 2005; Ivanov *et al.* 2005; Mansergh *et al.* 2004; Wride *et al.* 2003; Xiao *et al.* 2006) were examined to ascertain the PCR confirmation rate achieved for the genes demonstrating differential expression. Three of the studies looked at used semi-quantitative PCR to confirm the preferential expression of the genes identified in a particular cell type/strain (Hawse *et al.* 2005; Mansergh *et al.* 2004; Wride *et al.* 2003). The results of these studies varied between a 47% and 100% confirmation rate.

Two studies used quantitative PCR to confirm the difference in expression observed from the array results. The confirmation rate for this technique also varied; from 50% (Xiao *et al.* 2006) to 100% (Ivanov *et al.* 2005). Confirmation rate was seen to decrease with number of genes examined; Ivanov *et al.* confirmed the expression of 9 genes, Xiao *et al.* examined 80 and confirmed the expression of 40.

The results from the arrays and subsequent PCR confirmations show that the arrays used, although good at providing an overall profile of gene expression, may not be able to accurately demonstrate differential expression between time points. Quantitative PCR should be used to analyse the differences in gene expression more accurately.

The observation that these genes are expressed in the lens, does not necessarily suggest that they are involved in the processes of organelle degradation and/or denucleation. They could be involved in the general remodelling of the lens epithelium during development. However, the developmental time points for identification of apoptosis genes were selected because they represent periods during which the formation of the OFZ (involving apoptosis signalling) is progressing rapidly.

3.4.4. Discussion of Western Blotting Results

Protein expression of both axl and mcl-1 was observed at all the developmental time points examined. Axl had previously been shown to be expressed in the epithelial cells of both rat and bovine lenses (Valverde *et al.* 2004). The results from this study demonstrated the expression of axl in the postnatal mouse lens. No statistically significant difference in expression of axl was observed between any of the stages examined.

Previously the expression of the ligand for axl, Gas6, was demonstrated in the aqueous humor (Valverde *et al.* 2004). The localisation of expression of axl and its ligand have lead to the suggestion that these proteins may play a role in the proliferating epithelial cells but not in fibre cells. Gas6 has been shown to have an anti-apoptotic role, protecting cells from TNFα induced apoptosis (Valverde *et al.* 2004). It has been hypothesised that the presence of these proteins could help regulate the normal development of the lens epithelium.

The western blotting results presented in this chapter demonstrated the expression of both the long and short forms of mcl-1 in the postnatal mouse lens. Looking at the results produced it has been observed that the short isoform of mcl-1 (the pro-apoptotic form), is expressed at higher levels than the long isoform. The long and short isoforms have been observed to form heterodimers and the balance between the two has been suggested to determine the fate of the cell (Bae *et al.* 2000). The presence of a higher quantity of the short isoform could suggest the activation of a pro-apoptotic pathway in the lens. A significant increase in the long isoform was observed between the newborn and P7 results.

Although densitometry is a useful tool for measuring the relative protein expressions, there are some negative factors that need to be considered. It is highly reliant on the gel being of the utmost quality. If there are any imperfections (such as samples running at slightly different speeds) then it is more difficult to obtain an accurate value for the molecular weight for each band. Problems encountered during the transfer process from gel to membrane can also impact the results obtained.

The western blotting results produced from this study do not determine the localisation of these proteins; merely demonstrate their expression in the mouse lens. There is a large variation in results obtained from the western blotting experiments.

In summary the results included in this chapter show:

- Over 100 apoptosis-related genes (86 at P7 and 161 at P14) were shown to be expressed above background + 2SDs in at least one of the stages.
- 20 genes were shown to be significantly differentially regulated between the two time points examined, all with highest expression at P14.
- Semi-quantitative PCR was used to confirm differential expression for 52% of the genes identified.
- Two genes were selected to undergo further investigation, *axl* and *mcl-1*, which could possibly lead to future functional studies. Protein expression of these two genes was confirmed at all developmental time points examined.

Chapter 4: Examination of the Role of Huntingtin in Mouse Lens Development

4.1. Introduction

Huntington's disease is an autosomal dominant neurological disorder caused by triplet CAG repeat, encoding glutamine, in first exon of the huntingtin gene (*hd*) (reviewed in Reddy *et al.* 1999). This disease is characterised by involuntary movements, intellectual impairment and emotional disturbances. Huntington's tends to be an age-related disease mainly affecting people in middle-age, although individuals with an increased number of triplet repeats present with an earlier onset of the disease (reviewed in Young 2003). The toxicity of huntingtin is directly correlated to the number of CAG repeats it contains; in an unaffected individual *huntingtin* will contain 9-34 CAG repeats whilst in those affected the gene will include more than 40 repeats (Snell *et al.* 1993).

The extended CAG repeat which leads to the toxic function of huntingtin, results in the inclusion of a long polyglutamine tract at the N-terminus of the protein (Sharp *et al.* 1995). This polyglutamine tract has been observed to increase the chance of protein aggregation (reviewed in Walker 2007). The huntingtin protein has been shown to interact with proteins that regulate transcription (Kegel *et al.* 2002), apoptosis (Zhang *et al.* 2006) and axonal transport (Velier *et al.* 1998). In addition to its interactions with other proteins, the mutant form of the protein is thought to have an effect on the function of the normal protein and this dominant negative effect has been proposed as a mechanism for Huntington's pathogenesis (reviewed in Walker 2007).

A number of mouse models have been generated to elucidate the mechanism of Huntington's disease. The mouse model used in this study was generated on a C57/Bl6 background. Gene targeting was utilised to introduce an extended (150bp) CAG repeat into exon 1 of *huntingtin*. A two-step gene targeting strategy was utilised; firstly exon 1 of the gene was replaced in embryonic stem cells (ES cells) with a selectable marker, hprt. The ES cells containing this modification were then identified and used in the second stage where the hprt marker was replaced with an extended repeat version of exon 1. The result of this

ensures that the ES cells containing the modification only differ from the wild-type cells by the length of the CAG repeat (Lin *et al.* 2001). Expression of the mutant hd protein has been previously confirmed by western blotting in both the ES cells and in the brains of mutant mice (Lin *et al.* 2001). Mice with this knock-in mutation demonstrated late-onset behavioural and neuroanatomic abnormalities. No early developmental phenotype was noted and the mice were seen to develop normally with no severe neurological defects observed.

Results from **Chapter 3** showed that *huntingtin* was differentially expressed between postnatal days 7 and 14 in the mouse lens, with highest expression at P14. Semi-quantitative PCR results confirmed this differential expression and also demonstrated expression in both newborn and 4 week old mice. The aim of this study was to examine the morphology of the lens from eyes collected from mice with a mutant knock-in CAG repeat. The morphology was compared between wild type ($^{-}/^{-}$), heterozygotes ($^{+}/^{-}$) and homozygotes ($^{+}/^{+}$).

4.2. Experimental Design

The methods used in this chapter have already been described in the general methods chapter (**Chapter 2**). This part of the study used eyes from the mouse line described previously in **Section 4.1**. Eyes were collected from P2 mice (provided by Dr. Lesley Jones' lab based at the Heath Hospital). By P2, the OFZ in the centre of the lens has been established (Bassnett 2002). At this time point an alteration in the formation of the OFZ should be apparent, so the affect of this knock-in mutation could be identified. Tail tips were also collected from each pup to allow the genotype of each mouse to be established.

Following collection, excess tissue was removed from around the eyeball and small incisions were made in the back of the eye; this allowed for the fixative to enter the eye effectively. The eyeballs were then fixed in 4% PFA overnight before dehydrating and embedding in wax. Eyeballs were embedded with the optic nerve orientated towards the right of the embedding ring. Following sectioning (7μm sections) haematoxylin and eosin staining was utilised to examine the lenses and to note the morphological differences that were present, between the wild-type (WT), heterozygous (Hets) and homozygous (Homs) mice.

Images were taken of the haematoxylin and eosin staining using a Leica DMRA2 microscope using the Lecia QWin V3 software (Leica Systems, UK). Photographs were taken of sections seen to include the optic nerve, these sections should be through the centre of the lens. Three eyes for each genotype, each from a different pup, were photographed with five sections from each eye collected for analysis.

Following the generation of images of the eyes from each of the genotypes, image analysis was performed using ImageProPlus (MediaCybernetics, UK). This allowed for measurements to be made of the overall size of the lens as well as measurements of the OFZ dimensions (see **Figure 4.1** for details of the

measurements made). The images were coded prior to analysis to avoid any bias of the results generated.

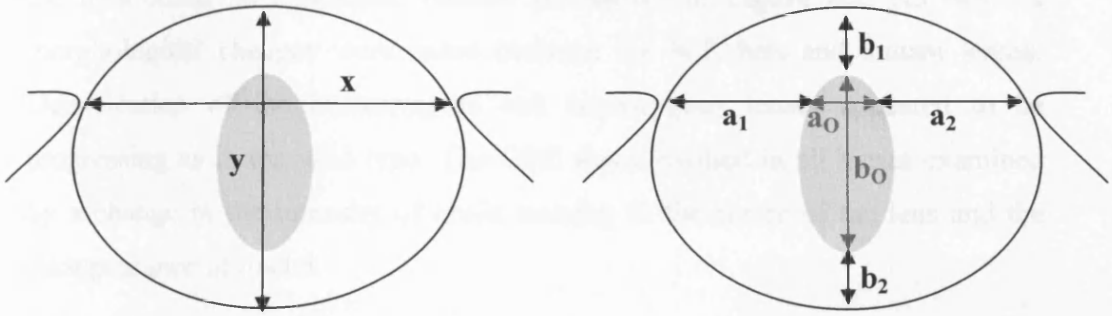

Figure 4.1: ***Diagram demonstrating the measurements taken for each lens using the image analysis software.*** *Measurements for a_o and b_o were not taken; instead these values were calculated using the results from the other measurements. Measurements for x were made in line with the iris.*

4.3. Results

Wax sections were stained with haematoxylin and eosin so the morphology of the lens could be examined. Results are shown in **Figure 4.2**. No obvious morphological changes were noted between the WT, hets and mutant lenses. Denucleation of the heterozygous and homozygous lenses appeared to be progressing as in the wild type. The OFZ was identified in all lenses examined by a change in the intensity of eosin staining in the centre of the lens and the disappearance of nuclei.

To examine the morphology of the lenses more closely measurements were taken using the image analysis software (Image-Pro Plus, UK). This allowed for more subtle changes in the lens morphology, e.g. alterations in the overall lens size or in the size of the OFZ, to be examined. Results are shown in **Table 4.1**.

Usable sections through the centre of the lens were not obtained for the heterozygote eyes, due to excessive tearing of the tissue during the sectioning process. The images gathered for this genotype were therefore not used for the image analysis as they could possibly skew the results obtained. An unpaired t-test was used to compare the average dimensions of the lenses from wild-type and homozygote lenses. No statistically significant differences were observed between Wt, Hets and mutants for any of the lens dimensions measured.

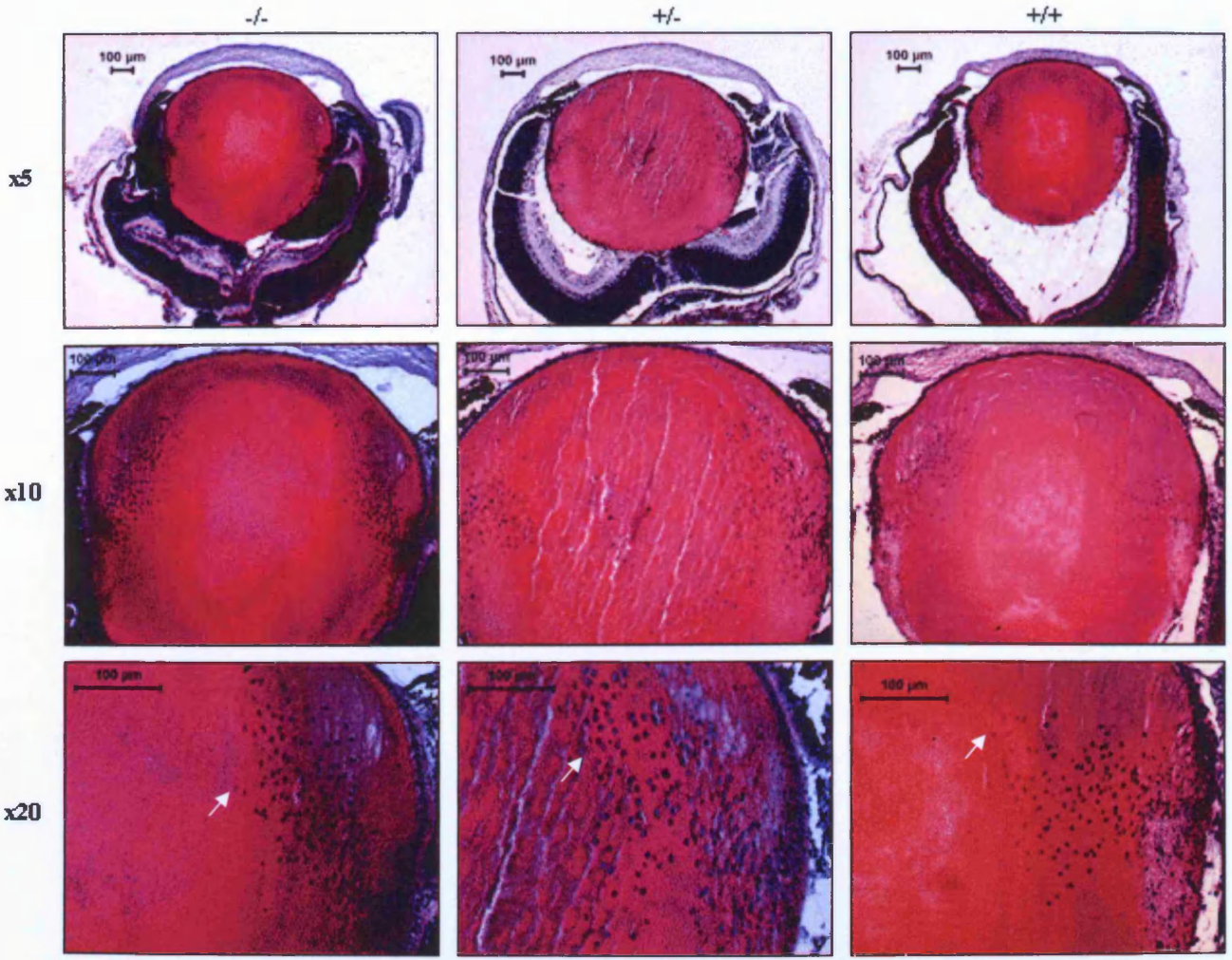

Figure 4.2: ***Histological examination of lens morphology in Huntingtin mutant Vs WT, Vs Het mouse lenses.*** *Lenses were stained with haematoxylin and eosin so the morphology of the lenses could be examined. Lenses were compared between wild-type (-/-), heterozygotes (+/-) and homozygotes (+/+). Numbers on the left hand side of the figure represent the magnification under which the picture was taken. Scale bars represent 100µm. White arrows indicate the position of the nuclei nearest the centre of the lens i.e. at the border of the OFZ. Measurements were made as detailed in* ***Figure 4.1****.*

Measurement	Wild-type			Homozygote			*p*-value
	1	2	3	1	2	3	
x	803.70	766.94	705.95	768.58	738.31	724.05	0.652
y	847.71	758.31	880.69	812.47	792.38	746.62	0.338
a_1	189.14	174.94	211.1	209.26	193.55	214.17	0.318
a_2	184.99	193.37	203.52	222.70	200.67	226.93	0.079
a_o	429.56	398.63	291.33	336.61	344.09	282.95	0.323
b_1	63.89	66.32	92.68	100.40	66.81	125.35	0.295
b_2	176.36	119.17	138.74	162.87	142.80	144.12	0.788
b_o	607.47	572.82	649.28	549.21	582.77	477.15	0.127

Table 4.1*: **Results from image analysis of haematoxylin and eosin staining of Huntingin mutant Vs WT, Vs Het mouse lenses.** The sections from 3 lenses from each genotype were photographed for analysis. Four or five sections from the middle of each lens (seen to include the optic nerve) were analysed (see **Figure 4.1** for details of the measurements made) and the average calculated. One measurement was made for each dimension for each of the 5 sections from the 3 eyes from each genotype; the average measurement is presented here. The average measurements for each of the distances were compared between the two genotypes using an unpaired t-test; the p-value is presented. All values given in the table (except the p-value) are given in microns.*

4.4. Discussion

The mouse model used in this study was generated to contain an extended CAG repeat (150bp) in the first exon of *huntingtin*. Lenses were collected from wild-type, heterozygous and homozygous mice. Following the examination of the structure of 3 lenses from each genotype no obvious morphological difference was observed. Denucleation was still seen to proceed along with formation of the OFZ in all the lenses examined. Further analysis was completed for the images produced from lenses from the wild-type and homozygous mice; no statistically significant differences were observed for any of the lens dimensions. This was not unexpected as Huntington's is an age-related disease and there are no recorded developmental problems with the eyes of Huntington's patients. Further work could look at the effect of the mutated gene in ageing mice, to see if any lens abnormalities arise later in life.

This model system demonstrated no developmental problems in the lens linked to the mutant form of *hd*. There is a possibility that the mutant protein is not expressed in the lens, this could explain the lack of an observed phenotype. Western blotting could be utilised to examine the specific expression of the mutant protein to confirm its presence or absence in the lens. The use of a knockout mouse could possibly provide a greater insight into the role hd plays in lens development. Deletion of the huntingtin protein has shown to be embryonic lethal (Duyao *et al.* 1995), so a conditional knockout would have to be used to knock-out this gene in the lens selectively.

In summary the results of this chapter show:

- Lens morphology was not affected by the mutant form of the huntingtin protein.
- Denucleation was still seen to occur, suggesting that the mutant *huntingtin* gene does not affect this process during development.

Chapter 5: Apoptosis Gene Expression in the Embryonic Chick Lens: A Comparative Study

5.1. Introduction

In **Chapter 3** the results for the mouse apoptosis arrays are presented. Genes shown to have high expression or demonstrating differential expression between the time points were identified. Following the identification of these genes, the expression of the genes shown to be differentially regulated was confirmed using RT-PCR. The aim of this part of the study was to examine the expression of genes identified from the mouse arrays in embryonic chick lenses. This would enable a cross-species comparison between the mouse and chick with a view to completing functional studies in the future.

Previous morphological studies suggest that the process of organelle degradation between mouse and chick is relatively similar although it is unknown whether the underlying biochemical mechanism is the same in both species (Bassnett 2002). Underlying differences in this process have been observed; chromatin marginalisation and subsequent collapse has been noted in the chick lens but not in the mouse.

In this study, six embryonic stages have been used to examine gene expression, ranging from embryonic day 6 (E6) to embryonic day 16 (E16). From previous studies it has been observed that organelle degradation begins at approximately E12 and by E21 (hatching) the organelle free zone is as large as the diameter of the pupil of the eye (Bassnett and Beebe 1992). Previous studies have examined the disappearance of intracellular organelles in the embryonic chick lens; a brief description is given here.

Fragmented mitochondria were observed as early as E8 in the central fibre cells. By E10 the mitochondria were swollen and by E12 the central region of the lens lacked mitochondria. Coincidently, the nuclei were found to decrease in size (at E8) and disappeared from the central fibre cells by E12 (Bassnett and Beebe 1992). Loss of nuclei and mitochondria was seen to occur simultaneously and abruptly (2-4hr). The endoplasmic reticulum was seen to disappear with the nucleus at the edge of the OFZ. The Golgi apparatus was seen to fragment in the cells at the lens equator (Bassnett 1995).

The chick system is relatively cheap and easy to manipulate making it ideal for developmental studies. With the development of the *in ovo* electroporation technique very large complex constructs can be injected into a specific population of cells, allowing loss-of-function or gain-of-function studies to be completed (Chen *et al.* 2004; Nakamura *et al.* 2004). The use of this model system is further promoted with the recent availability of the chick genome. Genes shown to be expressed in the chick lens during this study could be knocked out using *in ovo* electroporation to investigate their function in the lens.

Also, the lens epithelial cell culture developed by Menko *et al.* demonstrated the formation of lentoid bodies following 3 days in culture (Menko *et al.* 1984). These lentoid bodies were seen to demonstrate characteristics of fibre cells. This culturing method has been demonstrated to be useful in determining the role of certain proteins in the lens. This method of cell culture has subsequently been used to look at the role of members of the apoptotic pathway in lens differentiation. Synthetic peptides were added to the lens epithelial cell cultures to knockdown the expression of caspases -1, -2, -4, -6 and -9; following the addition of these peptides to the cultures a decrease was observed in the number of degenerating nuclei (Wride *et al.* 1999). This system has also been used to examine the role of the TNF family in this process. The addition of TNFα to lens cell cultures induced nuclear degeneration, whereas when antibodies to TNFα, TNFR1 and TNFR2 were added to the cultures, blocking the function of these proteins, the number of degenerating nuclei was seen to decrease suggesting a role for this family of proteins in nuclear degradation in the lens (Wride and Sanders 1998).

5.2. Experimental Design

The methods used in this chapter were previously described in the general methods chapter (**Chapter 2**). RNA was isolated from lenses of embryos at two day intervals between E6 and E16. These time points were chosen as they encompassed stages of development both proceeding and following the onset of organelle degradation. These RNA samples were quantified and used to synthesise cDNA. This cDNA was subsequently used in semi-quantitative PCR reactions to examine the expression of the genes identified from the apoptosis arrays (results discussed in **Chapter 3**). Each PCR was completed three times, each time with a different cDNA sample collected from pooled lenses extracted from 20-24 embryos. PCR products were run out on a 2% agarose gel and the resulting intensities of the individual bands were quantified using Scion Image software (USA). The three sets of results were combined to give the average band intensity for each of the stages examined.

Primers were designed for the genes shown to have the highest expression from the array results as well as those shown to be differentially expressed. Eighteen of these genes had a known nucleotide sequence included in the NCBI database, Gene, and the FASTA sequence was used to design primers using the primer design programme Primer3 (http://frodo.wi.mit.edu/cgi-bin/primer3/primer3_www.cgi). For the remaining 12 genes BLAST searches were completed; comparing the mouse accession number for the gene to the chick genome. Primer sequences are included in **Appendix 4**.

Following the completion of the BLAST search, four nucleotide sequences were identified with high homology to that of the mouse genes. Primers could not be designed for one of the highly expressed genes (*mts-1*) and 5 of the differentially expressed genes (*a1, axl, cdk4, DAXX* and *p2rx1*); this was due to the limitations of the availability of the chick genome at the time this study was completed.

5.3. Results

5.3.1. PCR Results

Before completing the PCR reactions, standard curves were generated to confirm that the results produced as a result of the PCR reaction are a result of the linear part of the reaction. A number of PCR reactions were completed using different cycle numbers to produce a standard curve. Standard curves for three genes; *GAPDH* (housekeeping gene used for normalisation), *14-3-3 eta* (gene shown to have the highest expression from the array results) and *mdm2* (gene shown to have the lowest expression from the array results) are shown in **Figure 5.1.**

Expression of the genes identified from the mouse arrays was examined using semi-quantitative RT-PCR (results shown in **Figures 5.2.** and **5.4**). The average normalised band intensity was calculated and is presented graphically in **Figures 5.3** and **5.5**. Normalised band intensities and fold differences observed from the PCR results are shown in **Appendix 5**.

80% (12/15) of the differentially expressed genes examined were shown to be expressed in the embryonic chick lens (see **Figure 5.2**). 90% (8/9) of the highly expressed genes examined were shown to be expressed in the embryonic chick lens (see **Figure 5.3**). Statistical analysis was completed to identify any significant differences in expression between the time points. Using a one-way ANOVA with Tukey's post-hoc test no statistical significant differences were observed between any of the stages examined for any of the genes. An example of the statistical analysis is given in **Appendix 6**.

Galectin-3, IGF-1 and *caspase-7* were not shown to be expressed at any of the time points examined. Whole embryo cDNA samples were used as a positive control to investigate whether these genes are truly not expressed in the lens or whether the primers are faulty. PCR reactions were completed under the same conditions as the original unsuccessful experimental PCRs. Following the completion of PCR reactions using the whole embryo samples, bands were

observed for all three sets of primers suggesting that these genes are not expressed in the lens at the developmental stages examined.

The PCR reaction for *TGFβ2* was unsuccessful; despite trying many different cycle numbers and annealing temperatures multiple bands were observed.

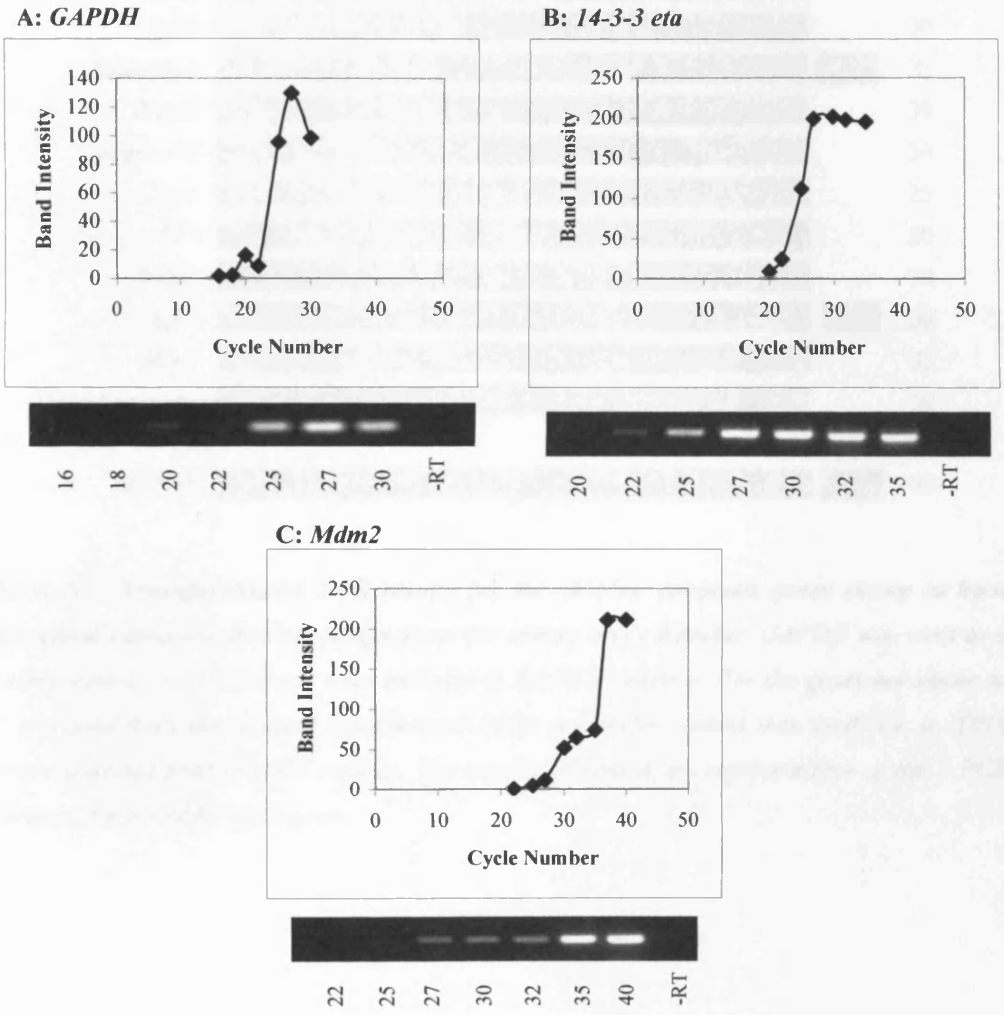

Figure 5.1: ***Standard curves for semi-quantitative PCR of chicken embryo lens.*** *Standard curves were completed for three genes to check that the results obtained from the PCR reactions were a result of the linear part of the reaction. Shown in this figure are the results for GAPDH, 14-3-3 eta and mdm2. The gel used to produce the curve is shown underneath each graph. –RT: no RT control. From these results it was decided that the cycle number used for each of these primer pairs would be as follows: GAPDH: 22 cycles, 14-3-3 eta: 25 cycles, mdm2: 30 cycles.*

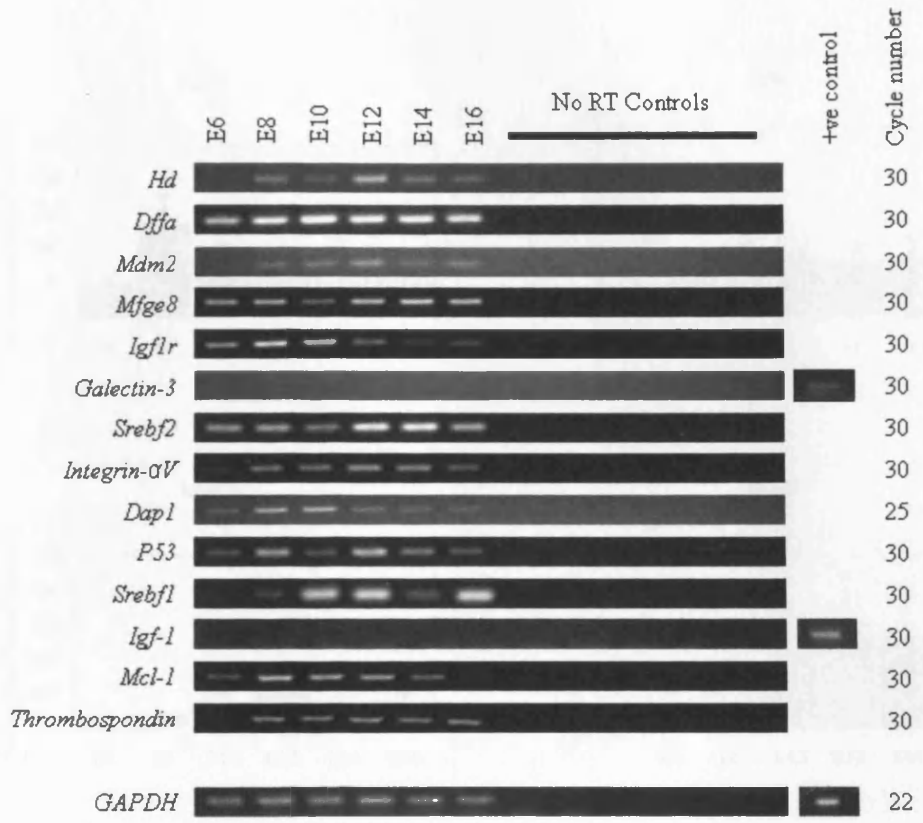

Figure 5.2: ***Semi-quantitative PCR results for the chicken apoptosis genes shown to have differential expression between stages from the mouse array Results.*** *GAPDH was used as a loading control, no RT controls were included in the PCR reaction. For the genes not shown to be expressed from the original experimental PCRs a positive control was used; i.e. a cDNA sample collected from a whole embryo. The results presented are representative of the 3 PCR reactions completed for each gene.*

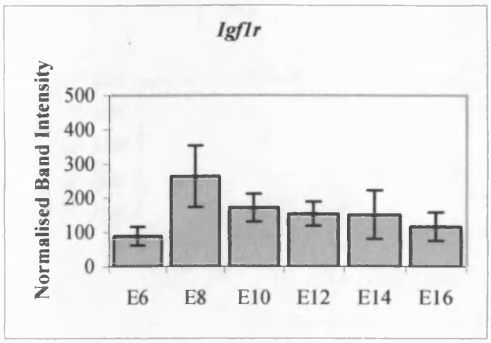

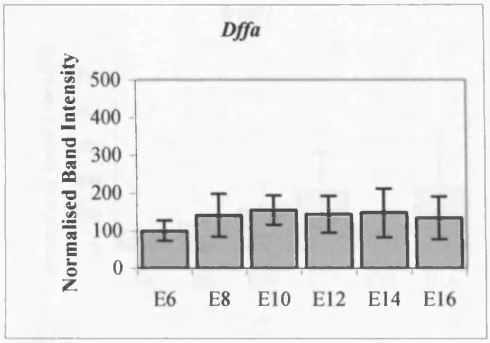

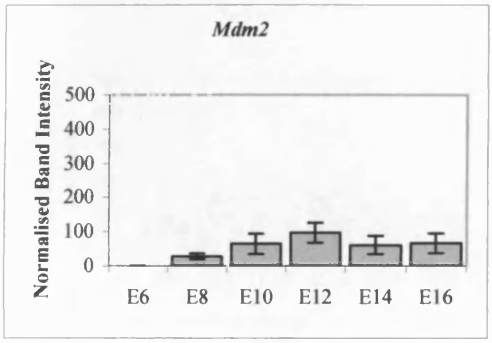

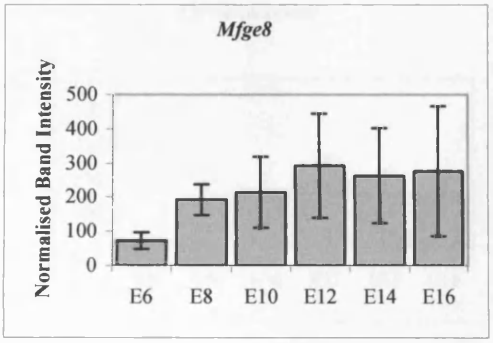

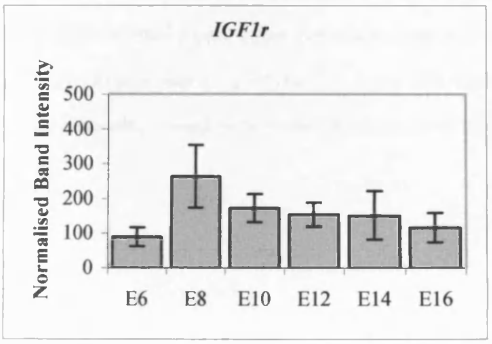

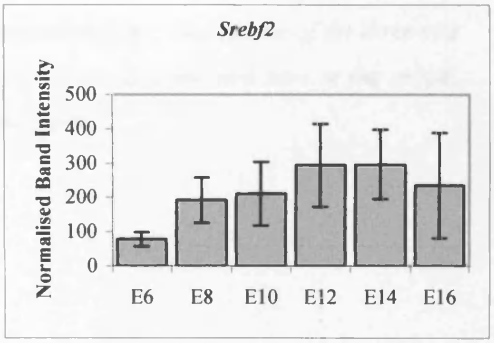

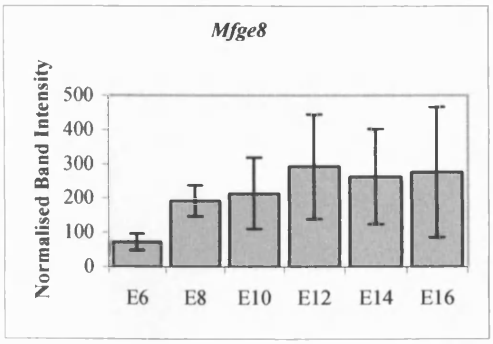

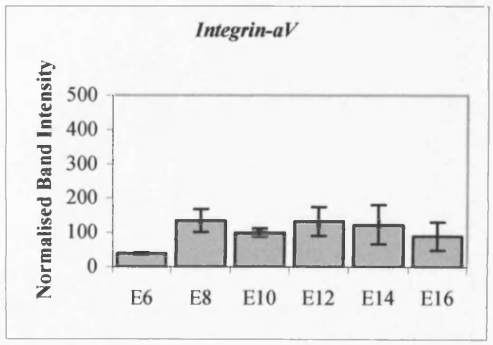

Figure 5.3 continues overleaf

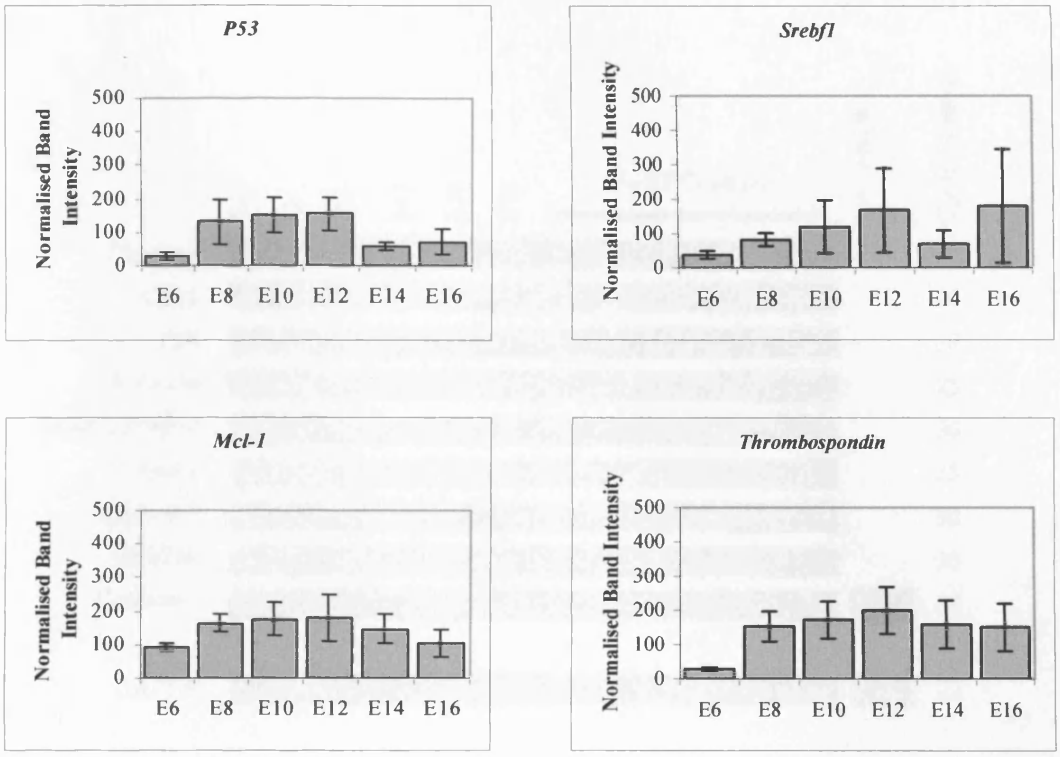

Figure 5.3: ***Graphical representation of PCR results for the chicken apoptosis genes shown to have differential expression between stages from the mouse arrays.*** *The results of the three sets of PCR results were combined to give the average band intensity presented here in the graph. Error bars displayed represent the standard error of the mean.*

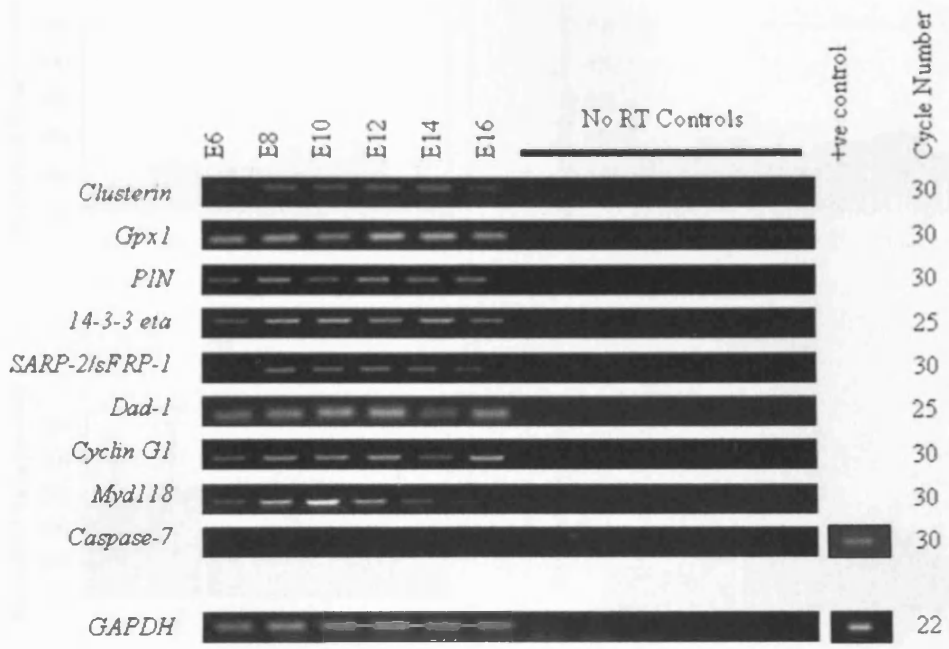

Figure 5.4: ***Semi-quantitative PCR results for the chicken apoptosis genes identified as having the highest expression from the mouse apoptosis arrays.*** *GAPDH was used as a loading control, no RT controls were included in the PCR reaction. Caspase-7 was shown not to be expressed; a positive control (whole embryo cDNA) was used to confirm that this gene was not expressed in the lens. The results presented are representative of the 3 PCR reactions completed for each gene.*

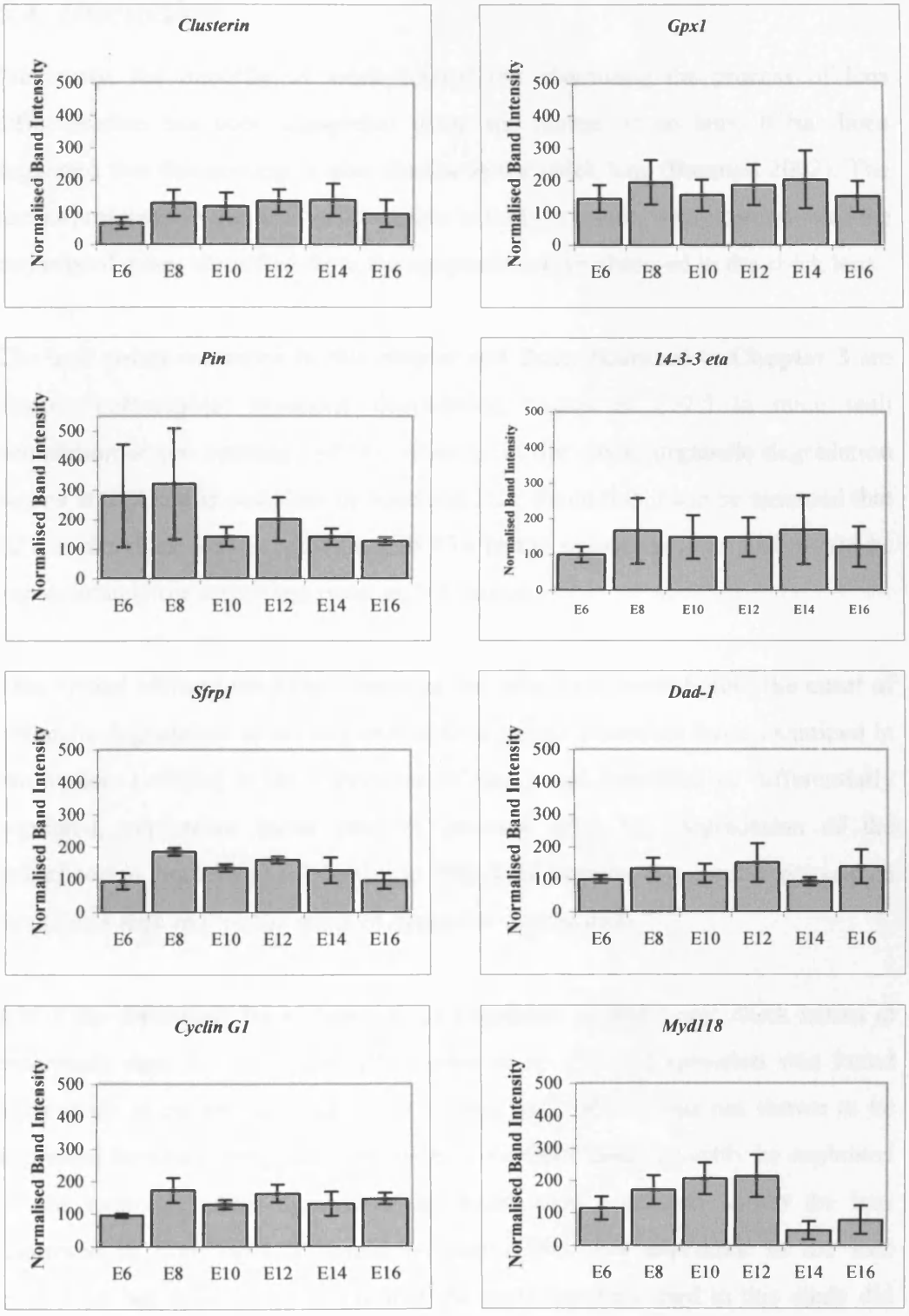

Figure 5.5: ***Graphical representation of the PCR results obtained for the chicken apoptosis genes shown to be highly expressed from the mouse arrays.*** *The results from the three sets of PCR reactions were combined to give the average band intensity presented here in the graphs. Error bars displayed represent the standard error of the mean.*

5.4. Discussion

Previously, the majority of work carried out examining the process of lens differentiation has been completed using the mouse or rat lens. It has been suggested that this process is also similar in the chick lens (Bassnett 2002). The results presented in this study add weight to that argument, with expression of the majority of genes identified from the apoptosis arrays observed in the chick lens.

The time points examined in this chapter and those examined in **Chapter 3** are directly comparable: organelle degradation begins at E17.5 in mice with completion at eye opening (~P14), whereas in the chick, organelle degradation begins at E12 and is complete by hatching E21. From this it can be assumed that E21 in the chick lens is equivalent to P14 in the mouse lens, so E14 would be approximately the same time point as NB mouse.

This system allowed the examination of the gene expression before the onset of organelle degradation at developmental time points preceding those examined in the mouse. Looking at the expression of the genes identified as differentially regulated, expression levels tend to increase after E6 (degradation of the mitochondria, nuclei and ER begins at E8). This increase in expression could be the signals required for the onset of organelle degradation.

IGF-1 has previously been shown to be expressed in embryonic chick lenses at embryonic days 8, 12, 15 and 19 (Caldes *et al.* 1991). Expression was found exclusively in the epithelial cells. From this study *IGF-1* was not shown to be expressed between embryonic days 6-16. This result could possibly be explained by the relatively small number of epithelial cells contained within the lens compared to fibre cells. It could be that *IGF-1* was expressed in the lens epithelium but at such low levels that the cycle numbers used in this study did not provide sufficient amplification for detection. *Galectin-3* and *caspase-7* were also shown to not be expressed from the PCR results presented here. There is no evidence in the published literature to suggest the presence of these genes in the embryonic chick lens.

In conclusion, the results presented here provide evidence for the process of lens differentiation to be biochemically similar between the mouse and chick. Expression of the genes at the earlier time points examined from this study, could also suggest a role for these genes in the onset of organelle degradation. However, from these results there is no evidence that these genes are translated. Protein studies, i.e. western blotting and immunohistochemistry, should be completed to examine the expression of these proteins, in order to confirm a role for these genes in organelle degradation.

In summary, the results from this chapter show:

- 20 of the 23 genes identified from the mouse arrays were also shown to be expressed in the embryonic chick lens, suggesting similarities in the biochemical process of lens differentiation in these two species.
- *Galectin-3, IGF-1* and *caspase-7* were not shown to be expressed in the chick lens at the time points examined.

Chapter 6: Discussion and Conclusions

6.1. Discussion of Results

During terminal differentiation of lens epithelial cells to fibre cells, all intracellular organelles are degraded. This ensures the formation of an optically clear tissue with no potentially light-scattering organelles. This process has been suggested to be an attenuated form of apoptosis (Bassnett 2002; Dahm 1999; Wride 2000). However, a number of recent studies have thrown doubt on this hypothesis.

Zandy *et al.* (2005) demonstrated that the executioner caspases are not required for organelle degradation. Knockout mice, generated with the inactivation of one or more of the executioner caspases, showed no difference in the size of the OFZ (Zandy *et al.* 2005). A number of studies have also been completed examining alternatives to the apoptosis pathway in this process of organelle degradation in the lens, including the ubiquitin pathway (Girao *et al.* 2005; Pereira *et al.* 2003; Shang *et al.* 1997), lipoxygenase (van Leyen *et al.* 1998) and autophagy (Matsui *et al.* 2006). Results of these previous studies have identified a functioning ubiquitin pathway in the lens and have shown that the components of the ubiquitin pathway are redistributed in the lens during differentiation (Girao *et al.* 2005; Pereira *et al.* 2003; Shang *et al.* 1997). A recent study by Zandy and Bassnett also demonstrated that the increase in VEIDase activity in the lens at the onset of organelle degradation is not due to the activation of caspase-6 but is instead attributable to the proteasome (Zandy and Bassnett 2007).

However, in support of the hypothesis that the classical apoptosis pathway is utilised during lens development and differentiation, this study has shown that over a hundred apoptosis genes were shown to be expressed above background **at** the two time points examined (**Chapter 3**). Twenty genes were shown to be differentially regulated between P7 and P14; these are developmental stages where a significant amount of organelle degradation occurs. Semi-quantitative PCR confirmed expression of all the genes identified from the arrays; corroborating the differential expression in approximately 50% of cases.

The relatively low confirmation rate could be due to one of two things, either the nylon membrane arrays are not good at accurately demonstrating differential gene expression or semi-quantitative PCR is not accurate enough to confirm the array results. However, the results from this study do show that these arrays give a good overview of gene expression; no genes tested were shown to be expressed on the arrays but not in PCR reactions.

It cannot be determined from these results in which sub-compartments of the developing lens (e.g. epithelium, outer fibres, central fibres) the genes identified from the arrays are expressed. Also, from this study it is uncertain whether the genes identified from the array results would also be identified in any normal non-lens epithelial cell undergoing differentiation and remodelling.

Some of the genes identified from the arrays are known to interact with one another. Mdm2, p53 and Daxx have all been linked. Mdm2 inhibits the function of p53, and increases its susceptibility to degradation by the proteasome (reviewed in Michael and Oren 2003). Daxx has been noted to affect the expression of mdm2, and enhances the E3 ligase activity of mdm2 (Tang *et al.* 2006). A number of genes identified from the arrays play a role in cell cycle progression. This is not unexpected as during terminal differentiation, epithelial cells have to exit the cell cycle in order to allow them to differentiate.

Two of the genes, axl and mcl-1, shown to be differentially expressed, were also shown to be present at the protein level using western blotting (**Chapter 3**). Mcl-1 has two isoforms, the short pro-apoptotic form, and the longer anti-apoptotic form. From the western blotting results obtained from this study, higher expression of the short isoform of mcl-1 was observed when compared to the long isoform. This could suggest a role for the pro-apoptotic pathway in the differentiation of the lens.

The process of denucleation during terminal differentiation has not only been observed in lens fibre cells but also in erythroblasts and keratinocytes. The terminal differentiation of mammalian erythrocytes has been shown to include the condensation of the nucleus and chromatin as observed in classical apoptosis as well as the destruction of the intracellular organelles. The DNA fragmentation pattern noted, however, was not as expected from an apoptosis process. Rather than the DNA laddering as seen in apoptosis, smears of DNA were observed when it was run on a gel, as seen in necrosis (Morioka *et al.* 1998). The role of caspases in this process has been examined (Carlile *et al.* 2004; Krauss *et al.* 2005; Zermati *et al.* 2001). Results from these studies suggest an essential role for caspase in early erythropoiesis of mammalian erythrocytes, although they seem to play no role in the later stages, where enucleation occurs (Krauss *et al.* 2005).

Differentiation of keratinocytes was seen to include the fragmentation of DNA (Weil *et al.* 1999) and the loss of mitochondrial membrane potential (Allombert-Blaise *et al.* 2003). Fragmented DNA, as seen during classical apoptosis, and the activation of caspase-3 have both been demonstrated in differentiating keratinocytes (Polakowska *et al.* 1994; Weil *et al.* 1999). Following the addition of caspase inhibitors to cultured keratinocytes, nuclear loss was inhibited, although some aspects of keratinocyte differentiation were still seen to occur (e.g. flattening of the keratinocytes) (Weil *et al.* 1999). The terminal differentiation process of lens fibre cells, keratinocytes and erythrocytes have all been suggested to utilise members of the apoptotic pathway, in an attenuated form of apoptosis in order to complete denucleation. Although the pathways in these cell types have not been fully elucidated, the presence of these key apoptotic proteins suggests similar mechanisms are operating.

A transgenic mouse has been generated containing an extended CAG repeat in the first exon of *huntingtin* (Lin *et al.* 2001). This extended repeat has been shown to result in a toxic gain-of-function. In this study the morphology of lenses of wild-type, heterozygotes and homozygotes was examined. No obvious morphological changes were noted and there was seen to be no statistically significant difference observed for any of the lens dimensions between wild-type

and homozygous lenses (**Chapter 4**). This was not unexpected as there is no recorded evidence of developmental eye problems in Huntington's patients.

The normal physiological function of huntingtin remains to be elucidated. It has been shown to play an important role during development. The deletion of *huntingtin* in mice was shown to result in early embryonic lethality (Duyao *et al.* 1995) and observations have also been made that mice expressing less than 50% of the normal level of wild-type hd demonstrate abnormalities of the central nervous system and were seen to die shortly after birth (White *et al.* 1997). A number of roles have been proposed for the wild-type protein due to the wide variety of proteins with which it interacts. An anti-apoptotic role has been suggested; wild-type huntingtin has been shown to protect cells from apoptosis induced by serum withdrawal and exposure to mitochondrial toxins (Rigamonti *et al.* 2000). Cells expressing the mutant form of this protein were shown to be more sensitive to these apoptotic stimuli. This anti-apoptotic role is thought to be attributable to the inhibition of caspase-3 by the huntingtin protein (Zhang *et al.* 2006). A role for huntingtin in transcriptional regulation has also been proposed; the wild-type protein has been shown to repress transcription (Kegel *et al.* 2002). It has been shown to interact with transcription factors including p53, TATA-binding protein and the C-terminal binding protein (CtBP) (reviewed in Harjes and Wanker 2003). Other roles have been suggested in both postsynaptic signalling and vesicle transport, transporting vesicles along the microtubules or cytoskeleton (reviewed in Harjes and Wanker, 2003).

With no blood supply and low level metabolism, the lens would be a good model system to examine the normal physiological function of huntingtin, but this would require a conditional knockout in which *hd* is selectively knocked out in the developing lens. Looking at the interacting partners of huntingtin, the presence of this gene in the lens suggests it could be involved in a number of processes; it could be expressed as an anti-apoptotic protein preventing complete apoptosis through its inhibition of caspase-3, although caspase-3 has been shown to not be essential for organelle degradation (Zandy *et al.* 2005). It could possibly be involved in the repression of transcription during differentiation of the lens epithelial cells or in membrane transport.

The expression of the genes shown to be highly or differentially expressed from the mouse array results was tested in the embryonic chick lens. The majority of genes tested were shown to be expressed (**Chapter 5**). The time points examined in this study include a range of stages before and after the onset of organelle degradation. In chicks, organelle degradation begins at E12, so an increase in expression immediately before this time point could suggest a role for this gene in triggering this process. These data presented here also suggests that the biochemical nature of the process of lens differentiation in both mouse and chick could be similar.

In conclusion the arrays used during this study give a good overall picture of apoptosis gene expression in the lens, though future studies still need to be completed to further elucidate the role of these genes/proteins in the process of lens development and differentiation. The observation that p53 and a number of its interacting partners are expressed in the lens could suggest an important role for this pathway in lens differentiation.

6.2. Future Work

The results presented in this study show apoptosis gene expression at the developmental time points examined although they do not demonstrate where these genes are expressed. Laser capture microdissection could be completed separating the lens epithelial cells from the lens fibre cells. Quantitative PCR could then be completed allowing the gene expression of epithelial cells to be compared to fibre cells. The localisation of these genes could lead to the generation of hypothesises about their role in the lens.

Also, from this study the gene expression has been examined but there is nothing to demonstrate that these genes are translated, so protein studies could be completed to study the changes in expression during development and also localise the protein to compartments within the lens.

The method of lens epithelial cell culture utilised by Menko *et al.* (1984) demonstrated the formation of lentoid bodies after 3 days in culture. These lentoid bodies demonstrated characteristics of lens fibre cells. Using this cell

culture method antibodies or siRNA could be used to knockdown expression of genes and the affect on the lentoid bodies could be observed. This technique could be used to look at the role of the interaction between p53, mdm2 and Daxx. By suppressing the expression of one of these genes, the affect on the other genes could be examined.

An alternative method to examine the gene function could be *in ovo* electroporation. This technique has been successfully completed introducing RNAi into the cells of the lens vesicle to knockdown endogenous gene products (Chen *et al.* 2004). This technique could be utilised to complete loss-of-function studies, introducing RNAi to knockdown the expression of some of the genes identified in this study to examine their affect on lens development

Huntingtin has been suggested to play a role in membrane trafficking. To examine whether huntingtin is involved in the trafficking process in the lens immunohistochemical studies could be completed to localise the huntingtin protein and components of the membrane trafficking system. Further studies could also be completed using a conditional knockout mouse. The Cre/LoxP system could be utilised under a crystallin promoter to dampen expression of huntingtin in the lens, to elucidate its function in the development of the lens.

References

Adams, J.C. and Lawler, J. 2004. The thrombospondins. *The International Journal of Biochemistry and Cell Biology* **36**, pp.961-968.

Adams, J.M. and Cory, S. 1998. The Bcl-2 protein family: Arbiters of cell survival. *Science* **281**, pp.1322-1326.

Akao, Y. Otsuki, Y. Kataoka, S. Ito, Y. Tsujimoto, Y. 1994. Multiple subcellular localization of Bcl-2: Detection in nuclear outer membrane, endoplasmic reticulum membrane, and mitochondrial membranes. *Cancer Research* **54**, pp.2468-2471.

Allombert-Blaise, C. Tamiji, S. Mortier, L. Fauvel, H. Tual, M. Delaporte, E. Piette, F. Martin DeLassale, E. Formstecher, P. Marchetti, P. Polakowska, R. 2003. Terminal differentiation of human epidermal keratinocytes involves mitochondria- and caspase-dependent cell death pathway. *Cell Death and Differentiation* **10**, pp.850-852.

Ameisen, J.C. 2002. On the origin, evolution, and nature of programmed cell death: A timeline of four billion years. *Cell Death and Differentiation* **9**, pp.367-393.

Andley, U.P. Song, Z. Wawrousek, E.F. Bassnett, S. 1998. The molecular chaperone alpha A-crystallin enhances lens epithelial cell growth and resistance to UVA stress. *Journal of Biological Chemistry* **273**, pp.31252-31261.

Andley, U.P. Song, Z. Wawrousek, E.F. Fleming, T.P. Bassnett, S. 2000. Differential protective activity of alpha A- and alpha B- crystallin in lens epithelial cells. *Journal of Biological Chemistry* **275**, pp.36823-36831.

Andley, U.P. Song, Z. Wawrousek, E.F. Brady, J.P. Bassnett, S. Fleming, T.P. 2001. Lens epithelial cells derived from alpha B-crystallin knockout mice demonstrate hyperproliferation and genomic instability. *The FASEB Journal* **15**, pp.221-229.

Antonsson, B. Conti, F. Ciavatta, A. Montessuit, S. Lewis, S. Martinou, I. Bernasconi, L. Bernard, A. Mermod, J.J. Mazzei, G. Maundrell, K. Gambale, F. Sadoul, R. Martinou, J.C. 1997. Inhibition of Bax channel-forming activity by Bcl-2. *Science* **277**, pp.370-372.

Antonsson, B. 2001. Bax and other pro-apoptotic Bcl-2 family "Killer-proteins" And their victim, the mitochondrion. *Cell and Tissue Research* **306**, pp.347-361.

Bae, J. Leo, C.P. Hsu, S.Y. Hsueh, A.J.W. 2000. Mcl-1s, a splicing variant of the antiapoptotic Bcl-2 family member Mcl-1, encodes a proapoptotic protein possessing only the BH3 domain. *Journal of Biological Chemistry* **275**, pp.25255-25261.

Bassnett, S. 1992. Mitochondrial dynamics in differentiating fiber cells of the mammalian lens. *Current Eye Research* **11**, pp.1227-1232.

Bassnett, S. and Beebe, D.C. 1992. Coincident loss of mitochondria and nuclei during lens fiber cell differentiation. *Developmental Dynamics* **194**, pp.85-93.

Bassnett, S. 1995. The fate of the golgi apparatus and the endoplasmic reticulum during lens fiber cell differentiation. *Investigative Ophthalmology & Visual Science* **36**, pp.1793-1803.

Bassnett, S. and Mataic, D. 1997. Chromatin degradation in differentiating fiber cells of the eye lens. *Journal of Cell Biology* **137**, pp.37-49.

Bassnett, S. 2002. Lens organelle degradation. *Experimental Eye Research* **74**, pp.1-6.

Bassnett, S. and McNulty, R. 2003. The effect of elevated intraocular oxygen on organelle degradation in embryonic chicken lens. *Journal of Experimental Biology* **206**, pp.4353-4361.

Beebe, D.C. Feagans, D.E. Jebens, H.A.H. 1980. Lentropin - a factor in vitreous-humor which promotes lens fiber cell differentiation. *Proceedings of the National Academy of Sciences of the United States of America* **77**, pp.490-493.

Beebe, D.C. Silver, M.H. Belcher, K.S. Van Wyk, J.J. Svoboda, M.E. Zelenka, P.S. 1987. Lentropin, a protein that controls lens fiber formation, is related functionally and immunologically to the insulin-like growth factors. *Proceedings of the National Academy of Sciences of the United States of America* **84**, pp.2327-2330.

Billingsley, G. Santhiya, S.T. Paterson, A.D. Ogata, K. Wodak, S. Hosseini, S.M. Manisastry, S.M.V., P. Gopinath, P.M. Graw, J. Heon, E. 2006. *Cryba4*, a novel human cataract gene, is also involved in microphthalmia. *American Journal of Human Genetics* **79**, pp.702-709.

Boyle, D.L. and Takemoto, L. 2000. A possible role for alpha-crystallins in lens epithelial cell differentiation. *Molecular Vision* **6**, pp.63-71.

Brady, J.P. Garland, D. Duglas-Tabor, Y. Robison, W.G. Groome, A. Wawrousek, E.F. 1997. Targeted disruption of the mouse αA-cystallin gene induces cataract and cytoplasmic inclusion bodies containing the small heat shock protein αB-crystallin. *Proceedings of the National Academy of Sciences of the United States of America* **94**, pp.884-889.

Burlacu, A. 2003. Regulation of apoptosis by Bcl-2 family proteins. *Journal of Cellular and Molecular Medicine* **7**, pp.249-257.

Caldes, T. Alemany, J. Robcis, H.L. de Pablo, F. 1991. Expression of insulin-like growth factor I in developing lens is compartmentalized. *Journal of Biological Chemistry* **266**, pp.20786-20790.

Carlile, G.W. Smith, D.H. Wiedmann, M. 2004. Caspase-3 has a nonapoptotic function in erythroid maturation. *Blood* **103**, pp.4310-4316.

Carter, J.M. Hutcheson, A.M. Quinlan, R.A. 1995. In vitro studies on the assembly properties of the lens proteins CP49, CP115: Coassembly with α-crystallin but not with vimentin. *Experimental Eye Research* **60**, pp.181-192.

Chen, Y.X. Krull, C.E. Reneker, L.W. 2004. Targeted gene expression in the chicken eye by in ovo electroporation. *Molecular Vision* **10**, pp.874-883.

Chittenden, T. Flemington, C. Houghton, A.B. Ebb, R.G. Gallo, G.J. Elangovan, B. Chinnadurai, G. Lutz, R.J. 1995. A conserved domain in Bak, distinct from BH1 and BH2, mediates cell death and protein binding functions. *The EMBO Journal* **14**, pp.5589-5596.

Chow, R.L. and Lang, R.A. 2001. Early eye development in vertebrates. *Annual Review of Cell and Developmental Biology* **17**, pp.255-296.

Cohen, D. Bar-Yosef, U. Levy, J. Gradstein, L. Belfair, N. Ofir, R. Joshua, S. Lifbitz, T. Carmi, R. Birk, O.S. 2007. Homozygous *crybb1* deletion mutation underlies autosomal recessive congenital cataract. *Investigative Ophthalmology and Vision Science* **48**, pp.2208-2213.

Congdon, N.G. 2001. Prevention strategies for age related cataract: Present limitations and future possibilities. *British Journal of Ophthalmology* **85**, pp.516-520.

Coulombre, J.L. and Coulombre, A.J. 1963. Lens development: Fiber elongation and lens orientation. *Science* **142**, pp.1489-1490.

Counis, M. Chaudun, E. Arruti, C. Oliver, L. Sanwai, M. Courtois, Y. Torriglia, A. 1998. Analysis of nuclear degradation during lens cell differentiation. *Cell Death and Differentiation* **5**, pp.251-261.

Cvekl, A. and Piatigorsky, J. 1996. Lens development and crystallin gene expression: Many roles for pax-6. *Bioessays* **18**, pp.621-630.

Dahm, R. Gribbon, C. Quinlan, R.A. Prescott, A.R. 1998. Changes in the nucleolar and coiled body compartments precede lamina and chromatin reorganization during fibre cell denucleation in the bovine lens. *European Journal of Cell Biology* **75**, pp.237-246.

Dahm, R. 1999. Lens fibre cell differentiation - a link with apoptosis? *Ophthalmic Research* **31**, pp.163-183.

Dahm, R. and Prescott, A.R. 2002. Morphological changes and nuclear pore clustering during nuclear degradation in differentiating bovine lens fibre cells. *Ophthalmic Research* **34**, pp.288-294.

Dahm, R. Bramke, S. Dawczynski, J. Nagaraj, R.H. Kasper, M. 2003. Developmental aspects of galectin-3 expression in the lens. *Histochemistry and Cell Biology* **119**, pp.219-226.

de Iongh, R.U. Lovicu, F.J. Overbeek, P.A. Schneider, M.D. Joya, J. Hardeman, E.D. McAvoy, J.W. 2001. Requirement for TGF beta receptor signaling during terminal lens fiber differentiation. *Development* **128**, pp.3995-4010.

Degli Esposti, M. 2003. The mitochondrial battlefield and membrane lipids during cell death signalling. *Italian Journal of Biochemistry* **52**, pp.43-50.

Del Vecchio, P.J. MacElroy, K.S. Rosser, M.P. Church, R.L. 1984. Association of alpha-crystallin with actin in cultured lens cells. *Current Eye Research* **3**, pp.1213-1219.

Deveraux, Q.L. and Reed, J.C. 1999. IAP family proteins - suppressors of apoptosis. *Genes and Development* **13**, pp.239-252.

Ding, R. Pommier, Y. Kang, V.H. Smulson, M. 1992. Depletion of poly(ADP-ribose) polymerase by antisense RNA expression results in a delay in DNA strand break rejoining. *Journal of Biological Chemistry* **267**, pp.12804-12812.

Ding, R. and Smulson, M. 1994. Depletion of nuclear poly(ADP-ribose) polymerase by antisense RNA expression: Influences on genomic stability, chromatin organization and carcinogen cytotoxicity. *Cancer Research* **54**, pp.4627-4634.

Duncan, M.K. Xie, L. David, L.L. Robinson, M.L. Taube, J.R. Cui, W. Reneker, L.W. 2004. Ectopic Pax6 expression disturbs lens fiber cell differentiation. *Investigative Ophthalmology and Vision Sciences* **45**, pp.3589-3598.

Duyao, M.P. A.B., A. Ryan, A. Persichetti, F. Barnes, G.T. McNeil, S.M. Ge, P. Vonsattel, J.P. Gusella, J.F. Joyner, A.L. al., e. 1995. Inactivation of the mouse huntington's disease gene homolog hdh. *Science* **269**, pp.407-410.

Evan, G. and Littlewood, T. 1998. A matter of life and cell death. *Science* **281**, pp.1317-1322.

Faulkner-Jones, B. Zandy, A.J. Bassnett, S. 2003. RNA stability in terminally differentiating fibre cells of the ocular lens. *Experimental Eye Research* **77**, pp.463-476.

Fokina, V.M. and Frolova, E.I. 2006. Expression patterns of wnt genes during development of an anterior part of the chicken eye. *Developmental Dynamics* **235**, pp.496-505.

Foley, J.D. Rosenbaum, H. Griep, A.E. 2004. Temporal regulation of VEID-AFC cleavage activity and caspase 6 correlates with organelle loss during lens development. *The Journal of Biological Chemistry* **279**, pp.32142-32150.

Francis, P.J. Berry, V. Moore, A.T. Bhattacharya, S. 1999. Lens biology: Development and human cataractogenesis. *Trends in Genetics* **15**, pp.191-196.

Francis, P.J. Berry, V. Bhattacharya, S.S. Moore, A.T. 2000. The genetics of childhood cataract. *Journal of Medical Genetics* **37**, pp.481-488.

Fromm, L. and Overbeek, P.A. 1997. Inhibition of cell death by lens-specific overexpression of Bcl-2 in transgenic mice. *Developmental Genetics* **20**, pp.276-287.

Furuta, Y. and Hogan, B.L.M. 1998. BMP4 is essential for lens induction in the mouse embryo. *Genes & Development* **12**, pp.3764-3775.

Gao, C.Y. Rampalli, A.M. Cai, H. He, H. Zelenka, P.S. 1999. Changes in cyclin dependent kinase expression and activity accompanying lens fiber cell differentiation. *Experimental Eye Research* **69**, pp.695-703.

Giancotti, F.G. 1997. Integrin signaling: Specificity and control of cell survival and cell cycle progression. *Current Opinion in Cell Biology* **9**, pp.691-700.

Gilbert, S. 2003. The emergence of the ectoderm: The central nervous system and the epidermis. In: Gilbert, S. ed./eds. *Developmental biology.* Massachusetts: Sinauer Associates Inc. pp.391-425.

Girao, H. Pereira, P. Taylor, A. Shang, F. 2005. Subcellular redistribution of components of the ubiquitin-proteasome pathway during lens differentiation and maturation. *Investigative Ophthalmology and Vision Sciences* **46**, pp.1386-1392.

Gonen, T. Donaldson, P. Kistler, J. 2000. Galectin-3 is associated with the plasma membrane of lens fiber cells. *Investigative Ophthalmology and Vision Science* **41**, pp.199-203.

Gong, X. Li, E. Klier, G. Huang, Q. Wu, Y. Lei, H. Kumar, N.M. Horwitz, J. Gilula, N.B. 1997. Disruption of a3 connexin gene leads to proteolysis and cataractogenesis in mice. *Cell* **91**, pp.833-843.

Gong, X. Cheng, C. Xia, C. 2007. Connexins in lens development and cataractogenesis. *Journal of Membrane Biology*, pp.Epub ahead of print.

Graw, J. 1996. Genetic aspects of embryonic eye development in vertebrates. *Developmental Genetics* **18**, pp.181-197.

Graw, J. 1999. Cataract mutations and lens development. *Progress in Retinal and Eye Research* **18**, pp.235-267.

Graw, J. and Loster, J. 2003. Developmental genetics in ophthalmology. *Ophthalmic Genetics* **24**, pp.1-33.

Graw, J. 2004. Congenital hereditary cataracts. *International Journal of Developmental Biology* **48**, pp.1031-1044.

Green, D.R. and Reed, J.C. 1998. Mitochondria and apoptosis. *Science* **281**, pp.1309-1312.

Gregg, N.M. and Banatvala, J.E. 2001. Congenital cataract following german measles in the mother (reprinted from transactions ophthalmological society of australia 3, pg 35-46, 1942). *Reviews in Medical Virology* **11**, pp.277-283.

Grindley, J.C. Davidson, D.R. Hill, R.E. 1995. The role of Pax-6 in eye and nasal development. *Development* **121**, pp.1433-1442.

Gross, A. Jockel, J. Wei, M.C. Korsmeyer, S.J. 1998. Enforced dimerization of Bax results in its translocation, mitochondrial dysfunction and apoptosis. *The EMBO Journal* **17**, pp.3878-3885.

Grullich, C. Duvoisin, R.M. Wiedmann, M. van Leyen, K. 2001. Inhibition of 15-lipoxygenase leads to delayed organelle degradation in the reticulocyte. *FEBS Letters* **489**, pp.51-54.

Guo, W. Shang, F. Liu, Q. Urim, L. Zhang, M. Taylor, A. 2006. Ubiquitin-proteasome pathway function is required for lens cell proliferation and differentiation. *Investigative Ophthalmology and Vision Science* **47**, pp.2569-2575.

Hanayama, R. Tanaka, M. Miwa, K. Shinohara, A. Iwamatsu, A. Nagata, S. 2002. Identification of a factor that links apoptotic cells to phagocytes. *Nature* **417**, pp.182-187.

Harding, J. 1991. The normal lens. In: Harding, J. ed./eds. *Cataract biochemistry epidemiology and pharmacology*. London: Chapman & Hall. pp.1-70.

Harjes, P. and Wanker, E.E. 2003. The hunt for huntingtin function: Interaction partners tell many different stories. *TRENDS in Biochemical Sciences* **28**, pp.425-433.

Hawse, J. Hejtmancik, J. Huang, Q.L. Sheets, N. Hosack, D. Lempicki, R. Horwitz, J. Kantorow, M. 2003. Identification and functional custering of global gene expression differences between human age-related cataract and clear lenses. *Molecular Vision* **9**, pp.515-537.

Hawse, J.R. Hejtmancik, J.F. Horwitz, J. Kantorow, M. 2004. Identification and functional clustering of global gene expression differences between age-related cataract and clear human lenses and aged human lenses. *Experimental Eye Research* **79**, pp.935-940.

Hawse, J.R. DeAmicis-Tress, C. Cowell, T.L. Kantorow, M. 2005. Identification of global gene expression differences between human lens epithelial and cortical fibre cells reveals specific genes and their associated pathways important for specialized lens cell functions. *Molecular Vision* **11**, pp.274-283.

He, H.Y. Gao, C. Vrensen, G. Zelenka, P. 1998. Transient activation of cyclin b/CDC2 during terminal differentiation of lens fiber cells. *Developmental Dynamics* **211**, pp.26-34.

Hiscott, P. Paraoan, L. Choudhary, A. Ordonez, J.L. Al-Khaier, A. Armstrong, D.J. 2006. Thrombospondin 1, thrombospondin 2 and the eye. *Progress in Retinal and Eye Research* **25**, pp.1-18.

Horwitz, J. 1992. Alpha-crystallin can function as a molecular chaperone. *Proceedings of the National Academy of Sciences of the United States of America* **89**, pp.10449-10453.

Hunter, J.J. and Parslow, T.G. 1996. A peptide sequence from bax that converts Bcl-2 into an activator of apoptosis. *Journal of Biological Chemistry* **271**, pp.8521-8524.

Hyatt, G.A. and Beebe, D.C. 1993. Regulation of lens cell growth and polarity by an embryo-specific growth factor and by inhibitors of lens cell proliferation and differentiation. *Development* **117**, pp.701-709.

Ireland, M.E. Wallace, P. Sandilands, A. Poosch, M. Kasper, M. Graw, J. Liu, A. Maisel, H. Prescott, A.R. Hutcheson, A.M. Goebel, D. Quinlan, R.A. 2000. Up-regulation of novel intermediate filament proteins in primary fiber cells: An indicator of all vertebrate lens fiber differentiation. *The Anatomical Record* **258**, pp.25-33.

Ishizaki, Y. Jacobson, M.D. Raff, M.C. 1998. Role for caspases in lens fiber differentiation. *Journal of Cell Biology* **140**, pp.153-158.

Ivanov, D. Dvoriantchikova, G. Pestova, A. Nathanson, L. Shestopalov, V.I. 2005. Microarray analysis of fiber cell maturation in the lens. *FEBS Letters* **579**, pp.1213-1219.

Kastan, M. Onyekwere, O. Sidransky, D. Vogelstein, B. Craig, R.W. 1991. Participation of p53 protein in the cellular response to DNA damage. *Cancer Research* **51**, pp.6304-6311.

Kegel, K.B. Melon, A.R. Yi, Y. Kim, Y.J. Doyle, E. Cuiffo, B.G. Sapp, E. Wang, Y. Qin, Z.H. Chen, J.D. Nevins, J.R. Aronin, N. DiFiglia, M. 2002. Huntingtin is present in the nucleus, interacts with the transcriptional corepressor c-terminal binding protein, and represses transcription. *Journal of Biological Chemistry* **277**, pp.7466-7476.

Kerr, J. Wyllie, A. Currie, A. 1972. Apoptosis: A basic biological phenomenon with wide-ranging implications in tissue kinetics. *British Journal of Cancer* **26**, pp.239-257.

Khakh, B. and North, A. 2006. P2x receptors as cell-surface ATP sensors in health and disease. *Nature* **442**, pp.527-532.

Kozopas, K.M. Yang, T. Buchan, H.L. Zhou, B.P. Craig, R.W. 1993. Mcl1, a gene expressed in programmed myeloid cell differentiation, has sequence similarity to Bcl-2. *Proceedings of the National Academy of Sciences of the United States of America* **90**, pp.3516-3520.

Krauss, S.W. Lo, A.J. Short, S.A. Koury, M.J. Mohandas, N. Chasis, J.A. 2005. Nuclear substructure reorganization during late stage erythropoiesis is selective and does not involve caspase cleavage of major nuclear substructural proteins. *Blood* **106**, pp.2200-2205.

Kroemer, G. Petit, P. Zamzami, N. Vayssiere, J. Mignotte, B. 1995. The biochemistry of programmed cell death. *The FASEB Journal* **9**, pp.1277-1287.

Kuerbitz, S. Plunkett, B. Walsh, W. Kastan, M. 1992. Wild-type p53 is a cell cycle checkpoint determinant following irradiation. *Proceedings of the National Academy of Sciences of the United States of America* **89**, pp.7491-7495.

Kuwabara, T. and Imaizumi, M. 1974. Denucleation process of the lens. *Investigative Ophthalmology* **13**, pp.973-981.

Lang, R.A. 1999. Which factors stimulate lens fiber cell differentiation in vivo? *Investigative Ophthalmology & Visual Science* **40**, pp.3075-3078.

Lazebnik, Y.A. Kaufmann, S.H. Desnoyers, S. Poirier, G.G. Earnshaw, W.C. 1994. Cleavage of poly(ADP-ribose) polymerase by a proteinase with properties like ice. *Nature* **371**, pp.346-347.

Lazebnik, Y.A. Takahashi, A. Moir, R.D. Goldman, R.D. Poirier, G.G. Kaufmann, S.H. Earnshaw, W.C. 1995. Studies of the lamin proteinase reveal multiple parallel biochemical pathways during apoptotic execution. *Proceedings of the National Academy of Sciences of the United States of America* **92**, pp.9042-9046.

Levy-Strumpf, N. and Kimchi, A. 1998. Death associated proteins (daps): From gene identification to the analysis of their apoptotic and tumor suppressive functions. *Oncogene* **17**, pp.3331-3340.

Li, P. Nijhawan, D. Budihardjo, I. Srinivasula, S.M. Ahmad, M. Alnemri, E.S. Wang, X. 1997. Cytochrome c and dATP-dependent formation of apaf-1/caspase-9 complex initiates an apoptotic protease cascade. *Cell* **91**, pp.479-489.

Li, W.C. Kuszak, J.R. Dunn, K. Wang, R.R. Ma, W.C. Wang, G.M. Spector, A. Leib, M. Cotliar, A.M. Weiss, M. Espy, J. Howard, G. Farris, R.L. Auran, J. Donn, A. Hofeldt, A. Mackay, C. Merriam, J. Mittl, R. Smith, T.R. 1995. Lens epithelial-cell apoptosis appears to be a common cellular basis for non-congenital cataract development in humans and animals. *Journal of Cell Biology* **130**, pp.169-181.

Li, W.C. and Spector, A. 1996. Lens epithelial, cell apoptosis is an early event in the development of uvb-induced cataract. *Free Radical Biology and Medicine* **20**, pp.301-311.

Lin, C. Tallaksen-Greene, S. Chien, W. Cearley, J.A. Jackson, W.S. Crouse, A.B. Ren, S. Li, X. Albin, R.L. Detloff, P.J. 2001. Neurological abnormalities in a knock-in mouse model of huntington's disease. *Human Molecular Genetics* **10**, pp.137-144.

Liou, M.L. and Liou, H.C. 1999. The ubiquitin-homology protein dap-1 associates with tumor necrosis factor receptor (p60) death domain and induces apoptosis. *Journal of Biological Chemistry* **274**, pp.10145-10153.

Liu, J. Chamberlain, C.G. McAvoy, J.W. 1996. Igf enhancement of FGF-induced fibre differentiation and DNA synthesis in lens explants. *Experimental Eye Research* **63**, pp.621-629.

Liu, X. Li, P. Widlak, P. Zou, H. Luo, X. Garrard, W.T. Wang, X. 1998. The 40-kda subunit of DNA fragmentation factor induces DNA fragmentation and chromatin condensation during apoptosis. *Proceedings of the National Academy of Sciences of the United States of America* **95**, pp.8461-8466.

Liu, X.S. Zou, H. Slaughter, C. Wang, X.D. 1997. DFF, a heterodimeric protein that functions downstream of caspase-3 to trigger DNA fragmentation during apoptosis. *Cell* **89**, pp.175-184.

Lockshin, R.A. and Zakeri, Z. 2004. Caspase-independent cell death? *Oncogene* **23**, pp.2766-2773.

Lovicu, F.J. Chamberlain, C.G. McAvoy, J.W. 1995. Differential effects of aqueous and vitreous on fiber differentiation and extracellular matrix accumulation in lens epithelial explants. *Investigative Ophthalmology and Vision Sciences* **36**, pp.1459-1469.

Lovicu, F.J. and McAvoy, J.W. 2005. Growth factor regulation of lens development. *Developmental Biology* **280**, pp.1-14.

Malecaze, F. Decha, A. Serre, B. Penary, M. Duboue, M. Berg, D. Levade, T. Lubsen, N.H. Kremer, E.J. Couderc, B. 2005. Prevention of posterior capsule opacification by the induction of therapeutic apoptosis of residual lens cells. *Gene Therapy*, pp.1-8.

Mansergh, F.C. Wride, M.A. Walker, V.E. Adams, S. Hunter, S.M. Evans, M.J. 2004. Gene expression changes during cataract progression in sparc null mice: Differential regulation of mouse globins in the lens. *Molecular Vision* **10**, pp.490-511.

Mao, Y.W. Liu, J.P. Xiang, H. Li, D.W.C. 2004. Human αA- and αB-crystallins bind to Bax and Bcl-x_S to sequester their translocation during staurosporine-induced apoptosis. *Cell Death and Differentiation* **11**, pp.512-526.

Marcantonio, J. and Vrensen, G. 1999. Cell biology of posterior capsular opacification. *Eye* **13**, pp.484-488.

Matsui, M. Yamamoto, A. Kuma, A. Ohsumi, Y. Mizushima, N. 2006. Organelle degradation during the lens and erythroid differentiation is independent of autophagy. *Biochemical and Biophysical Research Communications* **339**, pp.485-489.

McAlister Gregg, N. 2001. Congenital cataract following german measles in the mother. 1942. [classical article]. *Reviews in Medical Virology* **11**, pp.277-283; discussion 284-275.

McAvoy, J.W. and Chamberlain, C.G. 1989. Fibroblast growth-factor (FGF) induces different responses in lens epithelial-cells depending on its concentration. *Development* **107**, pp.221-228.

McAvoy, J.W. Chamberlain, C.G. de Iongh, R.U. Hales, A.M. Lovicu, F.J. 1999. Lens development. *Eye* **13**, pp.425-437.

Menko, A.S. and Philip, N.J. 1995. B_1 integrins in epithelial tissues: A unique distribution in the lens. *Experimental Cell Research* **218**, pp.516-521.

Menko, S. Klukas, K. Johnson, R. 1984. Chicken embryo lens culture mimic differentiation in the lens. *Developmental Biology* **103**, pp.129-141.

Michael, D. and Oren, M. 2003. The p53 - mdm3 module and the ubiquitin system. *Seminars in Cancer Biology* **13**, pp.49-58.

Michaelson, J.S. Bader, D. Kuo, F. Kozak, C. Leder, P. 1999. Loss of DAXX, a promiscuously interacting protein, results in extensive apoptosis in early mouse development. *Genes and Development* **13**, pp.1918-1923.

Michaelson, J.S. and Leder, P. 2003. RNAi reveals anti-apoptotic and transcriptionally repressive activities of DAXX. *Journal of Cell Science* **116**, pp.345-352.

Modak, S.P. and Perdue, S.W. 1970. Terminal lens cell differentiation. I. Histological and microspectrophotometric analysis of nuclear degeneration. *Experimental Cell Research* **59**, pp.43-56.

Mohamed, Y.H. and Amemiya, T. 2003. Apoptosis and lens vesicle development. *European Journal of Ophthalmology* **13**, pp.1-10.

Momand, J. Wu, H. Dasgupta, G. 2000. Mdm2 - master regulator of the p53 tumor suppressor protein. *Gene* **242**, pp.15-29.

Morioka, K. Tone, S. Mukaida, M. Takano-Ohmuro, H. 1998. The apoptotic and nonapoptotic nature of the terminal differentiation of erythroid cells. *Experimental Cell Research* **240**, pp.206-217.

Morozov, V. and Wawrousek, E.F. 2006. Caspase-dependent secondary lens fiber cell disintegration in {alpha}A-/{alpha}B-crystallin double-knockout mice. *Development* **133**, pp.813-821.

Nagata, S. 1997. Apoptosis by death factor. *Cell* **88**, pp.355-365.

Nakahara, M. Nagasaka, A. Koike, M. Uchida, K. Kawane, K. Uchiyama, Y. Nagata, S. 2007. Degradation of nuclear DNA by DNase ii-like DNase in cortical fiber cells of mouse eye lens. *FEBS* **274**, pp.3055-3064.

Nakamura, H. Katahira, T. Sato, T. Watanabe, Y. Funahashi, J. 2004. Gain- and loss-of-function in chick embryos by electroporation. *Mechanisms of Development* **121**, pp.1137-1143.

Nakamura, T. Pichel, J. Williams-Simons, L. Westphal, H. 1995. An apoptotic defect in lens differentiation caused by p53 is rescued by a mutant allele. *Proceedings of the National Academy of Sciences of the United States of America* **92**, pp.6142-6146.

Newmeyer, D.D. and Ferguson-Miller, S. 2003. Mitochondria: Releasing power for life and unleashing the machineries of death. *Cell* **112**, pp.481-490.

Nicholson, D.W. Ali, A. Thornberry, N.A. Vaillancourt, J.P. Ding, C.K. Gallat, M. Gareau, Y. Griffin, P.R. Labelle, M. Lazebnik, Y.A. Munday, N.A. Raju, S.M. Smulson, M.E. Yamin, T.T. Yu, V.L. Miller, D.K. 1995. Identification and inhibition of the ice/ced-3 protease necessary for mammalian apoptosis. *Nature* **376**, pp.37-43.

Nishimoto, S. Kawane, K. Watanabe-Fukunaga, R. Fukuyama, H. Ohsawa, Y. Uchiyama, Y. Hashida, N. Ohguro, N. Tano, Y. Morimoto, T. Fukuda, Y. Nagata, S. 2003. Nuclear cataract caused by a lack of DNA degradation in the mouse eye lens. *Nature* **424**, pp.1071-1074.

Nishutani, K. and Sasaki, K. 2006. Macrophage localization in the developing lens primordium of the mouse embryo - an immunohistochemical study. *Experimental Eye Research* **83**, pp.223-228.

Oltvai, Z.N. Milliman, C.L. Korsmeyer, S.J. 1993. Bcl-2 heterodimerizes in vivo with a conserved homolog, bax, that accelerates programmed cell death. *Cell* **74**, pp.609-619.

Ozaki, L. Jap, P. Bloemendal, H. 1985. Protein synthesis in bovine and human nuclear fiber cells. *Experimental Eye Research* **41**, pp.569-575.

Pandey, S.K. Apple, D.J. Werner, L. Maloof, A.J. Milverton, E.J. 2004. Posterior capsule opacification: A review of the aetiopathogenesis, experimental and clinical studies and factors for prevention. *Indian Journal of Ophthalmology* **52**, pp.99-112.

Pauli, S. Soker, T. Klopp, N. Illig, T. Engel, W. Graw, J. 2007. Mutation analysis in a german family identified a new cataract-causing allele in the *crybb2* gene. *Molecular Vision* **13**, pp.962-967.

Peek, R. McAvoy, J.W. Lubsen, N.H. Schoenmakers, J.G. 1992. Rise and fall of crystallin gene messenger levels during fibroblast growth factor induced terminal differentiation of lens cells. *Developmental Biology* **152**, pp.152-160.

Peller, S. Frenkel, J. Lapidot, T. Kahn, J. Rahimi-Levene, N. Yona, R. Nissim, L. Goldfinger, N. Sherman, D. Rotter, V. 2003. The onset of p53-dependent apoptosis plays a role in terminal differentiation of human normoblasts. *Oncogene* **22**, pp.4648-4655.

Pendergrass, W. Penn, P. Possin, D. Wolf, N. 2005. Accumulation of DNA, nuclear and mitochondrial debris, and ROS at sites of age-related cortical cataract in mice. *Investigative Ophthalmology and Vision Science* **46**, pp.4661-4670.

Pereira, P. Shang, F. Hobbs, M. Girao, H. Taylor, A. 2003. Lens fibers have a fully functional ubiquitin-proteasome pathway. *Experimental Eye Research* **76**, pp.623-631.

Piatigorsky, J. 1981. Lens differentiation in vertebrates - a review of cellular and molecular-features. *Differentiation* **19**, pp.134-153.

Pokroy, R. Tendler, Y. Pollack, A. Zinder, O. Weisinger, G. 2002. P53 expression in the normal murine eye. *Investigative Ophthalmology and Vision Science* **43**, pp.1736-1741.

Polakowska, R.R. Piacentini, M. Bartlett, R. Goldsmith, L.A. Haake, A.R. 1994. Apoptosis in human skin development: Morphogenesis, periderm, and stem cells. *Developmental Dynamics* **199**, pp.176-188.

Reddy, P.H. Williams, M. Tagle, D.A. 1999. Recent advances in understanding the pathogenesis of huntington's disease. *Trends in Neurosciences* **22**, pp.248-255.

Richardson, N.A. Chamberlain, C.G. McAvoy, J.W. 1993. IGF-1 enhancement of FGF-induced lens fiber differentiation in rats of different ages. *Investigative Ophthalmology and Vision Science* **34**, pp.3303-3312.

Rigamonti, D. Bauer, J.H. De-Fraja, C. Conti, L. Sipione, S. Sciorati, C. Clementi, E. Hackam, A. Hayden, M.R. Li, Y. Cooper, J.K. Ross, C.A. Govoni, S. Vincenz, C. Cattaneo, E. 2000. Wild-type huntingtin protects from apoptosis upstream of caspase-3. *The Journal of Neuroscience* **20**, pp.3705-3713.

Robman, L. and Taylor, H. 2005. External factors in the development of cataract. *Eye* **19**, pp.1074-1082.

Ruotolo, R. Grassi, F. Percudani, R. Rivetti, C. Martorana, D. Maraini, G. Ottonello, S. 2003. Gene expression profiling in human age-related nuclear cataract. *Molecular Vision* **9**, pp.538-548.

Sanders, E.J. and Parker, E. 2002. The role of mitochondria, cytochrome c and caspase-9 in embryonic lens fibre cell denucleation. *Journal of Anatomy* **201**, pp.121-135.

Sanders, E.J. and Parker, E. 2003. Retroviral overexpression of Bcl-2 in the embryonic chick lens influences denucleation in differentiating lens fiber cells. *Differentiation* **71**, pp.425-433.

Segev, F. Mor, O. Segev, A. Belkin, M. Assia, E.I. 2004. Downregulation of gene expression in the ageing lens: A possible contributory factor in senile cataract. *Eye*, pp.1-6.

Semina, E.V. Murray, J.C. Reiter, R. Hrstka, R.F. Graw, J. 2000. Deletion in the promoter region and altered expression of *pitx3* homeobox gene in *aphakia* mice. *Human Molecular Genetics* **9**, pp.1575-1585.

Shang, F. Gong, X. Palmer, H.J. Nowell, T.R., Jr. Taylor, A. 1997. Age-related decline in ubiquitin conjugation in response to oxidative stress in the lens. *Experimental Eye Research* **64**, pp.21-30.

Shang, F. Gong, X. McAvoy, J.W. Chamberlain, C. Nowell, T.R., Jr. Taylor, A. 1999. Ubiquitin-dependent pathway is up-regulated in differentiating lens cells. *Experimental Eye Research* **68**, pp.179-192.

Sharp, A.H. Loev, S.J. Schilling, G. Li, S.H. Li, X.J. Bao, J. Wagster, M.V. Kotzuk, J.A. Steiner, J.P. Lo, A. Hedreen, J. Sisodia, S. Snyder, S.H. Dawson, T.M. Ryugo, D.K. Ross, C.A. 1995. Widespread expression of huntington's disease gene (it15) protein product. *Neuron* **14**, pp.1065-1074.

Shaw, P. Bovey, R. Tardy, S. Sahli, R. Sordat, B. Costa, J. 1992. Induction of apoptosis by wild-type p53 in a human colon tumor-derived cell line. *Proceedings of the National Academy of Sciences of the United States of America* **89**, pp.4495-4499.

Sherr, C.J. 1993. Mammalian G1 cyclins. *Cell* **73**, pp.1059-1065.

Shestopalov, V.I. and Bassnett, S. 1999. Exogenous gene expression and protein targeting in lens fiber cells. *Investigative Ophthalmology & Visual Science* **40**, pp.1435-1443.

Shimano, H. 2001. Sterol regulatory element-binding proteins (SREBSs): Transcriptional regulators of lipid synthetic genes. *Progress in Lipid Research* **40**, pp.439-452.

Shirke, S. Faber, S. Hallem, E. Makarenkova, H. Robinson, M. Overbeek, P.A. Lang, R.A. 2001. Misexpression of IGF-i in the mouse lens expands the transitional zone and pertubs lens polarization. *Mechanisms of Development* **101**, pp.167-174.

Slee, E.A. Adrain, C. Martin, S.J. 2001. Executioner caspase-3, -6 and -7 perform distinct, non-redundant roles during the demolition phase of apoptosis. *Journal of Biological Chemistry* **276**, pp.7320-7326.

Snell, R.G. MacMillan, J.C. Cheadle, J.P. Fenton, I. Lazarou, L.P. Davies, P. MacDonald, M.E. Gusella, J.F. Harper, P.S. Shaw, D.J. 1993. Relationship between trinucleotide repeat expansion and phenotypic variation in huntington's disease. *Nature Genetics* **4**, pp.393-397.

Spalton, D. 1999. Posterior capsular opacification after cataract surgery. *Eye* **13**, pp.489-492.

Spemann, H. 1901. Uber correlationen in der entwicklung des auges. *Verhand. Anat. Ges.* **15**, pp.61-79. Cited in Piatigorsky 1981

Stubbs, J.D. Lekutis, C. Singer, K.L. Bui, A. Yuzuki, D. Srinivasan, U. Parry, G. 1990. cDNA cloning of a mouse mammary epithelial cell surface protein reveals the existence of epidermal growth factor-like domains linked to factor VIII-like sequences. *Proceedings of the National Academy of Sciences of the United States of America* **87**, pp.8417-8421.

Stump, R.J.W. Ang, S.J. Chen, Y. van Bahr, T. Lovicu, F.J. Pinson, K. de Iongh, R.U. Yamaguchi, T.P. Sassoon, D.A. McAvoy, J.W. 2003. A role for wnt/β-catenin signaling in lens epithelial differentiation. *Developmental Biology* **259**, pp.48-61.

Talla, V. Narayanan, C. Srinivasan, N. Balasubramanian, D. 2006. Mutation causing self-aggregation in human gc-crystallin leading to congenital cataract. *Investigative Ophthalmology and Vision Science* **47**, pp.5212-5217.

Tang, J. Qu, L.K. Zhang, J. Wang, W. Michaelson, J.S. Degenhardt, Y.Y. El-Deiry, W.S. Yang, X. 2006. Criticial role for DAXX in regulating mdm2. *Nature Cell Biology* **8**, pp.855-862.

Thornberry, N.A. Ranon, T.A. Pieterson, E.P. Rasper, D.M. Timkey, T. GarciaCalvo, M. Houtzager, V.M. Nordstrom, P.A. Roy, S. Vaillancourt, J.P. Chapman, K.T. Nicholson, D.W. 1997. A combinatorial approach defines specificities of members of the caspase family and granzyme b - functional, relationships established for key mediators of apoptosis. *Journal of Biological Chemistry* **272**, pp.17907-17911.

Trousse, F. Esteve, P. Bovolenta, P. 2001. BMP4 mediates apoptotic cell death in the developing chick eye. *Journal of Neuroscience* **21**, pp.1292-1301.

Valverde, P. Obin, M.S. Taylor, A. 2004. Role of gas6/axl signaling in lens epithelial cell proliferation and survival. *Experimental Eye Research* **78**, pp.27-37.

van Gurp, M. Festjens, N. van Loo, G. Saelens, X. Vandenabeele, P. 2003. Mitochondrial intermembrane proteins in cell death. *Biochemical and Biophysical Research Communications* **304**, pp.487-497.

van Leyen, K. Duvoisin, R.M. Engelhardt, H. Wiedmann, M. 1998. A function for lipoxygenase in programmed organelle degradation. *Nature* **395**, pp.392-395.

Varshavsky, A. 2005. Regulated protein degradation. *TRENDS in Biochemical Sciences* **30**, pp.283-286.

Vaux, D.L. and Strasser, A. 1996. The molecular biology of apoptosis. *Proceedings of the National Academy of Sciences of the United States of America* **93**, pp.2239-2244.

Velier, J. Kim, M. Schwarz, C. Kim, T.W. Sapp, E. Chase, K. Aronin, N. DiFiglia, M. 1998. Wild-type and mutant huntingtins function in vesicle trafficking in the secretory and endocytic pathways. *Experimental Neurology* **152**, pp.34-40.

Verhagen, A.M. Ekert, P.G. Pakusch, M. Silke, J. Connolly, L.M. Reid, G.E. Moritz, R.L. Simpson, R.J. Vaux, D.L. 2000. Identification of DIABLO, a mammalian protein that promotes apoptosis by binding to and antagonizing IAP proteins. *Cell* **102**, pp.43-53.

Vrensen, G.F. Graw, J. De Wolf, A. 1991. Nuclear breakdown during terminal differentiation of primary lens fibres in mice: A transmission electron microscopic study. *Experimental Eye Research* **52**, pp.647-659.

Walker, F.O. 2007. Huntington's disease. *Lancet* **369**, pp.218-228.

Wang, K. Cheng, C. Li, L. Liu, H. Huang, Q. Xia, C. Yao, K. Sun, P. Horwitz, J. Gong, X. 2007. Gd-crystallin-associated protein aggregation and lens fiber cell denucleation. *Investigative Ophthalmology and Vision Science* **48**, pp.3719-3728.

Weber, G.F. and Menko, A.S. 2006. Actin filament organization regulates the induction of lens cell differentiation and survival. *Developmental Biology* **295**, pp.714-729.

Wederall, E. and De Longh, R.U. 2006. Extracellular matrix and integrin signaling in lens development and cataract. *Seminars in Cell and Developmental Biology* **17**, pp.759-776.

Weil, M. Raff, M.C. Braga, V.M. 1999. Caspase activation in the terminal differentiation of human epidermal keratinocytes. *Current Biology* **9**, pp.361-364.

Werner, A.B. de Vries, E. Tait, S.W. Bontjer, I. Borst, J. 2002. Bcl-2 family member bfl-1/a1 sequesters truncated bid to inhibit is collaboration with pro-apoptotic Bak or Bax. *Journal of Biological Chemistry* **277**, pp.22781-22788.

White, J.K. Auerbacj, W. Duyao, M.P. Vonsattel, J.P. Gusella, J.F. Joyner, A.L. MacDonald, M.E. 1997. Huntingtin is required for neurogenesis and is not impaired by the huntington's disease CAG expansion. *Nature Genetics* **17**, pp.404-410.

White, T.W. Goodenough, D.A. Paul, D.L. 1998. Targeted ablation of connexin50 in mice results in microphthalmia and zonular pulverulent cataracts. *Journal of Cell Biology* **143**, pp.815-825.

Wilson, A.S. Hobbs, B.G. Speed, T.P. Rakoczy, P.E. 2002. The microarray: Potential applications for ophthalmic research. *Molecular Vision* **8**, pp.259-270.

Wilson, S.E. 1999. Stimulus-specific and cell type-specific cascades: Emerging principles relating to control of apoptosis in the eye. *Experimental Eye Research* **69**, pp.255-266.

Wolter, K.G. Hsu, Y.T. Smith, C.L. Nechushtan, A. Xi, X.G. Youle, R.J. 1997. Movement of Bax from the cytosol to mitochondria during apoptosis. *Journal of Cell Biology* **139**, pp.1281-1292.

Wormstone, I.M. Tamiya, S. Anderson, I. Duncan, G. 2002. TGF-beta 2-induced matrix modification and cell transdifferentiation in the human lens capsular bag. *Investigative Ophthalmology & Visual Science* **43**, pp.2301-2308.

Wride, M.A. 1996. Cellular and molecular features of lens differentiation: A review of recent advances. *Differentiation* **61**, pp.77-93.

Wride, M.A. and Sanders, E.J. 1998. Nuclear degeneration in the developing lens and its regulation by TNF alpha. *Experimental Eye Research* **66**, pp.371-383.

Wride, M.A. Parker, E. Sanders, E.J. 1999. Members of the Bcl-2 and caspase families regulate nuclear degeneration during chick lens fibre differentiation. *Developmental Biology* **213**, pp.142-156.

Wride, M.A. 2000. Minireview: Apoptosis as seen through a lens. *Apoptosis* **5**, pp.203-209.

Wride, M.A. Mansergh, F.C. Adams, S. Everitt, R. Minnema, S.E. Rancourt, D.E. Evans, M.J. 2003. Expression profiling and gene discovery in the mouse lens. *Molecular Vision* **9**, pp.360-396.

Wride, M.A. Geatrell, J. Guggenheim, J.A. 2006. Proteases in eye development and disease. *Birth Defects Research Part C: Embryo Today: Reviews* **78**, pp.90-105.

Wyllie, A. Kerr, J. Currie, A. 1980. Cell death: The significance of apoptosis. *International Review of Cytology* **68**, pp.251-306.

Xi, J.H. Bai, F. Andley, U.P. 2003. Reduced survival of lens epithelial cells in the alpha A- crystallin-knockout mouse. *Journal of Cell Science* **116**, pp.1073-1085.

Xiao, W. Liu, W. Li, Z. Liang, D. Li, L. White, L.D. Fox, D.A. Overbeek, P.A. Chen, Q. 2006. Gene expression profiling in embryonic mouse lenses. *Molecular Vision* **12**, pp.1692-1698.

Xie, L. Chen, H. Overbeek, P.A. Reneker, L.W. 2007. Elevated insulin signaling disrupts the growth and differentiation pattern of the mouse lens. *Molecular Vision* **13**, pp.397-407.

Yang, J. Liu, X. Bhalla, K. Kim, C.N. Ibrado, A.M. Cai, J. Peng, T.I. Jones, D.P. Wang, X. 1997a. Prevention of apoptosis by Bcl-2: Release of cytochrome c from mitochondira blocked. *Science* **275**, pp.1129-1132.

Yang, R. Hsu, D.K. Liu, F. 1996. Expression of galectin-3 modulates T-cell growth and apoptosis. *Proceedings of the National Academy of Sciences of the United States of America* **93**, pp.6737-6742.

Yang, T. Kozopas, K.M. Craig, R.W. 1995. The intracellular distribution and pattern of expression of Mcl-1 overlap with, but are not identical to, those of Bcl-2. *Journal of Cell Biology* **128**, pp.1173-1184.

Yang, X. Khosravi-Far, R. Chang, H.Y. Baltimore, D. 1997b. DAXX, a novel FAS-binding protein that activates JNK and apoptosis. *Cell* **89**, pp.1067-1076.

Young, A.B. 2003. Huntingtin in health and disease. *Neurodegeneration* **111**, pp.299-302.

Zandy, A.J. Lakhani, S. Zheng, T. Flavell, R.A. Bassnett, S. 2005. Role of the executioner caspases during lens development. *Journal of Biological Chemistry* **280**, pp.30263-30272.

Zandy, A.J. and Bassnett, S. 2007. Proteolytic mechanisms underlying mitochondrial degradation in the ocular lens. *Investigative Ophthalmology and Vision Science* **48**, pp.293-302.

Zermati, Y. Garrido, C. Amsellem, S. Fishelson, S. Bouscary, D. Valensi, F. Varet, B. Solary, E. Hermine, O. 2001. Caspase activation is required for terminal erythroid differentiation. *Journal of Experimental Medicine* **193**, pp.247-254.

Zhang, J. Liu, X. Scherer, D.C. van Kaer, L. Wang, X. Xu, M. 1998. Resistance to DNA fragmentation and chromatin condensation in mice lacking the DNA fragmentation factor 45. *Proceedings of the National Academy of Sciences of the United States of America* **95**, pp.12480-12485.

Zhang, Y. Leavitt, B.R. van Raamsdonk, J.M. Dragatsis, I. Goldowitz, D. MacDonald, M.E. Hayden, M.R. Friedlander, R.M. 2006. Huntingtin inhibits caspase-3 activation. *EMBO Journal* **25**, pp.5896-5906.

Zhou, M. Leiberman, J. Xu, J. Lavker, R.M. 2006. A hierarchy of proliferative cells exists in mouse lens epithelium: Implications for lens maintenance. *Investigative Ophthalmology and Vision Science* **47**, pp.2997-3003.

Appendix 1: Composition of Solutions

RNA gel composition

Gel Volume	Formaldehyde	10 x MOPS	Double Autoclaved Water
100ml	18ml	10ml	72ml
150ml	27ml	15ml	108ml
200ml	36ml	20ml	144ml
250ml	45ml	25ml	180ml
300ml	54ml	30ml	216ml

Add sufficient agarose in water to give a final 1.5% agarose concentration (i.e. 1.5g in 100ml). Add the formaldehyde and 10 x MOPS in fume hood after the agarose has boiled.

Running buffer for RNA denaturing gels

83ml formaldehyde

100ml 10 x MOPS

817ml double distilled water

10 x MOPS

To make 1 litre:

Add 41.85g 4-morpholinepropanesulfonic acid (MOPS free acid) and 6.8g sodium acetate-$3H_2O$ and stir until completely dissolved. Add 20ml of 0.5M Na_2EDTA solution and adjust pH to 7.0 with 10M NaOH. Adjust volume to 1 litre with double autoclaved H_2O. Store protected from light at 4°C.

Loading buffer for RNA denaturing gels

50% glycerol

10mM EDTA

0.25% bromophenol blue

0.25% xylene cyanol FF

Wash Solution I for Apoptosis Arrays

To make 500ml:

12.5ml 20 x SSPE to make a final concentration of 0.5 x SSPE

50ml 10% SDS to make a final concentration of 1% SDS

437.5ml double autoclaved water

Wash Solution II for Apoptosis Arrays

To make 500ml:

2.5ml 20 x SSPE to make a final concentration of 0.1 x SSPE

50ml 10% SDS to make a final concentration of 1% SDS

447.5ml double autoclaved water

Stripping Solution for Apoptosis Arrays

To make up 1 litre:

10ml 1M Tris-HCL pH 8 to give a final concentration of 10mM

1mM EDTA

100ml 10% SDS

0.5M Tris-HCl pH6.8

6g Tris base

60ml distilled water

Adjust to pH6.8 with HCl

Bring up to 100ml with distilled water

Store at 4°C

1.5M Tris-HCl pH8.8

27.23g Tris base

80ml distilled water

Adjust to pH 8.8 with HCl

Bring up to 150ml with distilled water

Store at 4°C

10% APS

1g ammonium persulphate

Dissolve in 10ml distilled water.

10 x TBS

10mM Tris

150mM NaCl

pH 7.6

Make up to 1 litre with water

4% Paraformaldehyde (PFA)

Dissolve 4g paraformaldehyde powder in 100ml – heat until dissolved – store at 4°C

1 x PBS

40g NaCl

1g KCl

5.75g Na_2HPO_4

1g KH_2PO_4

5 litres distilled water

Stripping Solution for Western Blotting

15g glycine

1g SDS

10ml Tween20

Set pH to 2.2

Make up to 1 litre with double autoclaved water.

Appendix 2: List of Genes Included on the Array

Array Coordinate	Gene Family	Gene Name	Accession Number	Gene Description
A1	Genomic DNA	GEN	N/A	Genomic DNA
P1	Genomic DNA	GEN	N/A	Genomic DNA
B2	Apoptosis-Related Factors	ABP1	AA109909	mp10d09.r1 Life Tech mouse embryo 8 5dpc 10664019 Mus musculus cDNA clone IMAGE:568817 5' similar to gb:U11863 AMILORIDE-SENSITIVE AMINE OXIDASE (HUMAN);, mRNA sequence
C2	Apoptosis-Related Factors	ADAM17	NM_009615	Mus musculus a disintegrin and metalloproteinase domain 17 (Adam17), mRNA
D2	Apoptosis-Related Factors	API5	NM_007466	Mus musculus apoptosis inhibitor 5 (Api5), mRNA
E2	Apoptosis-Related Factors	ATM	NM_007499	Mus musculus ataxia telangiectasia gene mutated in human beings (Atm), mRNA
F2	Apoptosis-Related Factors	CAD	NM_007859	Mus musculus DNase inhibited by DNA fragmentation factor (Didff), mRNA
G2	Apoptosis-Related Factors	CAV2	AF141322	Mus musculus caveolin-2 mRNA, complete cds
H2	Apoptosis-Related Factors	CD47	NM_010581	Mus musculus integrin-associated protein (Itgp), mRNA
I2	Apoptosis-Related Factors	CHML	AF189156	Mus musculus rab escort protein-2 (Chml) gene, complete cds
J2	Apoptosis-Related Factors	CIDE-A	NM_007702	Mus musculus cell death-inducing DNA fragmentation factor, alpha subunit-like effector A (Cidea), mRNA
K2	Apoptosis-Related Factors	CLDN3	NM_009902	Mus musculus claudin 3 (Cldn3), mRNA
L2	Apoptosis-Related Factors	Cln3	NM_009907	Mus musculus ceroid lipofuscinosis, neuronal 3, juvenile (Batten, Spielmeyer-Vogt disease) (Cln3), mRNA
M2	Apoptosis-Related Factors	Clu	NM_013492	Mus musculus alpha-clustrin and beta-clustrin mRNA, complete cds
N2	Apoptosis-Related Factors	Cox-1/Ptgs1	NM_008969	Mus musculus prostaglandin-endoperoxide synthase 1 (Ptgs1), mRNA
O2	Apoptosis-Related Factors	Cox-2/Ptgs2	NM_011198	Mus musculus prostaglandin-endoperoxide synthase 2 (Ptgs2), mRNA
B3	Apoptosis-Related Factors	CAS/CSE1	AI549625	ve53d06.y1 Beddington mouse embryonic region Mus musculus cDNA clone IMAGE:821867 5' similar to SW:CAS_HUMAN P55060 CELLULAR APOPTOSIS SUSCEPTIBILITY PROTEIN. ;, mRNA sequence
C3	Apoptosis-Related Factors	Ctsd	NM_009983	Mus musculus cathepsin D (Ctsd), mRNA
D3	Apoptosis-Related Factors	Cytochrome p450 oxidoreductase	NM_008898	Mus musculus P450 (cytochrome) oxidoreductase (Por), mRNA
E3	Apoptosis-Related Factors	DAD-1	NM_010015	Mus musculus defender against cell death 1 (Dad1), mRNA

Array Coordinate	Gene Family	Gene Name	Accession Number	Gene Description
F3	Apoptosis-Related Factors	Dap1	AI196645	ui53d07.y1 Sugano mouse liver mlia Mus musculus cDNA clone IMAGE:1886125 5' similar to SW:DAP1_HUMAN P51397 DEATH-ASSOCIATED PROTEIN 1 ;, mRNA sequence
G3	Apoptosis-Related Factors	DAXX	NM_007829	Mus musculus Fas death domain-associated protein (Daxx), mRNA
H3	Apoptosis-Related Factors	DEDD	NM_011615	Mus musculus tumor necrosis factor (ligand) superfamily, member 19 (Tnfsf19-pending), mRNA
I3	Apoptosis-Related Factors	DNAse1	NM_010061	Mus musculus mRNA for deoxyribonuclease I, complete cds
J3	Apoptosis-Related Factors	DNAse2	NM_010062	Mus musculus deoxyribonuclease II (Dnase2), mRNA
K3	Apoptosis-Related Factors	Fem1B	NM_010193	Mus musculus feminization 1 b homolog (C. elegans) (Fem1b), mRNA
L3	Apoptosis-Related Factors	FLASH	NM_011997	Mus musculus caspase 8 associated protein 2 (Casp8ap2), mRNA
M3	Apoptosis-Related Factors	Galectin-3	X16834	Mouse mRNA for Mac-2 antigen
N3	Apoptosis-Related Factors	GAPDH	NM_008084	Mus musculus glyceraldehyde-3-phosphate dehydrogenase (Gapd), mRNA
O3	Apoptosis-Related Factors	GPX1	NM_008160	Mus musculus glutathione peroxidase 1 (Gpx1), mRNA
B4	Apoptosis-Related Factors	GSN	NM_010354	Mus musculus gelsolin (Gsn), mRNA
C4	Apoptosis-Related Factors	HD	U24233	Mus musculus huntingtin (Hd) mRNA, complete cds
D4	Apoptosis-Related Factors	HnrpA1	NM_010447	Mus musculus heterogeneous nuclear ribonucleoprotein A1 (Hnrpa1), mRNA
E4	Apoptosis-Related Factors	ICAD/DFFA	NM_010044	Mus musculus DNA fragmentation factor, alpha subunit (Dffa), mRNA
F4	Apoptosis-Related Factors	Integrin-αV	NM_008402	Mus musculus integrin alpha V (Cd51) (Itgav), mRNA
G4	Apoptosis-Related Factors	MFGE8	NM_008594	Mus musculus milk fat globule-EGF factor 8 protein (Mfge8), mRNA
H4	Apoptosis-Related Factors	PGES	AB041997	Mus musculus PGES mRNA for prostaglandin E synthase, complete cds.
I4	Apoptosis-Related Factors	MT-2	K02236	vf04g05.y1 Knowles Solter mouse blastocyst B3 Mus musculus cDNA clone IMAGE:834776 5' similar to gb:K02236 Mouse metallothionein II (MOUSE);, mRNA sequence
J4	Apoptosis-Related Factors	eNOS	NM_008713	Mus musculus nitric oxide synthase 3, endothelial cell (Nos3), mRNA
K4	Apoptosis-Related Factors	iNOS	NM_010927	Mus musculus nitric oxide synthase 2, inducible, macrophage (Nos2), mRNA
L4	Apoptosis-Related Factors	nNOS	NM_008712	Mus musculus nitric oxide synthase 1, neuronal (Nos1), mRNA
M4	Apoptosis-Related Factors	ODC	NM_013614	Mus musculus ornithine decarboxylase, structural (Odc), mRNA
N4	Apoptosis-Related Factors	P2RX1	NM_008771	Mus musculus purinergic receptor P2X, ligand-gated ion channel, 1 (P2rx1), mRNA
O4	Apoptosis-Related Factors	uPAR1	NM_011113	Mus musculus urokinase plasminogen activator receptor (Plaur), mRNA

Array Coordinate	Gene Family	Gene Name	Accession Number	Gene Description
B5	Apoptosis-Related Factors	PDCD1	NM_008798	Mus musculus programmed cell death 1 (Pdcd1), mRNA
C5	Apoptosis-Related Factors	PDCD2	NM_008799	Mus musculus programmed cell death 2 (Pdcd2), mRNA
D5	Apoptosis-Related Factors	PIGA	D26047	Mouse testis mRNA for Pig-a
E5	Apoptosis-Related Factors	PIN	AF020185	mj05g09.r1 Soares mouse embryo NbME13.5 14.5 Mus musculus cDNA clone IMAGE:475264 5' similar to WP:T26A5.9 CE00788 ;, mRNA sequence
F5	Apoptosis-Related Factors	PLA2G1B	NM_011107	Mus musculus phospholipase A2, group IB, pancreas (Pla2g1b), mRNA
G5	Apoptosis-Related Factors	ZAC1/PLAGL1	X95504	M.musculus mRNA for zinc finger protein
H5	Apoptosis-Related Factors	PRKR	NM_011163	Mus musculus eukaryotic translation initiation factor 2 alpha kinase 2 (Eif2ak2), mRNA
I5	Apoptosis-Related Factors	REQ	NM_011262	Mus musculus requiem (Req), mRNA
J5	Apoptosis-Related Factors	RP105/Ly78	NM_008533	Mus musculus lymphocyte antigen 78 (Ly78), mRNA
K5	Apoptosis-Related Factors	Mts-1	X16190	Mouse mts1 gene
L5	Apoptosis-Related Factors	SAG-1	AF092877	Mus musculus zinc RING finger protein SAG mRNA, complete cds
M5	Apoptosis-Related Factors	SARP-1	NM_009144	Mus musculus stromal cell derived factor 5 (Sdf5), mRNA
N5	Apoptosis-Related Factors	SARP-2/sFRP-1	U88566	Mus musculus secreted frizzled related protein sFRP-1 (Sfrp1) mRNA, complete cds
O5	Apoptosis-Related Factors	sFRP-5/SARP-3	AF117759	Mus musculus secreted frizzled-related protein 5 (Sfrp5) mRNA, complete cds
B6	Apoptosis-Related Factors	SIAH1	NM_009172	Mus musculus seven in absentia 1A (Siah1a), mRNA
C6	Apoptosis-Related Factors	SREBF1	AB017337	Mus musculus mRNA for sterol regulatory element-binding protein-1 (SREBP-1), partial cds
D6	Apoptosis-Related Factors	SREBF2	AW106709	um32e12.y1 Sugano mouse kidney mkia Mus musculus cDNA clone IMAGE:2236270 5' similar to SW:SRE2_CRIGR Q60429 STEROL REGULATORY ELEMENT BINDING PROTEIN-2 ;, mRNA sequence
E6	Apoptosis-Related Factors	TDAG8	NM_008152	Mus musculus G-protein coupled receptor 25 (Gpcr25), mRNA
F6	Apoptosis-Related Factors	TFAR15	AF159368	Mus musculus TF-1 cell apoptosis related protein-15 (Tfar15) mRNA, complete cds
G6	Apoptosis-Related Factors	Thrombospondin	NM_011580	Mouse thrombospondin 1 mRNA, complete cds
H6	Apoptosis-Related Factors	TIAF1	AF104984	Mus musculus TGF-b1-induced anti-apoptotic factor 1 mRNA, complete cds
I6	Apoptosis-Related Factors	TIAL1	NM_009383	Mus musculus Tial1 cytotoxic granule-associated RNA-binding protein-like 1 (Tial1), mRNA
J6	Apoptosis-Related Factors	TSSC3	NM_009434	Mus musculus tumor-suppressing subchromosomal transferable fragment 3 (Tssc3), mRNA

Array Coordinate	Gene Family	Gene Name	Accession Number	Gene Description
K6	Apoptosis-Related Factors	TXN	NM_011660	Mus musculus thioredoxin (Txn), mRNA
L6	Caspases and Regulators	Caspase-1	NM_009807	Mus musculus caspase 1 (Casp1), mRNA
M6	Caspases and Regulators	Caspase-2	NM_007610	Mus musculus caspase 2 (Casp2), mRNA
N6	Caspases and Regulators	Caspase-3	NM_009810	Mus musculus caspase 3, apoptosis related cysteine protease (Casp3), mRNA
O6	Caspases and Regulators	Caspase-6	NM_009811	Mus musculus caspase 6 (Casp6), mRNA
B7	Caspases and Regulators	Caspase-7	NM_007611	Mus musculus caspase 7 (Casp7), mRNA
C7	Caspases and Regulators	Caspase-8	AJ007749	Mus musculus mRNA for caspase-8
D7	Caspases and Regulators	Caspase-9	NM_015733	Mus musculus mRNA for caspase9, complete cds
E7	Caspases and Regulators	Caspase-11	NM_007609	Mus musculus caspase 11 (Casp11), mRNA
F7	Caspases and Regulators	Caspase-12	NM_009808	Mus musculus caspase 12 (Casp12), mRNA
G7	Caspases and Regulators	Caspase-14	NM_009809	Mus musculus caspase 14 (Casp14), mRNA
H7	Caspases and Regulators	FLIPL/Cash	NM_009805	Mus musculus caspase homolog (Cash), mRNA
I7	Caspases and Regulators	Granzyme B	NM_013542	Mus musculus granzyme B (Gzmb), mRNA
J7	Caspases and Regulators	Granzyme A	NM_010370	Mus musculus granzyme A (Gzma), mRNA
K7	Caspases and Regulators	cIAP-1	NM_007464	Mus musculus apoptosis inhibitor 1 (Api1), mRNA
L7	Caspases and Regulators	cIAP-2	NM_007465	Mus musculus apoptosis inhibitor 2 (Api2), mRNA
M7	Caspases and Regulators	NAIP	NM_010872	Mus musculus neuronal apoptosis inhibitory protein 2 (Naip2), mRNA
N7	Caspases and Regulators	PARP	NM_007415	Mus musculus ADP-ribosyltransferase (NAD+; poly (ADP-ribose) polymerase) 1 (Adprt1), mRNA
O7	Caspases and Regulators	PARP-2	NM_009632	Mus musculus ADP-ribosyltransferase (NAD+; poly (ADP-ribose) polymerase) 2 (Adprt2), mRNA
B8	Caspases and Regulators	Sentrin/UBL1	NM_009460	Mus musculus ubiquitin-like 1 (Ubl1), mRNA
C8	Caspases and Regulators	Survivin	NM_009689	Mus musculus apoptosis inhibitor 4 (Api4), mRNA
D8	Caspases and Regulators	XIAP	NM_009688	Mus musculus apoptosis inhibitor 3 (Api3), mRNA
E8	Cell Cycle Regulators	53BP2	U58881	Mus musculus p53 binding protein 2 homolog (p53BP2), partial cDNA
F8	Cell Cycle Regulators	APEX/Ref-1	NM_009687	Mus musculus apurinic/apyrimidinic endonuclease (Apex), mRNA
G8	Cell Cycle Regulators	Calcyclin	NM_011313	Mus musculus calcium binding protein A6 (calcyclin) (S100a6), mRNA
H8	Cell Cycle Regulators	CBP	S66385	CREB-binding protein [mice, brain, mRNA Partial, 7326 nt]

Array Coordinate	Gene Family	Gene Name	Accession Number	Gene Description
I8	Cell Cycle Regulators	CDC2	NM_007659	Mus musculus cell division cycle 2 homolog A (S. pombe) (Cdc2a), mRNA
J8	Cell Cycle Regulators	CDK2	NM_016756	Mus musculus mRNA for cyclin dependent kinase (CDK2L) - the 39 kDa variant of CDK2
K8	Cell Cycle Regulators	CDK4	NM_009870	Mus musculus cyclin-dependent kinase 4 (Cdk4), mRNA
L8	Cell Cycle Regulators	CDK5	NM_007668	Mus musculus cyclin-dependent kinase 5 (Cdk5), mRNA
M8	Cell Cycle Regulators	CDK6	AF132483	Mus musculus strain BALB/c cyclin-dependent kinase 6 (Cdk6) mRNA, complete cds
N8	Cell Cycle Regulators	Cyclin A	NM_009828	Mus musculus cyclin A2 (Ccna2), mRNA
O8	Cell Cycle Regulators	Cyclin D1	M64403	Mus domesticus cyclin-like protein (induced by colony-stimulating factor 1) (CYL-1) mRNA, complete cds
B9	Cell Cycle Regulators	Cyclin G1	NM_009831	Mus musculus cyclin G (Ccng), mRNA
C9	Cell Cycle Regulators	DP1	NM_009361	Mus musculus transcription factor Dp 1 (Tfdp1), mRNA
D9	Cell Cycle Regulators	MDM2	NM_010786	Mus musculus transformed mouse 3T3 cell double minute 2 (Mdm2), mRNA
E9	Cell Cycle Regulators	c-myc	NM_010849	Mus musculus myelocytomatosis oncogene (Myc), mRNA
F9	Cell Cycle Regulators	p15INK4b/CDKN2B	NM_007670	Mus musculus cyclin-dependent kinase inhibitor 2B (p15, inhibits CDK4) (Cdkn2b), mRNA
G9	Cell Cycle Regulators	p19/NSG2	NM_008741	Mus musculus neuron specific gene family member 2 (Nsg2), mRNA
H9	Cell Cycle Regulators	RBL1/p107	U27177	Mus musculus p107 (p107) mRNA, complete cds
I9	Cell Cycle Regulators	RBL2/p130	NM_011250	Mus musculus retinoblastoma-like 2 (Rbl2), mRNA
J9	Cell Cycle Regulators	P300	AA881090	vz06c10.r1 Soares_mammary_gland_NbMMG Mus musculus cDNA clone IMAGE:1314930 5' similar to TR:Q09472 Q09472 E1A-ASSOCIATED PROTEIN P300. ;, mRNA sequence
K9	Cell Cycle Regulators	PAK1	NM_011035	Mus musculus p21 (CDKN1A)-activated kinase 1 (Pak1), mRNA
L9	Cell Cycle Regulators	PCNA	NM_011045	Mus musculus proliferating cell nuclear antigen (Pcna), mRNA.
M9	Cell Cycle Regulators	pRB	NM_009029	Mus musculus retinoblastoma 1 (Rb1), mRNA
N9	Cell Cycle Regulators	RBBP4/RbAp48	NM_009030	Mus musculus retinoblastoma binding protein 4 (Rbbp4), mRNA
O9	Cell Cycle Regulators	RBP1	AA474808	ve62d06.r1 Beddington mouse embryonic region Mus musculus cDNA clone IMAGE:822731 5' similar to gb:S66427 RETINOBLASTOMA BINDING PROTEIN 1 (HUMAN);, mRNA sequence
B10	Cell Cycle Regulators	RBBP6/PACT/RBQ1	U28789	Mus musculus p53-associated cellular protein PACT mRNA, partial cds
C10	Cell Cycle Regulators	Sp1	NM_013672	Mus musculus transcription factor Sp1 mRNA, complete cds
D10	Cell Cycle Regulators	TRP53/p53	NM_011640	Mus musculus transformation related protein 53 (Trp53), mRNA

Array Coordinate	Gene Family	Gene Name	Accession Number	Gene Description
E10	Cytokines and Receptors	AR	NM_013476	Mouse mRNA for Tfm androgen receptor (inactive)
F10	Cytokines and Receptors	ART/Agrp	NM_007427	Mus musculus agouti related protein (Agrp), mRNA
G10	Cytokines and Receptors	Axl	NM_009465	Mus musculus AXL receptor tyrosine kinase (Axl), mRNA
H10	Cytokines and Receptors	Dtk/Tyro3	U18933	Mus musculus receptor tyrosine kinase (Dtk) mRNA, complete cds
I10	Cytokines and Receptors	EGF	J00380	mouse epidermal growth factor (egf) mrna
J10	Cytokines and Receptors	EGF R	NM_007912	Mus musculus epidermal growth factor receptor (Egfr), mRNA
K10	Cytokines and Receptors	erbB2	U71126	Mus musculus erbB2 mRNA, partial cds
L10	Cytokines and Receptors	erbB3	L47240	Mus musculus tyrosine kinase (erbB3) mRNA, partial cds
M10	Cytokines and Receptors	erbB4	AF059176	Mus musculus EGF-like growth factor receptor ErbB4 extracellular domain mRNA, partial cds
N10	Cytokines and Receptors	GAS1	NM_008086	Mus musculus growth arrest specific 1 (Gas1), mRNA
O10	Cytokines and Receptors	GAS2	NM_008087	Mus musculus growth arrest specific 2 (Gas2), mRNA
B11	Cytokines and Receptors	GM-CSF	X02333	Murine mRNA for granulocyte-macrophage colony stimulating factor (GM-GSF)
C11	Cytokines and Receptors	GM-CSF Rα	NM_009970	Mus musculus colony stimulating factor 2 receptor, alpha, low-affinity (granulocyte-macrophage) (Csf2ra), mRNA
D11	Cytokines and Receptors	IFN-γ R1	NM_010511	Mus musculus interferon gamma receptor (Ifngr), mRNA
E11	Cytokines and Receptors	IFN-γ R2	NM_008338	Mus musculus interferon gamma receptor 2 (Ifngr2), mRNA
F11	Cytokines and Receptors	IGF-I	NM_010512	Mus musculus insulin-like growth factor 1 (IGF1), mRNA
G11	Cytokines and Receptors	IGF-II	NM_010514	Mus musculus insulin-like growth factor 2 (IGF2), mRNA
H11	Cytokines and Receptors	IGF R	AF056187	Mus musculus insulin-like growth factor I receptor mRNA, complete cds
I11	Cytokines and Receptors	IL-1 R AcP	NM_008364	Mus musculus interleukin 1 receptor accessory protein (Il1rap), mRNA
J11	Cytokines and Receptors	IL-1ra	M57525	Mouse interleukin 1 receptor antagonist (IL1RA) mRNA, complete cds
K11	Cytokines and Receptors	IL-1 RI	NM_008362	Mus musculus interleukin 1 receptor, type I (Il1r1), mRNA
L11	Cytokines and Receptors	IL-1 RII	NM_010555	Mus musculus interleukin 1 receptor, type II (Il1r2), mRNA
M11	Cytokines and Receptors	IL-1α	NM_010554	Mus musculus interleukin 1 alpha (Il1a), mRNA
N11	Cytokines and Receptors	IL-1β	NM_008361	Mus musculus interleukin 1 beta (Il1b), mRNA
O11	Cytokines and Receptors	IL-2	NM_008366	Mouse mRNA for interleukin-2 (IL-2)
B12	Cytokines and Receptors	IL-2 Rα	NM_008367	Mus musculus interleukin 2 receptor, alpha chain (Il2ra), mRNA

Array Coordinate	Gene Family	Gene Name	Accession Number	Gene Description
C12	Cytokines and Receptors	IL-2 Rβ	NM_008368	Mus musculus interleukin 2 receptor, beta chain (Il2rb), mRNA
D12	Cytokines and Receptors	IL-2 Rγ	NM_013563	Mouse interleukin 2 receptor gamma chain mRNA, complete cds
E12	Cytokines and Receptors	IL-4	M25892	Mus musculus interleukin 4 (Il-4) mRNA, complete cds
F12	Cytokines and Receptors	IL-4 Rα	NM_010557	Mus musculus interleukin 4 receptor, alpha (Il4ra), mRNA
G12	Cytokines and Receptors	IL-10	NM_010548	Mus musculus interleukin 10 (Il10), mRNA
H12	Cytokines and Receptors	IL-10 Rα	NM_008348	Mus musculus interleukin 10 receptor, alpha (Il10ra), mRNA
I12	Cytokines and Receptors	IL-12 p35	M86672	Mus musculus interleukin 12 p35 subunit, complete cds
J12	Cytokines and Receptors	IL-12 p40	M86671	Mus musculus interleukin 12 p40 subunit, complete cds
K12	Cytokines and Receptors	IL-12 Rβ1	NM_008353	Mus musculus interleukin 12 receptor, beta 1 (Il12rb1), mRNA
L12	Cytokines and Receptors	IL-12 Rβ2	NM_008354	Mus musculus interleukin 12 receptor, beta 2 (Il12rb2), mRNA
M12	Cytokines and Receptors	IL-13	NM_008355	Mus musculus interleukin 13 (Il13), mRNA
N12	Cytokines and Receptors	IL-13 Rα1	S80963	NR4=IL-13 receptor alpha chain [mice, embryonal stem cell, Genomic/mRNA, 1680 nt]
O12	Cytokines and Receptors	IL-15	NM_008357	Mus musculus interleukin 15 (Il15), mRNA
B13	Cytokines and Receptors	IL-15 Rα	NM_008358	Mus musculus interleukin 15 receptor, alpha chain (Il15ra), mRNA
C13	Cytokines and Receptors	Mannose 6-phosphate R	U04710	Mus musculus domesticus C57 Black 6 x CBA cation-independent mannose 6-phosphate/insulin-like growth factor II receptor precursor mRNA, complete cds
D13	Cytokines and Receptors	M-CSF	NM_007778	Mus musculus colony stimulating factor 1 (macrophage) (Csf1), mRNA
E13	Cytokines and Receptors	M-CSF R	NM_007779	Mus musculus colony stimulating factor 1 receptor (Csf1r), mRNA
F13	Cytokines and Receptors	Prolactin	NM_011164	Mus musculus prolactin (Prl), mRNA
G13	Cytokines and Receptors	TGF-β	NM_011577	Mus musculus transforming growth factor, beta 1 (Tgfb1), mRNA
H13	Cytokines and Receptors	TGF-β2	NM_009367	Mus musculus transforming growth factor, beta 2 (Tgfb2), mRNA
I13	Cytokines and Receptors	TGF-β3	NM_009368	Mus musculus transforming growth factor, beta 3 (Tgfb3), mRNA
J13	Cytokines and Receptors	TGF-β RI	NM_007394	Mus musculus activin A receptor, type 1 (Acvr1), mRNA
K13	Cytokines and Receptors	TGF-β RII	NM_009371	Mus musculus transforming growth factor, beta receptor II (Tgfbr2), mRNA
L13	Cytokines and Receptors	TGF-β RIII	AF039601	Mus musculus betaglycan mRNA, complete cds
M13	Cytokines and Receptors	TrkB	NM_008745	Mus musculus neurotrophic tyrosine kinase, receptor, type 2 (Ntrk2), mRNA
N13	Cytokines and Receptors	TrkC	AF035400	Mus musculus neurotrophin-3 receptor non-catalytic isoform 2 (trkC) mRNA, complete cds

Array Coordinate	Gene Family	Gene Name	Accession Number	Gene Description
O13	Mitochondrial Associated	A1	L16462	Mus musculus hemopoietic-specific early response protein (A1) mRNA, complete cds
B14	Mitochondrial Associated	AIF/Pdcd8	NM_012019	Mus musculus programmed cell death 8 (apoptosis inducing factor) (Pdcd8), mRNA
C14	Mitochondrial Associated	Apaf1	NM_009684	Mus musculus apoptotic protease activating factor 1 (Apaf1), mRNA
D14	Mitochondrial Associated	Bad	NM_007522	Mus musculus Bcl-associated death promoter (Bad), mRNA
E14	Mitochondrial Associated	Bag-1	NM_009736	Mus musculus Bcl2-associated athanogene 1 (Bag1), mRNA
F14	Mitochondrial Associated	BAK	NM_007523	Mus musculus Bcl2 homologous antagonist/killer (Bak), mRNA
G14	Mitochondrial Associated	Bax-α	NM_007527	Mus musculus Bcl2-associated X protein (Bax), mRNA
H14	Mitochondrial Associated	Bcl-2	NM_009741	Mus musculus B-cell leukemia/lymphoma 2 (Bcl2), mRNA
I14	Mitochondrial Associated	Bcl-w	NM_007537	Mus musculus Bcl2-like 2 (Bcl2l2), mRNA
J14	Mitochondrial Associated	Bcl-x	NM_009743	Mus musculus Bcl2-like (Bcl2l), mRNA
K14	Mitochondrial Associated	BID	NM_007544	Mus musculus BH3 interacting domain death agonist (Bid), mRNA
L14	Mitochondrial Associated	Bim	NM_009754	Mus musculus Bcl2 interacting mediator of cell death (Bim), mRNA
M14	Mitochondrial Associated	Cytochrome C	NM_007808	Mus musculus cytochrome c, somatic (Cycs), mRNA
N14	Mitochondrial Associated	Mcl-1	NM_008562	Mus musculus myeloid cell leukaemia sequence 1 (Mcl1), mRNA
O14	Signal Transduction	14-3-3 eta	NM_011738	Mus musculus tyrosine 3-monooxygenase/tryptophan 5-monooxygenase activation protein, eta polypeptide (Ywhah), mRNA
B15	Signal Transduction	AKT/PKB	NM_009652	Mus musculus thymoma viral proto-oncogene (Akt), mRNA
C15	Signal Transduction	ALG4	AF055669	Mus musculus apoptosis-linked gene 4, F form (Alg-4) mRNA, partial cds
D15	Signal Transduction	ASK1/MAP3K5	NM_008580	Mus musculus mitogen activated protein kinase kinase kinase 5 (Map3k5), mRNA
E15	Signal Transduction	Bcl-10	NM_009740	Mus musculus B-cell leukemia/lymphoma 10 (Bcl10), mRNA
F15	Signal Transduction	CARDIAK	AA655189	vv13a12.r1 Stratagene mouse heart (#937316) Mus musculus cDNA clone IMAGE:1211518 5' similar to TR:G1236943 G1236943 RIP PROTEIN KINASE. ;, mRNA sequence
G15	Signal Transduction	CRADD	NM_009950	Mus musculus CASP2 and RIPK1 domain containing adaptor with death domain (Cradd), mRNA
H15	Signal Transduction	TRAF3/CRAF1	NM_011632	Mus musculus Tnf receptor-associated factor 3 (Traf3), mRNA
I15	Signal Transduction	DAP Kinase	AA620064	vl53d10.r1 Stratagene mouse skin (#937313) Mus musculus cDNA clone IMAGE:975955 5' similar to TR:G434847 G434847 DAP-KINASE. ;, mRNA sequence

Array Coordinate	Gene Family	Gene Name	Accession Number	Gene Description
J15	Signal Transduction	DRAK2	AI585389	vj56a01.y1 Knowles Solter mouse blastocyst B1 Mus musculus cDNA clone IMAGE:933000 5' similar to SW:DAPK_HUMAN P53355 DEATH-ASSOCIATED PROTEIN KINASE 1 ;, mRNA sequence
K15	Signal Transduction	E2F1	NM_007891	Mus musculus E2F transcription factor 1 (E2f1), mRNA
L15	Signal Transduction	FADD	NM_010175	Mus musculus Fas-associating protein with death domain (Fadd), mRNA
M15	Signal Transduction	FAN	NM_010945	Mus musculus neutral sphingomyelinase (N-SMase) activation associated factor (Nsmaf), mRNA
N15	Signal Transduction	GSK3B	AF156099	Mus musculus glycogen synthase kinase 3 beta mRNA, complete cds
O15	Signal Transduction	IKK-α	NM_007700	Mus musculus conserved helix-loop-helix ubiquitous kinase (Chuk), mRNA
B16	Signal Transduction	IKK-β	AF088910	Mus musculus IkB kinase-beta (Ikkb) mRNA, complete cds
C16	Signal Transduction	MADD	AI595199	mk16f10.y1 Soares mouse p3NMF19.5 Mus musculus cDNA clone IMAGE:493099 5' similar to TR:O08873 O08873 RAB3 GDP/GTP EXCHANGE PROTEIN. ;, mRNA sequence
D16	Signal Transduction	MEKK1	AF117340	Mus musculus MAP kinase kinase kinase 1 (Mekk1) mRNA, complete cds
E16	Signal Transduction	MYD118	NM_008655	Mus musculus myeloid differentiation primary response gene 118 (Myd118), mRNA
F16	Signal Transduction	NF-κB DNA binding subunit	NM_008689	Mus musculus nuclear factor of kappa light chain gene enhancer in B-cells 1, p105 (Nfkb1), mRNA
G16	Signal Transduction	NF-κB inducing kinase	NM_016896	Mus musculus Nfkb inducing kinase (Nik-pending), mRNA
H16	Signal Transduction	NFκBp65	NM_009045	Mus musculus avian reticuloendotheliosis viral (v-rel) oncogene homolog A (Rela), mRNA
I16	Signal Transduction	Par-4	AA023558	mh76e12.r1 Soares mouse placenta 4NbMP13.5 14.5 Mus musculus cDNA clone IMAGE:456910 5' similar to TR:G456282 G456282 CLONE PAR-4 INDUCED BY EFFECTORS OF APOPTOSIS. ;, mRNA sequence
J16	Signal Transduction	PI-3 Kinase	NM_011084	Mus musculus phosphatidylinositol 3-kinase, C2 domain containing, gamma polypeptide (Pik3c2g), mRNA
K16	Signal Transduction	PKC-α	NM_011101	Mus musculus protein kinase C, alpha (Pkca), mRNA
L16	Signal Transduction	PP2A	AI894369	mf46e11.y1 Soares mouse embryo NbME13.5 14.5 Mus musculus cDNA clone IMAGE:408140 5' similar to gb:M64929 PROTEIN PHOSPHATASE PP2A, 55 KD REGULATORY SUBUNIT, ALPHA (HUMAN);, mRNA sequence
M16	Signal Transduction	PTEN	NM_008960	Mus musculus phosphatase and tensin homolog (Pten), mRNA
N16	Signal Transduction	RARβ2	S56660	retinoic acid nuclear receptor isoform beta 2 [mice, embryonal carcinoma cell line, PCC7-MZ1, mRNA, 2971 nt]

Array Coordinate	Gene Family	Gene Name	Accession Number	Gene Description
O16	Signal Transduction	RIP	NM_009068	Mus musculus receptor (TNFRSF)-interacting serine-threonine kinase 1 (Ripk1), mRNA
B17	Signal Transduction	RxR-β	X66224	M.musculus mRNA for retinoid X receptor-beta (mRXR-beta)
C17	Signal Transduction	TANK	NM_011529	Mus musculus TRAF family member-associated Nf-kappa B activator (Tank), mRNA
D17	Signal Transduction	TRADD	AA013699	mh12f08.r1 Soares mouse placenta 4NbMP13.5 14.5 Mus musculus cDNA clone IMAGE:442311 5' similar to PIR:A56911 A56911 TRADD protein - human ;, mRNA sequence
E17	Signal Transduction	TRAF1	NM_009421	Mus musculus Tnf receptor-associated factor 1 (Traf1), mRNA
F17	Signal Transduction	TRAF2	L35303	Mus musculus TNF receptor associated factor 2 (TRAF2) mRNA, complete cds
G17	Signal Transduction	TRAF5	NM_011633	Mus musculus Tnf receptor-associated factor 5 (Traf5), mRNA
H17	Signal Transduction	TRAF6	NM_009424	Mus musculus Tnf receptor-associated factor 6 (Traf6), mRNA
I17	Signal Transduction	TRANK	NM_016764	Mus musculus peroxiredoxin 4 (Prdx4), mRNA
J17	Signal Transduction	TRIP	NM_011634	Mus musculus TRAF-interacting protein (Traip), mRNA
K17	Telomerase Related	TP1/Tep1	NM_009351	Mus musculus telomerase associated protein 1 (Tep1), mRNA
L17	Telomerase Related	TERT/TP2	NM_009354	Mus musculus telomerase reverse transcriptase (Tert), mRNA
M17	Telomerase Related	TR/TeRc	U33831	Mus musculus telomerase RNA component gene
N17	Telomerase Related	TRF1	NM_009352	Mus musculus telomeric repeat binding factor 1 (Terf1), mRNA
O17	Telomerase Related	TRF2	NM_009353	Mus musculus telomeric repeat binding factor 2 (Terf2), mRNA
B18	TNF Superfamily	DR-6	AW211328	uo79f09.y1 NCI_CGAP_Mam3 Mus musculus cDNA clone IMAGE:2648777 5' similar to TR:O75509 O75509 TNFR-RELATED DEATH RECEPTOR-6. ;, mRNA sequence
C18	TNF Superfamily	B-NGF	NM_013609	Mouse nerve growth factor (NGF) precursor mRNA, complete cds
D18	TNF Superfamily	NGF R	AF105292	Mus musculus nerve growth factor receptor mRNA, complete cds
E18	TNF Superfamily	TNF-α/TNFSF2	NM_013693	Mouse tumor necrosis factor (TNF) mRNA, complete cds
F18	TNF Superfamily	TNF-β/TNFSF1	NM_010735	Mus musculus lymphotoxin A (Lta), mRNA
G18	TNF Superfamily	OX40L/TNFSF4	NM_009452	Mus musculus tax-transcriptionally activated glycoprotein 1 ligand (Txgp1l), mRNA
H18	TNF Superfamily	FasL/TNFSF6	NM_010177	Mus musculus Fas antigen ligand (Fasl), mRNA
I18	TNF Superfamily	TRAIL/TNFSF10	NM_009425	Mus musculus tumor necrosis factor (ligand) superfamily, member 10 (Tnfsf10), mRNA
J18	TNF Superfamily	TRANCE/RANK L/TNFSF11	NM_011613	Mus musculus tumor necrosis factor (ligand) superfamily, member 11 (Tnfsf11), mRNA

Array Coordinate	Gene Family	Gene Name	Accession Number	Gene Description
K18	TNF Superfamily	TWEAK/TNFSF12	AF030100	Mus musculus TWEAK mRNA, partial cds
L18	TNF Superfamily	TALL-1/THANK/BAFF/TNFSF13B	AF119383	Mus musculus B-cell activating factor (Baff) mRNA, complete cds
M18	TNF Superfamily	LIGHT/TNFSF14	AB029155	Mus musculus mRNA for LIGHT protein, complete cds
N18	TNF Superfamily	TNF RI/TNFRSF1A	NM_011609	Mus musculus tumor necrosis factor receptor superfamily, member 1a (Tnfrsf1a), mRNA
O18	TNF Superfamily	TNF RII/TNFRSF1B	NM_011610	Mus musculus tumor necrosis factor receptor superfamily, member 1b (Tnfrsf1b), mRNA
B19	TNF Superfamily	OX40/TNFRSF4	NM_011659	Mus musculus tax-transcriptionally activated glycoprotein 1 (Txgp1), mRNA
C19	TNF Superfamily	CD40/TNFRSF5	NM_011611	Mus musculus tumor necrosis factor receptor superfamily, member 5 (Tnfrsf5), mRNA
D19	TNF Superfamily	Fas/TNFRSF6	NM_007987	Mus musculus Fas antigen (Fas), mRNA
E19	TNF Superfamily	RANK/TRANCE/TNFRSF11A	NM_009399	Mus musculus tumor necrosis factor receptor superfamily, member 11a (Tnfrsf11a), mRNA
F19	TNF Superfamily	OPG/TNFRSF11B	NM_008764	Mus musculus osteoprotegerin (Opg), mRNA
A24	Genomic DNA	GEN	N/A	Genomic DNA
B24	Housekeeping Genes	β2-Microglobulin	NM_009735	Mus musculus beta-2 microglobulin (B2m), mRNA
C24	Housekeeping Genes	β-Actin	X03672	Mouse cytoskeletal mRNA for beta-actin
D24	Housekeeping Genes	Cyclophilin A	NM_008907	Mus musculus peptidylprolyl isomerase A (Ppia), mRNA
E24	Housekeeping Genes	HPRT	J00423	Mouse hypoxanthine phosphoribosyltransferase (hprt) mRNA, complete cds
F24	Housekeeping Genes	L19	NM_009078	Mus musculus ribosomal protein L19 (Rpl19), mRNA
G24	Housekeeping Genes	Transferrin R	X57349	M.musculus mRNA for transferrin receptor
H24	Housekeeping Genes	α-Tubulin	M13446	Mouse alpha-tubulin isotype M-alpha-2 mRNA, complete cds
I24	Negative Control	1xTE Buffer	N/A	1x TE Buffer
J24	Negative Control	1xTE Buffer	N/A	1x TE Buffer
K24	Negative Control	pUC19	M77789	pUC19 cloning vector.
L24	Negative Control	E. coli b0658 gene	AE000170	*E. coli* b0658 gene (ybeX).
M24	Negative Control	E. coli b1444 gene	AE000241	*E. coli* b1444 gene, putative enzyme; not classified.
N24	Negative Control	E. coli b3535 gene	AE000430	*E. coli* b3535 gene (yhjR).
P24	Genomic DNA	GEN	N/A	Genomic DNA

Table A2.1: ***Table of genes printed onto the apoptosis arrays.*** *The table presents the information provided by Sigma. The table provides the gene name along with its array coordinates, gene family and a brief description of the gene.*

Appendix 3: List of Genes Expressed Above Background at P7 and P14

Genes Expressed Above Background at P7

Gene ID	Gene Family	Mean Normalised Value
ABP1	Apoptosis-Related Factors	2.20
CAS/CSE1	Apoptosis-Related Factors	2.30
GSN	Apoptosis-Related Factors	14.86
ADAM17	Apoptosis-Related Factors	3.04
Ctsd	Apoptosis-Related Factors	13.55
HD	Apoptosis-Related Factors	3.26
API5	Apoptosis-Related Factors	2.97
Cytochrome p450 oxidoreductase	Apoptosis-Related Factors	3.38
HnrpA1	Apoptosis-Related Factors	21.71
SREBF2	Apoptosis-Related Factors	5.03
ATM	Apoptosis-Related Factors	2.41
DAD-1	Apoptosis-Related Factors	32.63
ICAD/DFFA	Apoptosis-Related Factors	4.30
PIN	Apoptosis-Related Factors	50.64
CAD	Apoptosis-Related Factors	2.70
Dap1	Apoptosis-Related Factors	8.10
Integrin-αV	Apoptosis-Related Factors	7.10
MFGE8	Apoptosis-Related Factors	2.75
Thrombospondin	Apoptosis-Related Factors	3.27
CD47	Apoptosis-Related Factors	2.40
DEDD	Apoptosis-Related Factors	4.02
CHML	Apoptosis-Related Factors	2.73
DNAse1	Apoptosis-Related Factors	2.35
REQ	Apoptosis-Related Factors	8.89
TIAL1	Apoptosis-Related Factors	15.97
CIDE-A	Apoptosis-Related Factors	2.43
TSSC3	Apoptosis-Related Factors	2.66
CLDN3	Apoptosis-Related Factors	2.04
Fem1B	Apoptosis-Related Factors	4.66
Mts-1	Apoptosis-Related Factors	23.74
TXN	Apoptosis-Related Factors	14.74
Cln3	Apoptosis-Related Factors	2.53
FLASH	Apoptosis-Related Factors	3.41
nNOS	Apoptosis-Related Factors	2.41
SAG-1	Apoptosis-Related Factors	4.26
Clu	Apoptosis-Related Factors	75.36
Galectin-3	Apoptosis-Related Factors	2.71
ODC	Apoptosis-Related Factors	17.27
GAPDH	Apoptosis-Related Factors	123.30
SARP-2/sFRP-1	Apoptosis-Related Factors	39.34
Cox-2/Ptgs2	Apoptosis-Related Factors	2.12
GPX1	Apoptosis-Related Factors	55.09
sFRP-5/SARP-3	Apoptosis-Related Factors	5.02
Caspase-7	Caspases and Regulators	18.92
Caspase-2	Caspases and Regulators	3.23
PARP	Caspases and Regulators	7.25
Cyclin G1	Cell Cycle Regulators	28.61

Gene ID	Gene Family	Mean Normalised Value
RBBP6/PACT/RBQ1	Cell Cycle Regulators	7.50
DP1	Cell Cycle Regulators	5.08
MDM2	Cell Cycle Regulators	5.15
APEX/Ref-1	Cell Cycle Regulators	11.18
Calcyclin	Cell Cycle Regulators	3.61
CBP	Cell Cycle Regulators	13.23
RBL2/p130	Cell Cycle Regulators	3.49
CDK2	Cell Cycle Regulators	2.66
CDK4	Cell Cycle Regulators	3.04
pRB	Cell Cycle Regulators	3.60
RBBP4/RbAp48	Cell Cycle Regulators	6.14
Cyclin D1	Cell Cycle Regulators	3.11
GM-CSF Rα	Cytokines and Receptors	13.28
Mannose 6-phosphate R	Cytokines and Receptors	5.02
M-CSF	Cytokines and Receptors	7.28
IGF-II	Cytokines and Receptors	4.29
TGF-β	Cytokines and Receptors	4.92
TGF-β2	Cytokines and Receptors	4.14
GAS1	Cytokines and Receptors	4.19
β-Actin	Housekeeping Genes	100.56
Cyclophilin A	Housekeeping Genes	47.11
L19	Housekeeping Genes	108.63
α-Tubulin	Housekeeping Genes	19.58
Bag-1	Mitochondrial Associated	11.44
Bcl-w	Mitochondrial Associated	12.40
Cytochrome C	Mitochondrial Associated	9.57
AKT/PKB	Signal Transduction	13.23
ASK1/MAP3K5	Signal Transduction	6.37
MEKK1	Signal Transduction	8.59
MYD118	Signal Transduction	28.61
DAP Kinase	Signal Transduction	4.18
E2F1	Signal Transduction	4.25
PKC-α	Signal Transduction	7.71
PTEN	Signal Transduction	8.97
GSK3B	Signal Transduction	10.24
14-3-3 eta	Signal Transduction	47.45
TP1/Tep1	Telomerase Related	13.26
NGF R	TNF Superfamily	15.33

Table A3.1: ***Genes surviving the filtering process at P7.*** *Genes included in this table were shown to have an original spot intensity above the filtering value for at least half of the representative spots.*

Genes Expressed Above Background at P14

Gene ID	Gene Family	Mean Normalised Value
ABP1	Apoptosis-Related Factors	2.41
CAS/CSE1	Apoptosis-Related Factors	3.71
GSN	Apoptosis-Related Factors	15.89
PDCD1	Apoptosis-Related Factors	2.32
SIAH1	Apoptosis-Related Factors	3.36
ADAM17	Apoptosis-Related Factors	3.05
Ctsd	Apoptosis-Related Factors	15.06
HD	Apoptosis-Related Factors	21.96
PDCD2	Apoptosis-Related Factors	3.85
SREBF1	Apoptosis-Related Factors	5.43
API5	Apoptosis-Related Factors	3.90
Cytochrome p450 oxidoreductase	Apoptosis-Related Factors	4.62
HnrpA1	Apoptosis-Related Factors	13.35
PIGA	Apoptosis-Related Factors	2.26
SREBF2	Apoptosis-Related Factors	11.86
ATM	Apoptosis-Related Factors	2.20
DAD-1	Apoptosis-Related Factors	27.49
ICAD/DFFA	Apoptosis-Related Factors	15.03
PIN	Apoptosis-Related Factors	42.09
TDAG8	Apoptosis-Related Factors	5.02
CAD	Apoptosis-Related Factors	2.46
Dap1	Apoptosis-Related Factors	16.85
Integrin-αV	Apoptosis-Related Factors	14.61
PLA2G1B	Apoptosis-Related Factors	3.19
TFAR15	Apoptosis-Related Factors	4.00
CAV2	Apoptosis-Related Factors	2.37
DAXX	Apoptosis-Related Factors	4.32
MFGE8	Apoptosis-Related Factors	7.89
Thrombospondin	Apoptosis-Related Factors	6.04
CD47	Apoptosis-Related Factors	3.58
DEDD	Apoptosis-Related Factors	7.16
PRKR	Apoptosis-Related Factors	2.76
CHML	Apoptosis-Related Factors	2.84
DNAse1	Apoptosis-Related Factors	4.17
REQ	Apoptosis-Related Factors	10.51
TIAL1	Apoptosis-Related Factors	13.46
CIDE-A	Apoptosis-Related Factors	2.23
DNAse2	Apoptosis-Related Factors	2.43
CLDN3	Apoptosis-Related Factors	2.84
Fem1B	Apoptosis-Related Factors	5.91
Mts-1	Apoptosis-Related Factors	28.27
TXN	Apoptosis-Related Factors	12.88
Cln3	Apoptosis-Related Factors	2.90
FLASH	Apoptosis-Related Factors	3.02
SAG-1	Apoptosis-Related Factors	5.87
Clu	Apoptosis-Related Factors	63.25
Galectin-3	Apoptosis-Related Factors	6.67
ODC	Apoptosis-Related Factors	18.24
Cox-1/Ptgs1	Apoptosis-Related Factors	2.96
GAPDH	Apoptosis-Related Factors	169.87
P2RX1	Apoptosis-Related Factors	18.05
SARP-2/sFRP-1	Apoptosis-Related Factors	56.28
Cox-2/Ptgs2	Apoptosis-Related Factors	2.63
GPX1	Apoptosis-Related Factors	48.46
uPAR1	Apoptosis-Related Factors	2.47
sFRP-5/SARP-3	Apoptosis-Related Factors	6.87
Caspase-7	Caspases and Regulators	18.79

Gene ID	Gene Family	Mean Normalised Value
Sentrin/UBL1	Caspases and Regulators	3.57
Caspase-8	Caspases and Regulators	2.70
Survivin	Caspases and Regulators	2.76
Caspase-9	Caspases and Regulators	3.66
XIAP	Caspases and Regulators	4.35
FLIPL/Cash	Caspases and Regulators	3.25
Caspase-2	Caspases and Regulators	3.94
Caspase-3	Caspases and Regulators	4.87
PARP	Caspases and Regulators	7.69
PARP-2	Caspases and Regulators	3.62
Cyclin G1	Cell Cycle Regulators	51.28
RBBP6/PACT/RBQ1	Cell Cycle Regulators	6.50
DP1	Cell Cycle Regulators	6.76
Sp1	Cell Cycle Regulators	4.12
MDM2	Cell Cycle Regulators	16.80
TRP53/p53	Cell Cycle Regulators	7.01
53BP2	Cell Cycle Regulators	2.87
c-myc	Cell Cycle Regulators	3.23
APEX/Ref-1	Cell Cycle Regulators	10.20
p15INK4b/CDKN2B	Cell Cycle Regulators	2.63
Calcyclin	Cell Cycle Regulators	6.54
P19/NSG2	Cell Cycle Regulators	3.98
CBP	Cell Cycle Regulators	12.91
CDC2	Cell Cycle Regulators	3.81
CDK2	Cell Cycle Regulators	3.18
p300	Cell Cycle Regulators	4.01
CDK4	Cell Cycle Regulators	7.20
CDK5	Cell Cycle Regulators	4.63
pRB	Cell Cycle Regulators	3.62
RBBP4/RbAp48	Cell Cycle Regulators	7.75
Cyclin D1	Cell Cycle Regulators	5.61
RBP1	Cell Cycle Regulators	3.11
GM-CSF Rα	Cytokines and Receptors	15.58
Mannose 6-phosphate R	Cytokines and Receptors	5.36
IFN-γ R1	Cytokines and Receptors	3.47
M-CSF	Cytokines and Receptors	8.33
AR	Cytokines and Receptors	3.43
IFN-γ R2	Cytokines and Receptors	3.97
M-CSF R	Cytokines and Receptors	4.09
ART/Agrp	Cytokines and Receptors	3.00
IGF-I	Cytokines and Receptors	7.65
IL-4 Rα	Cytokines and Receptors	2.91
Prolactin	Cytokines and Receptors	2.55
Axl	Cytokines and Receptors	8.27
IGF-II	Cytokines and Receptors	3.55
TGF-β	Cytokines and Receptors	5.74
IGF R	Cytokines and Receptors	6.84
IL-10 Rα	Cytokines and Receptors	3.17
TGF-β2	Cytokines and Receptors	9.32
TGF-β3	Cytokines and Receptors	4.83
TGF-β RI	Cytokines and Receptors	3.08
GAS1	Cytokines and Receptors	5.05
β2-Microglobulin	Housekeeping Genes	2.91
β-Actin	Housekeeping Genes	105.54
Cyclophilin A	Housekeeping Genes	58.08
HPRT	Housekeeping Genes	5.03
L19	Housekeeping Genes	82.35
Transferrin R	Housekeeping Genes	3.69
α-Tubulin	Housekeeping Genes	32.61

Gene ID	Gene Family	Mean Normalised Value
Bag-1	Mitochondrial Associated	16.08
BAK	Mitochondrial Associated	5.24
Bax-α	Mitochondrial Associated	3.89
Bcl-2	Mitochondrial Associated	4.98
Bcl-w	Mitochondrial Associated	18.94
Bcl-x	Mitochondrial Associated	4.92
BID	Mitochondrial Associated	3.38
Cytochrome C	Mitochondrial Associated	7.13
Mcl-1	Mitochondrial Associated	8.04
A1	Mitochondrial Associated	6.53
1xTE Buffer	Negative Control	2.87
E. coli b1444 gene	Negative Control	1.92
E. coli b3535 gene	Negative Control	2.28
AKT/PKB	Signal Transduction	9.73
RxR-β	Signal Transduction	3.75
TANK	Signal Transduction	4.76
ASK1/MAP3K5	Signal Transduction	9.33
MEKK1	Signal Transduction	9.92
Bcl-10	Signal Transduction	4.03
MYD118	Signal Transduction	20.37
NF-κB DNA binding subunit	Signal Transduction	4.22
TRAF2	Signal Transduction	3.42
CRADD	Signal Transduction	3.21
TRAF3/CRAF1	Signal Transduction	4.06
NF-κBp65	Signal Transduction	6.72
TRAF6	Signal Transduction	6.60
DAP Kinase	Signal Transduction	5.09
TRANK	Signal Transduction	4.52
PI-3 Kinase	Signal Transduction	2.88
TRIP	Signal Transduction	2.45
E2F1	Signal Transduction	7.25
PKC-α	Signal Transduction	9.20
FADD	Signal Transduction	3.44
FAN	Signal Transduction	3.98
PTEN	Signal Transduction	13.30
GSK3B	Signal Transduction	7.99
RARβ2	Signal Transduction	4.72
14-3-3 eta	Signal Transduction	28.95
IKK-α	Signal Transduction	4.37
TP1/Tep1	Telomerase Related	7.85
TR/TeRc	Telomerase Related	5.80
NGF R	TNF Superfamily	12.18
FasL/TNFSF6	TNF Superfamily	3.93
TALL-1/THANK/BAFF/TNFSF13B	TNF Superfamily	4.60

Table A3.2: ***Genes surviving the filtering process at P14.*** *Genes included in this table were shown to have an original spot intensity above the filtering value for at least half of the representative spots.*

Appendix 4: Primer Sequences

Accession Number	*Gene*	*Forward Primer*	*Reverse Primer*	*Annealing Temperature (°C)*	*PCR Product Size (bp)*
NM_001001303	Gapdh	ACCACAGTCCATGCCATCAC	TCCACCACCCTGTTGCTGTA	61	450
Genes shown to be differentially expressed between the two time points					
NM_010414	Hd	CTGCCACTCACCATTCTCACC	CCTCATCCCATTCCTCCTCTC	62	213
NM_008771	P2rx1	CTTGGCTATGTGGTGCGAGAG	TTGAAGAGGTGACGACGGTTT	62	233
NM_010044	Dffa	ACTTCCTCTGCCTTCCTTCCA	GCCACATTCTTCCACTTCACC	62	160
NM_010786	Mdm2	GCACACACACACACACACACA	AACATAGGCAACCACCAGGAA	61	240
NM_008594	Mfge8	CAACAACTCCCACAAGAAGAACA	AGAAGGTCGTCAGCCACAGAA	61	220
NM_010513	IGF1r	GCGGCGATGAAGAGAAGAAA	TCAGGAAGGACAAGGAGACCA	62	216
NM_009465	Axl	AAGAGCGATGTGTGGTCCTTC	GGCAGAGCCTTCAGTGTGTTC	61	248
NM_010705	Galectin-3	ACAGTGAAACCCAACGCAAAC	GCACAGACACACAACACACAAA	61	594
NM_009742	A1	ATTGCCCTGGATGTATGTGCT	GGTTCTCTCTGGTCCGTAGTGTT	61	219
NM_009870	Cdk4	CGACGCAGAGTGAGAAGAGG	TCAGGGAGGGAAGAAGACAGA	61	231
NM_009367	Tgf-β2	TTGGATGCTGCCTACTGCTTT	GCTTCGGGATTTATGGTGTTG	61	212
NM_011640	p53	GCTGGATAGGAAAGAGCACAGA	GGTTGAGGGCAAGAAATGGA	61	239
NM_146057	Dapl	CTGTGTCGCTAAGGAGGGATG	TTACAACGGGAGAAACTGACGA	62	121
XM_127995.	Srebf2	CAAGTCAGCAGCCAAGGAGAG	TCACAAATCCCACAGAGTCCA	61	233
NM_008402	Itg-αV	GGCTGCTGTGGAGATAAGAGG	GCCTTGCTGAATGAACTTGGA	61	162
NM_007829	DAXX	AAAGAAGCAACTGGGCTCTGG	GAGAAGCAGGGATGGAGAAGG	63	214
NM_008562	Mcl-1	ATTTCTTTCGGTGCCTTTGTG	AAACCCATCCCAGCCTCTTT	59	144
NM_010512	IGF-1	CTCTGCTTGCTCACCTTCACC	CACTCATCCACAATGCCTGTCT	63	176
NM_011480	Srebf1	TGGCTTGGTGATGCTATGTTG	AGGGAACTGTGTGTGTTTCTGG	61	150
NM_011580	Thrombospondin	CTGTGACCCTGGACTTGCTGT	AGTATCCCTGAGCCCTTGTGG	64	203

Table A4.1: ***Mouse PCR Primers.*** *This table shows the sequence of the primers designed for the genes identified from the arrays along with the accession number of the sequence for which the primers were designed, the annealing temperatures of the primers and the expected product size.*

Accession Number	*Gene*	*Forward Primer*	*Reverse Primer*	*Annealing Temperature (°C)*	*PCR Product Size (bp)*
Housekeeping genes not shown to be expressed above background					
NM_009735	β2-Microglobulin	CCTGGTCTTTCTGGTGCTTGT	TATGTTCGGCTTCCCATTCTC	61	109
NM_013556	HPRT	TTGGGCTTACCTCACTGCTTT	CGCTCATCTTAGGCTTTGTATTTG	61	758
NM_016638	Transferrin R	TCGGCAAGTAGATGGAGATAACA	CACGCTTACAATAGCCCAGGTAG	61	197

Table A4.2: ***Mouse PCR primers designed for the housekeeping genes not shown to be expressed on the macroarrays.*** *This table shows the sequence of the primers designed for the housekeeping genes identified from the arrays along with the accession number of the sequence for which the primers were designed, the annealing temperatures of the primers and the expected product size.*

Accession Number	*Gene*	*Forward Primer*	*Reverse Primer*	*Annealing Temperature (°C)*	*PCR Product Size (bp)*
NM_001001303	Gapdh	GGAGAAACCAGCCAAGTATGATG	AAAGGTGGAAGAATGGCTGTCA	61	138
Genes shown to be differentially expressed between the two time points					
XM_420822	Hd	CCAGAAGGAGGTGGTGGTGT	AACAGGGCGAAGGGAAGAAG	62	250
-	**P2rx1**	Gene sequence not identified	-	-	-
XM_417610	Dffa	CTTGCCCAGAATCAAACCAAA	CGTGTCAACCACATCCATCTC	61	195
XM_416084	Mdm2	AACTGGTGCCGTCCTAATCT	TAATGTATGGTGGCTGGGTTG	59	148
XM_413867	Mfge8	GGAAGATGAGGCTGAGTGGTG	GCTGTGATGGGAGGGTCAAA	62	208
NM_205032	IGF1r	AAGTGCTCCGCTTTGTGATG	GAGGCTTGTTCTCTTCGCTGT	61	204
-	**Axl**	Gene sequence not identified	-	-	-
NM_214591	Galectin-3	CAGTTCCTCATTGTGCTTGG	GGACAGGGATTTGGTGTTAGG	59	165
-	**A1**	Gene sequence not identified	-	-	-
-	**Cdk4**	Gene sequence not identified	-	-	-
NM_001031045	Tgf-β2	CGGAAGGAGGAGGAAGAGGA	GAGGGAAGAAGTGATGGCAGA	62	325
NM_205264	p53	CGCTATGAGATGCTGAAGGAGA	CGTGGCTGAAGGGAAATGG	62	237
NM_001031003	Dapl	CACCAGCAGATTCAGGACAAA	TGCGTAAGGTAGGAACACATAGAG	61	345
XM_416222	Srebf2	GTGCCTCTCCTTCAACCCTTT	ATCATCCAGCCAAACCATCC	62	246
NM_205439	Itg-αV	TTGATTGTTGGAGCCTTTGGT	CTTTCCTTTGCCATCTGCTTT	60	189
-	**DAXX**	Gene sequence not identified	-	-	-
XM_001233734	Mcl-1	GAGGGCTTTGTTGACTTCTTCC	TCCACTTTGCCTTTCTCTCCT	61	178
NM_001004384	IGF-1	GATGCTCTTCAGTTCGTATGTGG	GCAGATTTAGGTGGCTTTATTGG	61	176
NM_204126	Srebf1	GCAGAAGAGCAAGTCCCTCAA	GTCGGCATCTCCATCACCTC	63	105
XM_421205	Thrombospondin	GGGTGAAGCAAGAGAAACCAA	CGCAAAGCAGGGATTAGACA	60	250

Table A4.3: ***Chick PCR primers designed for genes shown to be differentially expressed from the macroarray results.*** *This table shows the sequence of the primers designed for the genes identified from the arrays along with the accession number of the sequence for which the primers were designed, the annealing temperatures of the primers and the expected product size. Genes for which a sequence could not be identified are highlighted in bold.*

Accession Number	*Gene*	*Forward Primer*	*Reverse Primer*	*Annealing Temperature (°C)*	*PCR Product Size (bp)*
Genes shown to be highly expressed at both time points					
NM_204900	Clusterin	AAGCCCTGCCTCAAACACAC	AGATGTCCTCCACTCCGTCCT	62	232
BX935086	Gpx1	GCAAAGTGCTGCTGGTGGT	TCGTTGGTGGCGTTCTCCT	62	160
BX931030	Pin	ATCGTGGGAAGGAACTTTGG	CAAGAAGGCTGAAGGAACTGG	61	178
NM_001007839	14-3-3 eta	TTGCTGCTGGAGAGAAGAAGAA	TGACAGGGATTGTGAAGTGGA	61	382
NM_204553	Sfrp1	TGGGACTGACTGGTGTCTGG	GGAGCAATGTGGGACTATGGA	62	219
NM_001007473	Dad-1	GGCTCGGTAGGTTCTGTGGT	GGAAGGAGTTGAAGGGAAAGG	61	163
XM_414493	Cyclin G1	TACCTGGCTGTGAAGGCAAC	GCTGGGTCTCAAGTCTCTCAA	60	250
BX932320	Myd118	ATTACCGCTCGTAGGGCTTCT	AATCCGTCCTCCTCCATCAC	61	669
-	**Mts-1**	No primer pair found	-	-	-
XM_421764	Caspase-7	CCACCTTCTGCTTTCGCTTT	TCGGTTGTTCTTCTTCTCCATTC	61	202

Table A4.4: ***Chick PCR primers designed for genes shown to be highly expressed on the macroarrays at both time points examined.*** *This table shows the sequence of the primers designed for the genes identified from the arrays along with the accession number of the sequence for which the primers were designed, the annealing temperatures of the primers and the expected product size. Genes for which no primer pairs could be designed are highlighted in bold.*

Appendix 5: PCR Results

	NB		P7		P14		4wk		
	Normalised Value	Standard Error of Mean	Normalised Value	Standard Error of Mean	Normalised Value	Standard Error of Mean	Normalised Value	Standard Error of Mean	Fold Difference (P14/P7)
Hd	117.38	56.10	44.29	5.68	56.18	8.18	69.15	17.13	1.27
Dffa*	107.37	40.33	48.91	15.05	44.30	5.49	34.50	11.21	0.91
Mdm2	27.94	13.49	53.03	10.83	110.39	68.08	151.41	100.92	2.08
Mfge8	91.58	56.57	55.43	22.66	61.48	19.55	45.37	10.05	1.11
IGF1r	120.07	78.36	44.40	15.46	47.12	9.68	116.58	38.67	1.06
Axl*	160.10	95.61	88.17	16.93	31.65	2.56	39.11	16.71	0.36
Galectin-3	37.18	9.98	35.11	21.79	42.38	14.86	127.67	90.91	1.21
A1*	102.55	36.81	55.54	20.96	10.58	1.90	19.09	16.22	0.19
Cdk4	177.40	67.30	100.87	51.76	100.72	37.98	78.88	38.91	1.00
Srebf2*	153.12	113.93	56.87	12.31	69.16	21.16	176.61	70.64	1.22
TGFβ2	97.39	53.02	75.01	29.22	88.83	18.48	98.76	45.21	1.18
Dap1	58.87	28.60	56.92	15.63	56.21	16.59	48.52	17.48	0.99
Integrin-αV*	126.07	60.19	117.94	15.34	83.98	11.64	145.46	42.68	0.71
P53	36.04	19.14	16.76	9.57	26.61	6.74	32.88	15.97	1.59
DAXX*	54.40	27.75	29.71	21.13	34.75	22.40	62.17	50.04	1.17
Thrombospondin*	48.89	6.59	47.51	13.66	14.03	4.89	7.26	0.38	0.30
IGF-1*	85.37	20.23	108.07	34.72	15.84	3.59	10.55	4.55	0.15
Srebf1*	72.04	25.88	66.44	21.05	56.02	6.30	56.03	9.37	0.84
Mcl-1	43.92	20.13	4.88	1.50	34.51	11.54	108.41	46.93	7.07

Table A5.1: Densitometry Results for the differential gene expression observed by semi-quantitative PCR. *Each PCR was completed three times each time using a different cDNA sample and the resulting bands from the PCR reactions were quantified using Scion Image. First, the results were normalised to that obtained for gapdh. Then the average band intensity and standard error of the mean were calculated from the three sets of results. These results are presented here. The fold difference was calculated. The asterisks mark the genes for which primers were designed for the sequence identified as a result of a BLAST search.*

Appendix 6: Statistical Analysis of PCR Results

One way ANOVA was used with Tukey's post-hoc test in SPSS (USA) to compare the normalised band intensities across time points in an attempt to identify significant changes in expression.

Mouse PCR Results

From the results, a statistically significant difference in expression was only noted in 2 genes, *thrombospondin* and *IGF-1*. *Thrombospondin* showed significantly differential expression between newborn and 4 weeks, and P7 and 4 weeks. *IGF-1* showed significantly different expression between P7 and P14 and P7 and 4 weeks.

Thrombospondin

ANOVA

	Sum of Squares	df	Mean Square	F	Sig.
Between Groups	4302.712	3	1434.237	7.527	.010
Within Groups	1524.327	8	190.541		
Total	5827.039	11			

Table A6.1: ***ANOVA results obtained from analysis of the mouse thrombospondin PCR results.*** *Results are only significant if the sig. value is less than 0.05. A significant difference was observed (sig. value 0.010).*

Multiple Comparisons

Dependent Variable: Thrombospondin

Tukey HSD

(I) Timepoint	(J) Timepoint	Mean Difference (I-J)	Std. Error	Sig.	95% Confidence Interval	
					Lower Bound	Upper Bound
1	2	1.37333	11.27064	.999	-34.7192	37.4659
	3	34.85667	11.27064	.058	-1.2359	70.9492
	4	41.62667(*)	11.27064	.025	5.5341	77.7192
2	1	-1.37333	11.27064	.999	-37.4659	34.7192
	3	33.48333	11.27064	.069	-2.6092	69.5759
	4	40.25333(*)	11.27064	.030	4.1608	76.3459
3	1	-34.85667	11.27064	.058	-70.9492	1.2359
	2	-33.48333	11.27064	.069	-69.5759	2.6092
	4	6.77000	11.27064	.929	-29.3225	42.8625
4	1	-41.62667(*)	11.27064	.025	-77.7192	-5.5341
	2	-40.25333(*)	11.27064	.030	-76.3459	-4.1608
	3	-6.77000	11.27064	.929	-42.8625	29.3225

* The mean difference is significant at the .05 level.

Table A6.2: ***Post-hoc test results obtained from analysis of the mouse thrombospondin PCR results.*** *Results are only significant if the sig. value is less than 0.05. Timepoints 1: newborn, 2: P7, 3: P14, 4: 4 weeks.*

IGF-1

ANOVA

	Sum of Squares	df	Mean Square	F	Sig.
Between Groups	21742.623	3	7247.541	5.863	.020
Within Groups	9889.449	8	1236.181		
Total	31632.072	11			

Table A6.3: ***ANOVA results obtained from analysis of the mouse IGF-1 PCR results.*** *Results are only significant if the sig. value is less than 0.05. A significant difference was observed (sig. value 0.020).*

Multiple Comparisons

Dependent Variable: IGF1

Tukey HSD

(I) Timepoint	(J) Timepoint	Mean Difference (I-J)	Std. Error	Sig.	95% Confidence Interval	
					Lower Bound	Upper Bound
1	2	-22.70000	28.70750	.857	-114.6315	69.2315
	3	69.52333	28.70750	.150	-22.4082	161.4549
	4	74.82000	28.70750	.116	-17.1115	166.7515
2	1	22.70000	28.70750	.857	-69.2315	114.6315
	3	92.22333(*)	28.70750	.049	.2918	184.1549
	4	97.52000(*)	28.70750	.038	5.5885	189.4515
3	1	-69.52333	28.70750	.150	-161.4549	22.4082
	2	-92.22333(*)	28.70750	.049	-184.1549	-.2918
	4	5.29667	28.70750	.998	-86.6349	97.2282
4	1	-74.82000	28.70750	.116	-166.7515	17.1115
	2	-97.52000(*)	28.70750	.038	-189.4515	-5.5885
	3	-5.29667	28.70750	.998	-97.2282	86.6349

* The mean difference is significant at the .05 level.

Table A6.4: ***Post-hoc test results obtained from analysis of the mouse IGF-1 PCR results.*** *Results are only significant if the sig. value is less than 0.05. Timepoints 1: newborn, 2: P7, 3: P14, 4: 4 weeks.*

Chick PCR Results

No statistically significant differences in expression were observed. An example of the results obtained from the statistical analysis is shown below. Post-hoc test results are not included as there was no significant difference observed from the ANOVA results generated by the SPSS statistical package.

ANOVA

		Sum of Squares	df	Mean Square	F	Sig.
Hd	Between Groups	13067.128	5	2613.426	.824	.556
	Within Groups	38061.011	12	3171.751		
	Total	51128.139	17			
P53	Between Groups	43720.497	5	8744.099	1.600	.234
	Within Groups	65572.521	12	5464.377		
	Total	109293.018	17			
Mcl-1	Between Groups	21217.084	5	4243.417	.747	.603
	Within Groups	68125.536	12	5677.128		
	Total	89342.621	17			
Mdm2	Between Groups	17490.292	5	3498.058	2.100	.136
	Within Groups	19991.936	12	1665.995		
	Total	37482.228	17			

Table A6.5: ***Example of the statistical results obtained from analysis of the chick PCR results.*** *Results are only significant if the sig. value is less than 0.05.*

Appendix 7: Statistical Analysis of Western Blotting Results

One way ANOVA was used with Tukey's post-hoc test in SPSS (USA) to compare the normalised band intensities across timepoints in an attempt to identify significant changes in expression.

Axl

ANOVA

	Sum of Squares	df	Mean Square	F	Sig.
Between Groups	3.776	3	1.259	2.380	.145
Within Groups	4.232	8	.529		
Total	8.008	11			

Table A7.1: ***ANOVA results obtained from analysis of the mouse axl western blotting results.*** *Results are only significant if the sig. value is less than 0.05.*

No significant difference in expression was observed for Axl at any of the timepoints examined.

Mcl-1

Short Isoform: Mcl-1_S

ANOVA

	Sum of Squares	df	Mean Square	F	Sig.
Between Groups	.013	3	.004	.768	.543
Within Groups	.046	8	.006		
Total	.060	11			

Table A7.2: ***ANOVA results obtained from analysis of the mouse mcl-1_S western blotting results.*** *Results are only significant if the sig. value is less than 0.05.*

No significant difference in expression was observed for Mcl-1_S at any of the timepoints examined.

Long Isoform: Mcl-1_L

ANOVA

	Sum of Squares	df	Mean Square	F	Sig.
Between Groups	.001	3	.000	5.148	.028
Within Groups	.000	8	.000		
Total	.001	11			

Table A7.3: ***ANOVA results obtained from analysis of the mouse mcl-1_L western blotting results.*** *Results are only significant if the sig. value is less than 0.05. Results showed a significant difference (sig. value 0.028).*

Multiple Comparisons

Dependent Variable: Mcl-1_L

Tukey HSD

(I) Timepoint	(J) Timepoint	Mean Difference (I-J)	Std. Error	Sig.	95% Confidence Interval	
					Lower Bound	Upper Bound
1.00	2.00	-.01881036(*)	.00487130	.020	-.0344100	-.0032107
	3.00	-.00633032	.00487130	.588	-.0219299	.0092693
	4.00	-.00825779	.00487130	.385	-.0238574	.0073418
2.00	1.00	.01881036(*)	.00487130	.020	.0032107	.0344100
	3.00	.01248004	.00487130	.123	-.0031196	.0280797
	4.00	.01055257	.00487130	.212	-.0050470	.0261522
3.00	1.00	.00633032	.00487130	.588	-.0092693	.0219299
	2.00	-.01248004	.00487130	.123	-.0280797	.0031196
	4.00	-.00192748	.00487130	.978	-.0175271	.0136721
4.00	1.00	.00825779	.00487130	.385	-.0073418	.0238574
	2.00	-.01055257	.00487130	.212	-.0261522	.0050470
	3.00	.00192748	.00487130	.978	-.0136721	.0175271

* The mean difference is significant at the .05 level.

Table A7.4: ***Post-hoc test results obtained from analysis of the mouse mcl-1_L PCR results.*** *Results are only significant if the sig. value is less than 0.05. Timepoinst 1: newborn, 2: P7, 3: P14, 4: 4 weeks.*

Appendix 8: Publications and Poster Presentations

Publications

Wride M.A. **Geatrell J.** and Guggenheim J.A. 2006. Proteases in Eye Development and Disease. *Birth Defects Research Part C: Embryo C: Reviews* **78,** pp.90-105.

Poster Presentations

J.C. Geatrell, M.E. Boulton, M.A. Wride. Apoptosis Gene Expression Profiling in Mouse Lens Maturation. ARVO Conference, Fort Lauderdale, Florida, April 2006.

J.C. Geatrell, M.E. Boulton, M.A. Wride. Apoptosis Genes in Lens Differentiation: Identification by Array Analysis. International Society for Ocular Cell Biology (ISOCB) Conference, Cambridge, UK, September 2006.